Lorentz Lattice Gases on Graphs

A Thesis
Presented to
The Academic Faculty

by

Dmitry M. Kreslavskiy

In Partial Fulfillment
of the Requirements for the Degree
Doctor of Philosophy

School of Mathematics
Georgia Institute of Technology
November 2003

Lorentz Lattice Gases on Graphs

Approved by:

Leonid A. Bunimovich
School of Mathematics, Adviser

Mihai Ciucu
School of Mathematics

Prasad Tetali
School of Mathematics

Thomas Morley
School of Mathematics

Dana Randall
College of Computing

Date Approved November 24, 2003

To my parents,

Mikhail Kreslavskiy and Yevgeniya Kreslavskaya,

and to my grandfather,

Roman Kreslavskiy,

a manifestation of whose dream this thesis is.

ACKNOWLEDGEMENTS

First and foremost, I would like to thank my parents for the unending supply of inspiration and good advice, as well as for their tactful but goal-driven guidance. To a large degree, this thesis is a product of your effort, and it is a manifestation of their dream. They'll always remain role models for me.

My parents, my wife, my sister and nephew, and my grandparents have certainly given me unquestionable support of all sorts and kinds throughout my years in academia, and this work would not have been completed without them.

It has been a pleasure and an honor to work under the supervision of Dr. Leonid Bunimovich. In the few short years that I've been under his tutelage, he managed to completely revamp my attitude towards mathematics in general and towards modeling in particular. He always kept my work interesting for me. His help, guidance and support throughout these years is very precious to me.

I am grateful to Georgia Tech, particularly to the School of Mathematics, for contributing to my education and maturity through both teaching and learning opportunities, and also for providing an environment promoting scholarship and integrity, as well as for providing the financial support for me throughout my years in graduate school. On that note, I'd also like to thank my advisor, Dr. Bunimovich, for generously providing me with a research assistantship in my last year.

I would also like to thank Drs. Prasad Tetali, Richard Duke, Federico Bonetto and Thomas Morley from the School of Mathematics, as well as Drs. William Cook, Ellis Johnson and Jan Karel Lenstra from the School of Industrial and Systems Engineering for very helpful discussions and consultations regarding various topics in mathematics.

I am very thankful to the members of my Reading Committee – Drs. Mihai Ciucu,

Thomas Morley, Dana Randall and Prasad Tetali, – for their precious time and efforts on my behalf.

It is my pleasure to write a big "thank you" to Ms. Cathy Jacobson, who put in a lot of time and effort to proof-read this thesis on a very short notice. She helped me out immensely at a very crucial situation, and I am very much indebted to her for her assistance and support.

A special thanks to Ms. Jackie Smythe and to the other wonderful members of the staff from the School of Mathematics for their everyday dedication and support. A big thank you to my friends, without whom my life at Tech would not be an enjoyable experience.

Finally, I'd like to thank G-d, who gave life, and sustained it, and let me have and actualize an opportunity to achieve this monumental building block in my life.

TABLE OF CONTENTS

LIST OF TABLES

LIST OF FIGURES

SUMMARY

The present work consists of three parts. In the first part (chapters III and IV), the dynamics of Lorentz lattice gases (LLG) on graphs is analyzed. We study the fixed scatterer model on finite graphs. A tight bound is established on the size of the orbit for arbitrary graphs, and the model is shown to perform a depth-first search on trees. Rigidity models on trees are also considered, and the size of the resulting orbit is established.

In the second part (chapter V), we give a complete description of dynamics for LLG on the one-dimensional integer lattice, with a particular interest in showing that these models are not capable of universal computation. Some statistical properties of these models are also analyzed.

In the third part (chapter VI) we attempt to partition a pool of workers into teams that will function as independent TSS lines. Such partitioning may be aimed to make sure that all groups work at approximately the same rate. Alternatively, we may seek to maximize the rate of convergence of the corresponding dynamical systems to their fixed points with optimal production at the fastest rate. The first problem is shown to be **NP**-hard. For the second problem, a solution for splitting into pairs is given, and it is also shown that this solution is not valid for partitioning into teams composed of more than two workers.

CHAPTER I

INTRODUCTION

We will consider a class of discrete dynamical systems that model the motion of an object (e.g., the read/write head of a multi-tape Turing machine) on an undirected graph G. At each time step, the object hops from its current location $v \in V(G)$ to any one of its neighboring vertices. The destination of such a transition in unit time is completely determined by the edge that the object used to reach v and by the type of deterministic scattering rule at v. The scattering rule, or the *scatterer*, can be thought of as symbols, written on the tape of the Turing machine at the current vertex.

Initially, the scatterers are distributed among the vertices of the underlying graph. Unless otherwise specified, we will assume that this initial assignment is independent and identically distributed for each vertex. Most of the results, however, will be obtained for almost all (sometimes, for all) initial configurations of the scatterers.

Such models can be thought of as describing a deterministic walk in random media. Equivalent models have been independently introduced to model various phenomena in a wide range of applications, such as statistical physics, coding theory, the theory of artificial life, and theoretical computer science (e.g., see [27, 43, 52], the review [25] and its extensive bibliography). Mathematically, these models belong to the class of deterministic cellular automata (CA).

1.1 CA and Collision-Based Computing

CA are discrete dynamical systems, whose evolution is completely specified in terms of a local deterministic rule. In this light, one may look at CA as a discrete computer

counterpart to the physical concept of a field [55].

Alternatively, Langton suggested to think of CA as a "logical universe with its own local physics" [52]. We represent space by a uniform grid, or, more generally, by a graph, where each vertex, or *cell*, contains some data (in our case, scattering rules); time will advance in discrete steps; and the laws of the universe are expressed as one local relation, depending, say, on the cell and its immediate neighbors.

Another way of understanding CA is to take Wolfram's approach. He viewed such models as a parallel processing computer [69], where the initial configuration is considered as the input. Indeed, CA are considered a general paradigm for parallel computation, just like Turing machines are a general model of serial computation [55].

In addition to being very valuable in theoretical computer science, CA supply a useful and simple paradigm for modeling various phenomena in natural sciences and problems in combinatorial mathematics. For example, such models give a natural way for studying the evolution of spatially extended physical systems.

Historically, due to a wide range of phenomena that could be modeled through CA, equivalent models have been invented under different names in many areas. In pure mathematics, the study of CA belongs, e.g., to topological dynamics; in electrical engineering, CA are sometimes referred to as iterative arrays; and even kids are familiar with such systems, cleverly disguised as computer games.

In conventional models of computation, e.g., the Turing machine, the computer can neither operate on itself nor build other computers. The structural part of the computer is fixed, while the data on which the computer operates are variable.

To provide a more realistic model for the behavior of complex extended systems, von Neumann [65] introduced CA in the late 1940s, following a suggestion of Ulam [62]. Von Neumann was looking for a discrete analog of partial differential equations

to model various phenomena in biology. The mechanisms he utilized to model self-reproduction through CA are very similar to the ones actually employed by biological life.

Ulam and von Neumann are traditionally credited with the invention of CA. Historically, however, such models were independently developed close to the end of World War II by a German engineer Konrad Zuse [73], who was hiding from the Nazis at the time of his research. His interest was in digital models of mechanics, and his invention of "computing spaces" precisely characterizes cellular automata.

In the 1960s, Atrubin used CA to design a one-dimensional multiplicator [2], Fisher, to generate prime numbers [30], and Waksman, to obtain an 8-state solution to the firing squad synchronization problem [66]. In 1966, John Holland started to apply CA to optimization and adaptation problems [49]. Meanwhile, mathematicians became interested in iterated transformations acting on a discrete-state spatially-extended structures [47], and again came up with CA. Absence of uniform terminology and lack of communication lead to a lot of work being duplicated.

Models that explicitly reduce global phenomena to precisely defined local processes are of prime interest. As such, CA have been effectively used to provide models of common differential equations in physics, like the heat and wave equations [61] and the Navier-Stokes equation [46, 33]. In addition, CA have been successfully utilized in modeling phenomena of interest in dynamical systems theory. For example, in systems consisting of large numbers of components connected by a nonlinear couplings, CA were applied to study phenomena like ordering, chaos, symmetry-breaking and fractality. CA provide a rich collection of representative models, where such phenomena can be isolated and studied with relative ease [64, 29, 9]. Wolfram used CA extensively in similar contexts [67, 69, 68, 71, 57, 72].

In 1970, Gardner introduced John Conway's celebrated Game of Life to the public in a widely read column in Scientific American [38]. This gave CA an enormous

popularity, especially among the generation of young scientists. The result was an explosion of research activity in the field of CA.

In the early 1970s, Banks simulated a logical circuit by building logic gates and using particular stationary configurations of cell states in a two-dimensional binary CA to represent wires [3]. This introduced the idea of using CA as a paradigm for computation. In 1982, Berlekamp, Conway and Guy [10] used interactions of gliders to build logical gates. The lines along which the gliders move play the role of wires. They established the universality of this model of computation, i.e., they proved that Game of Life can be used to simulate computers, along the way introducing a wireless model of the logical circuit.

Meanwhile, the question of whether CA can be used to model directly the laws of physics has been raised by Fredkin and Toffoli. Their research culminated in construction of the so-called *conservative logic*. This new type of digital logic conserves the physical quantities in which the symbols were encoded. All information present in the logical circuit at any moment in time is conserved as well. In other words, not only were the Boolean states constant at all levels, but the logical circuit was reversible [32, 60, 31].

The corresponding model of computation can be thought of as an ensemble of balls, interacting with fixed reflectors through elastic collisions. The resulting model of computation was named the Billiard Ball model. These ideas were further developed in [31], giving birth to a concept of ballistic computing. Finally, in 1984, Margolus used the so-called Margolus neighborhood to invent the CA implementation of the Billiard Ball model [54].

In summary, CA have found a permanent and increasingly important role as conceptual and practical models of spatially-extended dynamical systems. They have been very effectively used as models of computation as well.

1.2 CA and Lorentz Lattice Gases

We will consider the class of CA that generalizes the Lorentz lattice gas (LLG) models. LLG models feature rich dynamics on the macroscopic level, while being very simple locally. An important feature of LLG is that these systems are neither purely deterministic nor purely stochastic. LLG and models equivalent to them have been introduced and applied in a variety of fields, including theory of artifical life and biochemistry [52], computational fluid dynamics [59, 11], graph theory [35, 36, 20], and theoretical computer science [52, 27, 14]. The applications for which the CA have been utilized as an effective paradigm feature studying the growth of the order-disorder or solid-liquid interface [56], simulating biomolecular functions or studying the evolution of aggregate systems, like insect colonies [52]. LLG could be useful in modeling partial differential equations. In hydrodynamics, the independent introduction of a perfectly isotropic lattice gas version of the Navier-Stokes equation by Wolfram [70], and simultaneously by Frisch, et al. [33], resulted in very significant research activity. Their model and its derivatives are still an effective simulation method for microemulsions and other complex fluids (see [13, 12] and the bibliography there.) Some LLG models, like Langton's ant [52], are able to simulate the dynamics of Turing machines and are thus capable of universal computation [36]. It has been shown that, given a little information about the structure of the orbits in a two-dimensional Turing machine, it may be possible to solve the inverse problem, i.e., recover the model from an observed orbit [23, 15].

In the classical Lorentz gas model, introduced in connection with the study of electrical conductivity in metals, a particle moves in Euclidean space, elastically colliding with randomly placed spheres [53]. In another classical model in statistical mechanics, called the Ehrenfest's wind-tree model, the moving particle (wind) is elastically scattered by randomly placed diamonds (trees) whose diagonals are parallel to the coordinate axes. These two models are considered to be the simplest for studying the

diffusion of a particle in a random environment. However, a rigorous analysis of these models turns out to be difficult. In fact, the time-irreversible macroscopic dynamics in Lorentz gas (diffusion) has been rigorously derived from the local time-reversible dynamics only when the configuration of the scatterers is periodic and when the free path of the particle is bounded [21, 22, 24].

Such difficulties in the classical models resulted in the introduction of new ones that were simpler to analyze. One of such classes of models are the Lorentz lattice gas cellular automata (LLGCA). These models embed either one of the above-mentioned classical models in a graph G, usually a lattice. Initially, the scatterers will be randomly distributed among the vertices of G and the particle will move along the edges of G.

Two types of generalizations can be applied to the models of this kind. First, various types of scatterers can be placed on the vertices of G. The second generalization is concerned with the possibility of the environment (type of the scatterer) to change (flip) after a collision with a moving object. It is this second generalization that makes such a model a type of a high-dimensional Turing machine [52, 27, 15, 18]. In these models, at each vertex v there will be a protocol that governs the changes of the environment (type of the scatterer) at v. These protocols are infinite tapes, subdivided into cells, with symbols of scattering rules written in each cell.

Applying the second generalization results in models of two types. In the first one, the environment will not change throughout the evolution of the system. This class of models is often called LLGCA *with fixed scatterers*, or the *fixed scatterer* model. In the second one, every time a particle visits a vertex v, the state of the scatterer at v will flip. This class is often called the *flipping-scatterer* model.

It is possible to obtain some rigorous results describing such systems without additional assumptions being made about these protocols (e.g., see [15].) However, such models are too general to analyze in detail. Thus, a more narrow class of

LLGCA, called *walks in rigid environments*, has been introduced in [17]. This class is big enough to generalize all models studied previously. We will sometimes refer to walks in rigid environments as *rigidity* models. In these models, all tapes (protocols) are periodic and each scattering rule occurs on any tape in strings of identical symbols of length r.

The number $r \in [1, \infty]$ is called the *rigidity of the environment*. To justify the term "rigidity," consider a dynamical interpretation of this model. The moving object must visit any vertex v of the underlying graph exactly r times, until the state (type) of the scatterer at v will flip.

Note that rigidity models include both fixed and flipping scatterer models as the extreme cases; LLGCA models with fixed environment correspond to $r = \infty$, while those with flipping scatterers correspond to $r = 1$. All of these LLGCA models describe a completely deterministic evolution of the system with random initial conditions (configuration of the scatterers). As such, they can serve as a paradigm for the deterministic motion of objects in random media.

The properties of such models are often counterintuitive. At first sight, there seems to be a resemblance between such models and random walks (RW). However, their properties are quite different because LLGCA, unlike RW, are not purely random. Both deterministic and stochastic phenomena make important contributions to the evolution of LLGCA models. One example of such a phenomenon is the ultimate propagation of a particle in a strip in a regular triangular lattice with flipping rotators [42]. As a result, the particle always builds a glider. However, this glider moves with random, rather than constant, velocity that depends on the initial states of the scatterers of the system. Recall that in Conway's Game of Life, a glider corresponds to a very specific initial condition. In the model under consideration, however, such gliders appear for any initial configuration of the scatterers.

Bunimovich [17] introduced rigidity models and explored their properties on $\mathbb{Z}$ under various rigidities. Gajardo, et al., considered the restriction of LLGCA to planar graphs and proved that the resulting two-dimensional model is capable of universal computation [34, 36]. Gajardo [37] also classified the rules of LLGCA dynamics on the $\mathbb{Z}$ lattice with forward, back, and delayed-back scatterers, proving some results about the behavior of each rule in the flipping model.

In the present work, we study LLGCA on graphs. The models with fixed environment are considered on arbitrary graphs. It is shown that under the dynamics of these models, the particle performs a depth-first search [26, 1] on the underlying graphs. We examine LLGCA rigidity models on trees and show that in many cases a depth-first search behavior emerges again. We also give estimates on the sizes of orbits of these models [20]. in the case $r = 1$, these estimates coincide with the ones obtained by Gajardo et al., [34, 37]. Additionally, LLGCA rigidity models are examined on the lattice $\mathbb{Z}$. We construct the AND and NOT logical gates for each of the sets of basic dynamics rules on $\mathbb{Z}$, considered in [37]. In addition, we introduce and study the pushback scattering rule, completing the classification of all scattering rules for LLGCA on $\mathbb{Z}$. We also give a complete description of dynamics and statistical properties of these models [51].

1.3 TSS Production Lines

A classical assembly line consists of some number of workstations. The workers are assigned to fixed workstations in order to complete the product. We will consider work-sharing manufacturing, which is a situation where no special advanced skills are required to work on any segment of the production line. This way, each worker can process an item at any point in the production line. Such a case is typical for the apparel industry. Also, two workers cannot work on the same machine at the same time. This way, the station with the greatest work content determines the rate of

production.

Traditionally, each worker is assigned his own machine or a set of machines, where he will work without interference from other workers. In other words, the production line gets divided into fixed sections, and each worker becomes responsible for one section on the line.

Such fixed assignments result in sub-optimal production rates, since a lot of parts may be produced, but not all of them will be connected together to form a complete product. For example, if one worker can produce and attach the collars faster than the other worker can sew on the sleeves for various shirts, a relatively small amount of shirts will be produced, and many produced collars will be left in the middle of the line.

In addition, zone manufacturing is very inflexible. The control of the production line is centralized. In other words, the only way to change the production rate is to redistribute tasks and sections. This is expensive and disruptive, as it may require a long time for workers to adjust to the new assignments. Such inflexibility is especially damaging when products have short life cycles. This occurs often in manufacturing, e.g., in the apparel industry, where clothing changes from season to season.

To increase the flexibility of production, a new idea has been introduced to apparel manufacturing by Aisin Seiki Co. Ltd, a subsidiary of Toyota. The new assembly line design was named "Toyota Sewn Products Management System," or TSS, which is a registered trademark of Aisin Seiki Co. Ltd and is marketed in the western hemisphere by Americas 21st, Inc. TSS has been successfully utilized in manufacturing of a variety of sewn products, such as furniture, shoes, and fish nets [6].

The evolution of TSS production lines can be viewed as a dynamical system [6, 4] where different workers can be thought of as particles moving along a production line and interacting via some potential. This potential represents the restriction that the workers cannot share any workstation on the production line at any moment in time.

The order of the workers on such a line remains fixed. The natural problem of finding an optimal sequencing of the workers has been addressed for both deterministic [6, 4, 16] and stochastic [8] work content. In both situations, the TSS arrangement is very effective. The various industrial sites in apparel manufacturing that applied this approach report increased production rates [6, 8]. In addition, essentially the same approach has been effectively applied in warehouse management, which is an intrinsically stochastic system [5, 7].

In this work, we examine partitioning a pool of workers into groups, where each group will work on its own TSS line. This partition may be optimized in one of two ways. We may see to form groups of workers with approximately the same production rate. Alternatively, we may attempt to form groups of workers for which the corresponding dynamical systems will converge at the fastest rate to their fixed points, where optimal production occurs.

CHAPTER II

PRELIMINARY NOTIONS

2.1 Graph Theory Background

We require a basic set of notions from graph theory, discussed below. For a more detailed discussion, refer to [28]. An ordered pair $G = (V, E)$, with $E \subseteq V \times V$, is called a *graph* with *vertices* V and *edges* E. A graph $G = (V, E)$ is called *finite* if $|V| < \infty$ and *undirected* if E is symmetric, i.e., $(y, x) \in E$ whenever $(x, y) \in E$. A graph G is called *simple* if no two edges of G have the same ends and if G has no *loops*, i.e., edges that start and end at the same vertex. A *path* in the graph G is a sequence $v_1, v_2, \ldots v_n$ of distinct vertices of G, such that $(v_k, v_{k+1}) \in E$ for all $k = 1, \ldots n-1$. A sequence $v_1, v_2, \ldots v_n, v_1$ of vertices of G, such that $v_1, v_2, \ldots v_n$ is a path and $(v_n, v_1) \in E$ (i.e., the ends of this sequence coincide) is called a *cycle*. A graph G is called *connected* if between any two distinct vertices of G there exists a path in G. In this paper, we only deal with undirected simple connected graphs.

A graph G is called *acyclic* if G contains no cycles. A connected and acyclic graph is called a *tree*. Any tree may have a special vertex, called the *root* of the tree. In that case, the tree T is called *rooted*. The set of vertices of the rooted tree at some distance n from the root is called the *n-th level* of the tree. In any rooted tree T, a path of infinite length starting at the root is called a *ray*.

A vertex v is a *neighbor* of a vertex u iff $(u, v) \in E$. A vertex v is *adjacent* to all of its neighbors and to all edges leading from itself to its neighbors. A vertex v is said to have *degree* n if it has precisely n neighbors in G. Every tree with finite number of vertices must have at least 2 vertices of degree 1. Such vertices are called *leaves*. If every non-leaf node of the tree has degree d, we call the tree *d-regular*. A

d-regular tree in which the first level contains d vertices and any other level $n > 1$ has $d(d-1)^{n-1}$ vertices is called *complete*. The length of the longest path in a tree T is called the *diameter* of T. Also, a tree on $n \geq 1$ vertices has exactly $2n-2$ edges. There exists a unique path between any pair of vertices in the tree. In particular, there exists a unique path between the root of the tree and any other vertex v in that tree. The predecessor of v on such a path, say u, is called the *parent* of the v, and v is called the *child* of u.

Any graph can be drawn in the plane in some way, by picking vertices to be points in $\mathbb{R}^2$ and letting edges be arbitrary curves between the corresponding points. Any such drawing of a graph in the plane where no two edges intersect is called a *planar drawing*. A graph is *planar* if and only if it has at least one planar drawing. In particular, any tree is a planar graph.

2.2 Dynamics Definitions

At any particular time, we may combine the states of the scatterers at each vertex (the *configuration* of the system), the position of the particle (i.e., the edge on which it is currently located) and the direction along which the particle is moving on this edge. Such a combination taken at some fixed time t is called the *state* of the system at time t. An *orbit of the particle* is a sequence of successive states $s_1, s_2, \ldots$, arising from the movement of the particle on the graph. This orbit is *periodic* if $\exists\ p, m \in \mathbb{Z}^+$ such that $s_{k+p} = s_k, \forall\ k \geq m$. In this case, the number p is called the *period* of the particle.

2.3 Measuring Algorithm Speed

We will also need some notions to measure the speed of an algorithm. For that, we use the standard $O(\cdot)$ and $\Theta(\cdot)$ notations of asymptotic growth, defined as follows. We say $f(n) = O(g(n))$ if and only if $\exists\ c, N \in (0, +\infty)$ such that $0 \leq f(n) \leq c \cdot g(n), \forall\ n \geq N$.

This way, $f(n) = O(g(n))$ means that f grows asymptotically not faster than g. We also say that $f(n) = \Theta(g(n))$ if and only if $f(n) = O(g(n))$ and $g(n) = O(f(n))$. For a more elaborate discussion, see [26].

2.4 Computational Complexity

A *decision problem* is a question, where for any given instance the answer is either "yes" or "no." Such a problem is *decidable* iff there exists an algorithm that answers the question correctly in finite time.

A system is said to be universal (or capable of universal computation) if it may simulate a universal Turing machine. This notion implies, in particular, the existence of undecidable problems.

Decidable problems are classified into *complexity classes* that describe the amount of resources (e.g., memory and processing time) that are necessary to solve the problems in the class. Some important classes are **P** and **NP**. The class **P** consists of problems for which there exists an algorithm to solve them in polynomial running time in terms of input size.

We can think of decision problems as being questions of the type "does there exist an object with property X within a set of objects Y?" A problem belongs to the class **NP** iff there is an algorithm that will be able to check in polynomial time whether a fixed member of Y possesses the property X. In other words, **NP** is a class of decision problems, an answer to which can be verified in polynomial time. Hence, $\mathbf{P} \subseteq \mathbf{NP}$. The question of whether $\mathbf{P} = \mathbf{NP}$, however, is one of the most challenging questions in modern mathematics.

We say that a problem A can be *reduced* to a problem B, if there is a function R, computable using logarithmic space in terms of size of the input, such that a is an instance of A if and only if $R(a)$ is an instance of B.

A problem to which any problem in any complexity class C can be reduced is

called C-hard. If a C-hard problem in addition belongs to C, it is said to be C-complete. Hence, to show that a problem is C-hard, it suffices to reduce any C-hard problem to it.

Intuitively, if a problem is **NP**-hard, then the most efficient way of solving it is to sift through all possible solutions, which is extremely cumbersome. Showing that a problem is **NP**-hard implies that there is an element in the problem that is intrinsically difficult to optimize quickly.

Complexity and undecidability are ways to measure the unpredictability of the system. A good account of the notions in computational complexity can be found, e.g., in [58].

CHAPTER III

FIXED SCATTERER MODEL

3.1 Dynamics of LGCA on Arbitrary Graphs

We will consider a connected undirected graph $G = (V, E)$, together with one of its drawings in the plane. Note that G is not necessarily planar, and so the drawing we will consider may possibly contain some non-vertex edge-crossings. Fixing the particular drawing of G allows us to define an order on the set of edges adjacent to a given vertex. For a given edge e adjacent to some $u \in V$, there always exists an edge e' that is next *to the left* of e. This edge e' can be found by moving clockwise around u, starting at the edge e. Notice that $e = e'$ if and only if $\deg_G v = 1$. The next edge to the right of e can be defined analogously by moving counter-clockwise from e around u. Henceforth, we follow the orientation of the particle when using directions right and left.

LLGCA can be defined on different lattices [42, 50]. We follow [34] to extend LLGCA to general graphs. We place a scatterer on every vertex of the underlying graph G. Denote the state of the scatterer at any $v \in V$ by $\phi(v)$. Initially, any scatterer will be in one of the two states: *to left* or *to right*. In accordance with this, $\phi : V \to \{L, R\}$. Later we will introduce the so-called *back-scatterers* by allowing the third state of the scatterer, *back*, and letting $\phi : V \to \{L, R, B\}$. Suppose the particle arrives to some $u \in V$ using some edge $e \in E$. If $\phi(u) = L$, the particle will use the next edge to the left of e to exit the vertex u. On the other hand, if $\phi(u) = R$, the particle will use the next edge to the right of e to exit the vertex u. in the case of a flipping LLGCA model, we will in addition switch $\phi(u)$ after each passage of the particle through u.

3.2 Previous Results

In this section, we summarize some relevant previous results. The models on $\mathbb{Z}$ have been studied in [17, 42]. In these one-dimensional models, if we do not allow back-scatterers in either the flipping or the fixed scatterer models (i.e., only the forward scatterers are present), the particle will propagate in one direction with unit velocity. When we allow back-scatterers, in the case of a model with fixed environment, the particle will oscillate between two back-scatterers to the right and to the left of its initial starting point. In the flipping model, the particle will proceed in one of the directions with random velocity due to a blocking mechanism [42].

Gajardo, Goles and Moreira [34, 37] studied the behavior of the flipping-scatterer model (also known as the Langton's ant model [52]) on planar graphs. Following their terminology, we will occasionally refer to this model as "Langton's ant" or as the "ant." They proved that on a tree with diameter D, the period of the ant is linear in the number of vertices of the graph and equals $4D$. They also proved that the period is linear for a larger class of planar graphs, where no edge can be shared by two distinct cycles. There exist non-planar drawings of planar graphs on which the period of the ant is exponential in the number of vertices of the underlying graph, while on planar drawings of the same graphs, the period is polynomial. There also are planar drawings of some graphs on which the period of the ant is exponential [34]. Thus, the behavior of the ant in the flipping model is dependent on the drawing of the graph.

3.3 Estimation of Period on Arbitrary Graphs

Throughout this section, we consider a particle of a LGCA with fixed environment moving on a simple graph $G = (V, E)$ with n vertices and m edges. Without loss of generality (WLOG) we may assume (WMA) that G is connected.

Proposition 1 *Period of a LGCA with fixed environment on a finite connected graph G is $O(m)$.*

Proof At any given time the particle can be positioned at one of the edges of the graph G, and it can be moving in either of the two directions along this edge. Because the scatterers at the vertices of the graph never change their state, there are at most $2m = O(m)$ distinct system states. Once the particle retraces the same edge in the same direction, it must be in a periodic orbit.

Q.E.D.

Any planar graph with $n \geq 3$ vertices satisfies $m \leq 3n - 6$ [28]. Hence,

Corollary 2 *Period of a LGCA with fixed environment on any finite planar graph is at most $O(n)$.*

3.4 Construction of a Quadratic-Period Graph

In view of Proposition 1, it is natural to ask if there exist non-planar graphs, for which the period of the LGCA with fixed environment is super-linear. For any prime $p > 3$, we construct a drawing in the plane of a non-planar graph G_p (i.e., the edges will be allowed to cross) such that the LGCA with fixed environment on it will have a quadratic period in n, the number of its vertices. Even though we consider a non-planar drawing, the senses of right and left are going to stay the same because we embed the graph in the plane. The algorithm is illustrated on figures 1 - 5 for $p = 5$. We proceed as follows.

1. Start with a cycle on p vertices, say $\{v_i\}_{i=1}^{p}$, forming the boundary of a regular p-gon. For each v_i we set $\phi(v_i) = R$. See figure 1. We may also refer to v_p as v_0 for notational convenience.

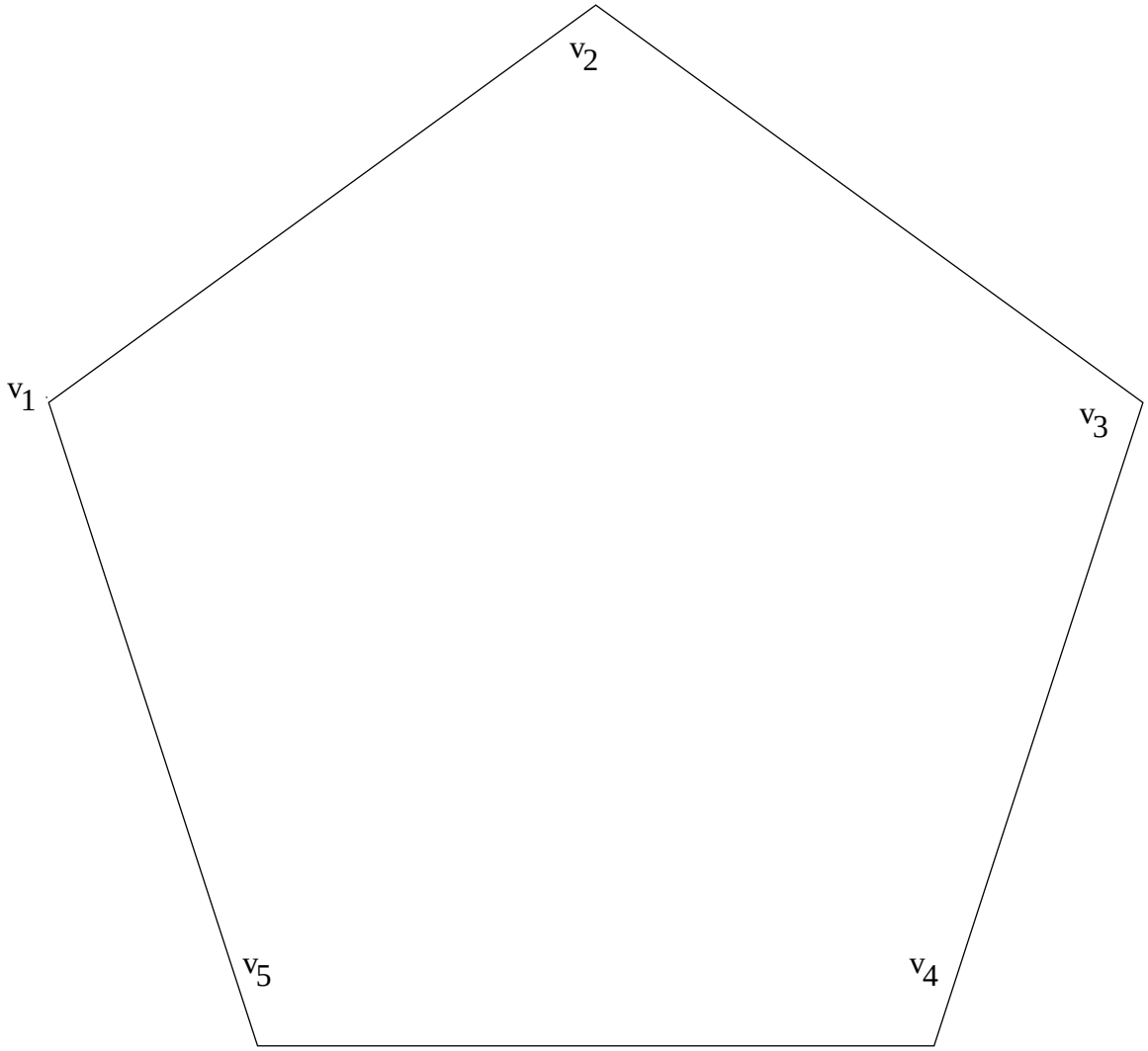

Figure 1: The Original Cycle

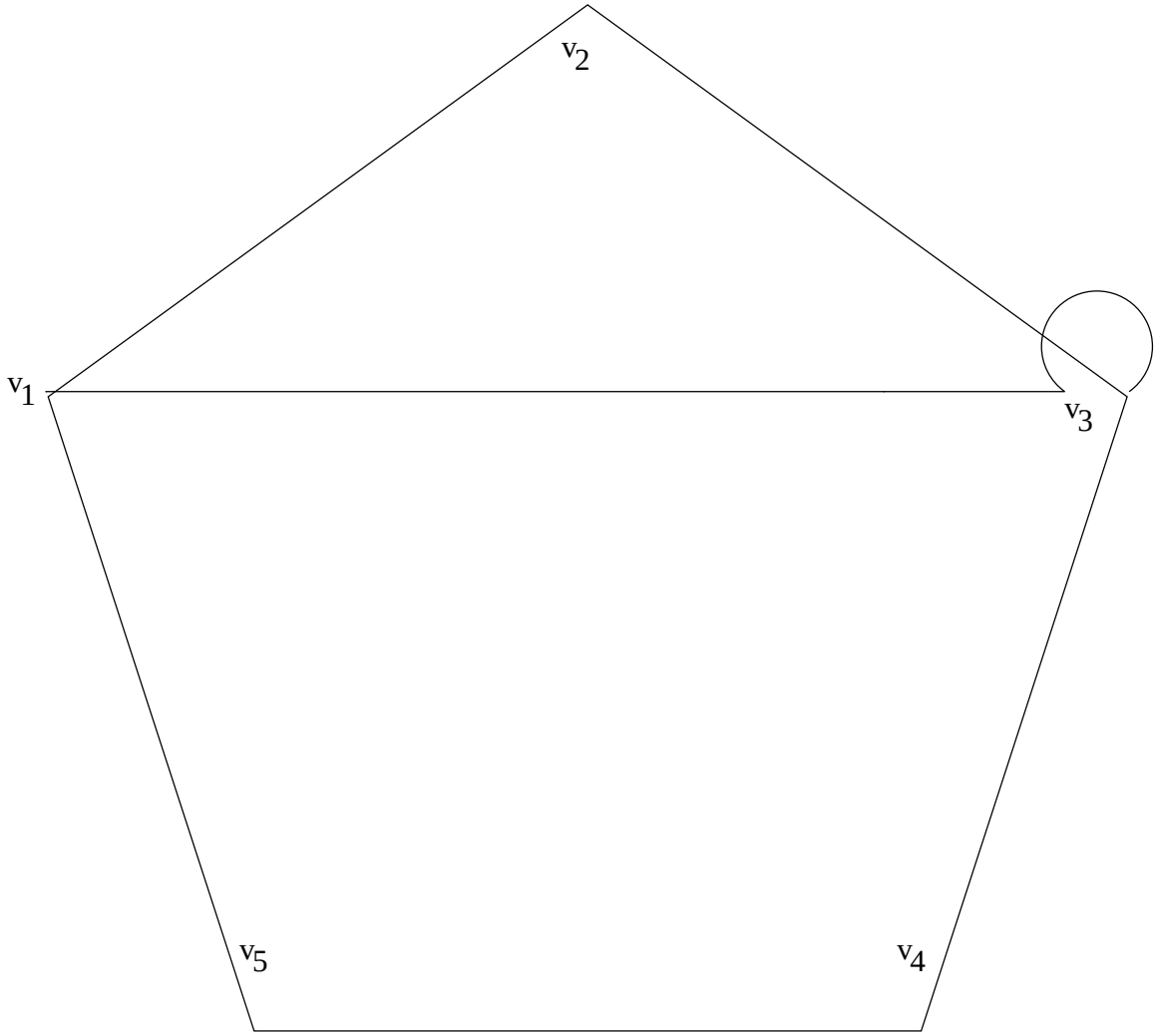

Figure 2: Drawing the Edge $\{v_1, v_3\}$

2. Draw an edge from v_1 to v_3, moving inside the cycle from v_1, leaving the cycle right before v_3 and hitting the destination from outside the cycle. See figure 2.

3. Now, between the edge just drawn and the edge next to its right, draw an edge e going outside the cycle from current vertex, say v_j. This edge must intersect the edge used to enter v_j and then proceed to v_k where $k = (j+2) \mod p$. The edge e must hit the destination v_k between the last edge drawn incoming to v_k and the edge $\left\{v_k, v_{(k+1) \mod p}\right\}$ to the next vertex along the original cycle. See figure 3.

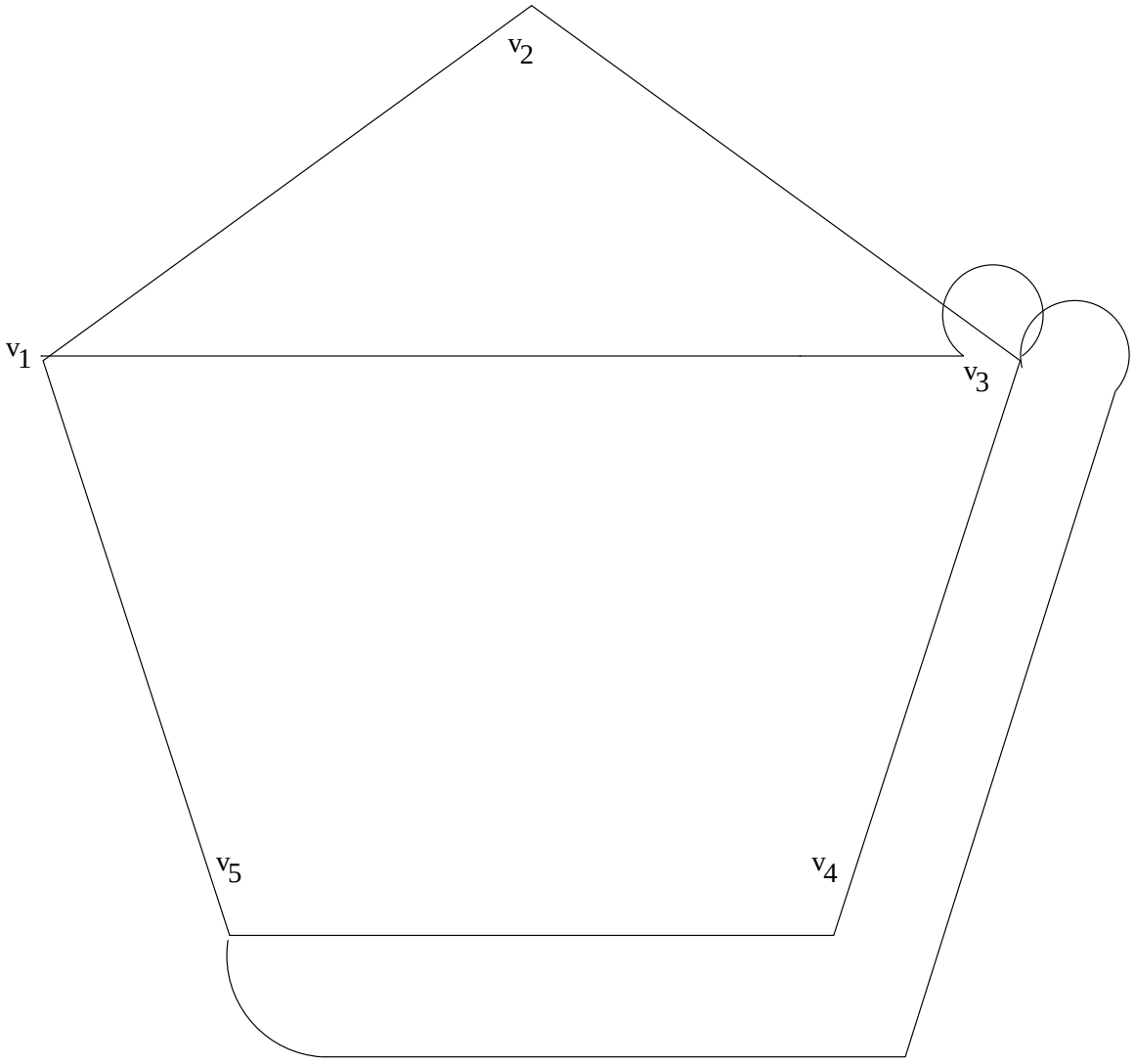

Figure 3: Drawing the Next Edge With Skip 1

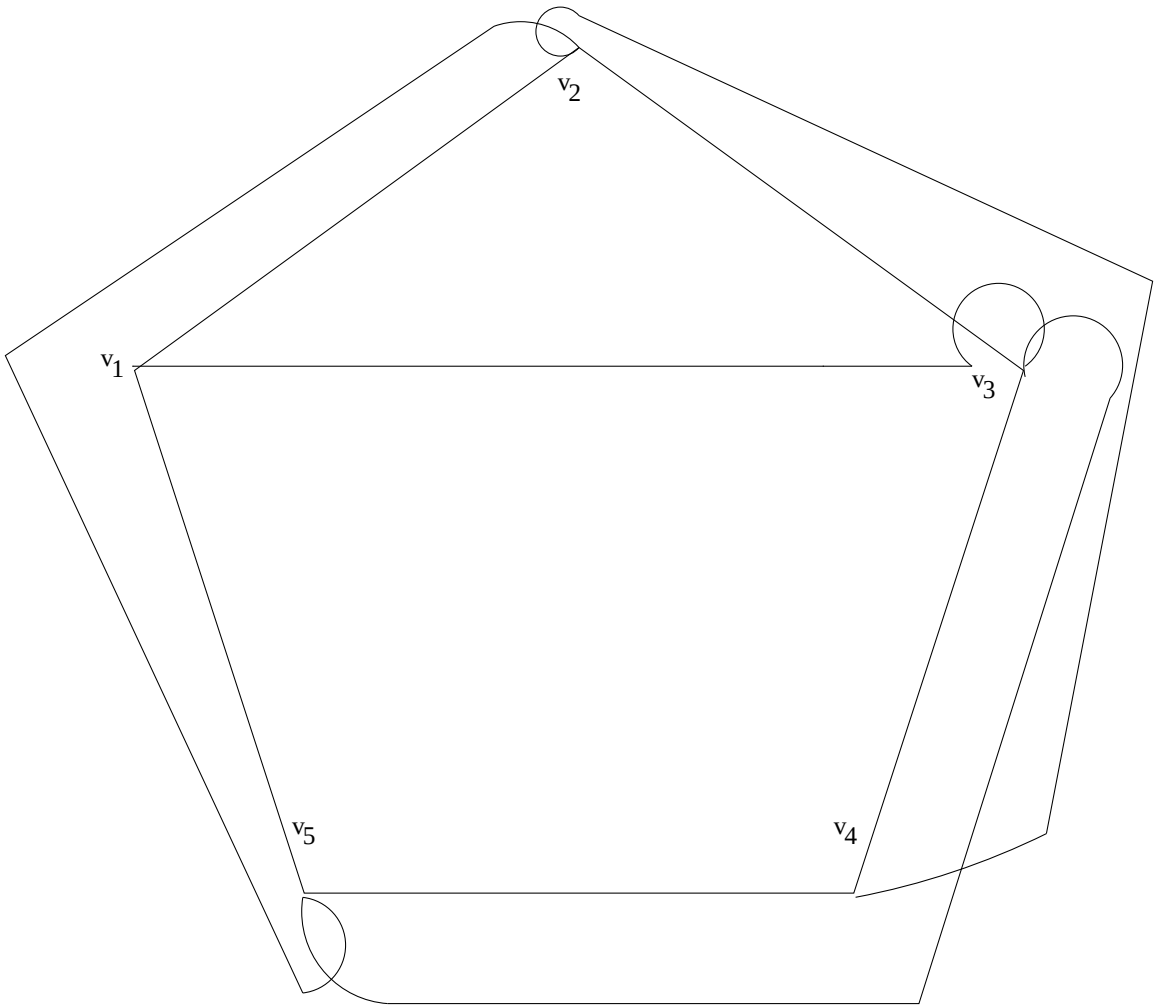

Figure 4: Complete the Cycle With Skip 1 Until v_1 Is Hit

4. Repeat the above until the vertex v_1 is hit. See figure 4.

5. Repeat the two preceding steps for all skips from 2 until $\frac{p-1}{2}$, except the very last edge to v_1 crosses into the cycle right before v_1 and enters v_1 between the edges $\{v_1, v_2\}$ and $\{v_1, v_3\}$. See figure 5.

6. Start the particle on the edge $\{v_1, v_2\}$ going from v_1 to v_2.

Lemma 1 *For any fixed $n \in \mathbb{Z}^+$, there is a graph G_n with n vertices, such that LGCA with fixed environment has a quadratic (i.e., $\Theta(n^2)$) period on G_n.*

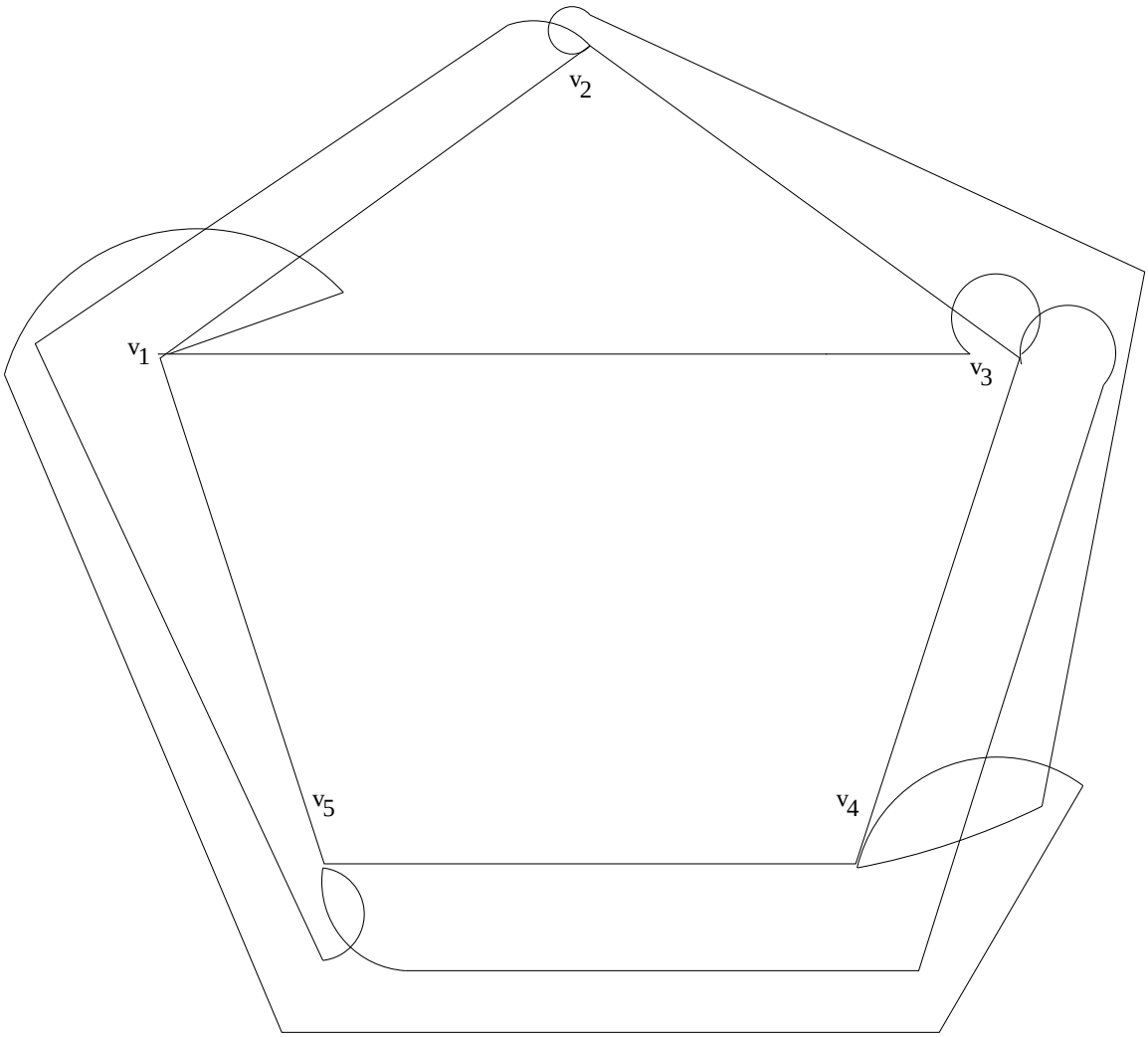

Figure 5: The Graph G_5

Proof First, let us assume that $n = p$ for some prime p. Consider the graph G_p, drawn by the above algorithm. Between any two distinct vertices of G_p there is an edge. Therefore, G_p is a complete graph on p vertices, and so it has $\frac{p(p-1)}{2} = \Theta(p^2)$ edges. Thus, it suffices to show that the particle visits every edge of G_p exactly once during the movement along its orbit in the same period. The proof of this will be given below.

Now, suppose an integer $n \geq 3$ is not prime. We can come up with largest prime number p smaller than n, i.e., let $p = \max\{\, q |\, q \leq n, q \text{ is prime}\}$. It has been shown that if $x \in \mathbb{N}$, then there is a prime q satisfying $x \leq q \leq 2x$ [45]. Then, $p = \Theta(n)$. Now construct the graph G_p, and replace any one edge $\{x, y\}$ of G_p with a path $x \to w_1 \to v_2 \to \ldots \to w_{n-p} \to y$, obtaining the graph G_n. Since $p = \Theta(n)$, LGCA with fixed environment has a $\Theta(n^2)$ period on G_n.

□

We now show that the particle visits every edge of G_p exactly once during the movement along its orbit in each period. Between any two distinct vertices of G_p there is an edge. So, G_p is a complete graph on p vertices. Thus, G_p has $\frac{p(p-1)}{2} = \Theta(p^2)$ edges. Consequently, it suffices to show that the particle visits every edge of G_p exactly once during each period.

It suffices to show that the particle will visit the edges of the graph G_p in the same order as they were drawn by the algorithm. We proceed by induction on the number of iterations in the algorithm.

Initially, the particle starts on the edge $\{v_1, v_2\}$ of the original cycle. Then it follows that cycle along every vertex until it reaches the vertex v_1 again. This happens because all added edges were drawn to the outside of the original cycle, except near the vertex v_1. At v_1 the particle will turn right, using the edge $\{v_1, v_3\}$, because that edge was drawn inside the circle. Assume that until step k (with $0 < k \leq \frac{p(p-1)}{2}$), the

particle precisely followed the order in which the edges were drawn by the constructing algorithm.

In the case $k < \frac{p(p-1)}{2}$, suppose the particle entered the vertex v after the step using the edge e_{in}. Notice that by the construction, the algorithm next drew the edge leaving v between e_{in} and the previous edge drawn incoming into v, say e_{prev}. Observe that all edges adjacent to v drawn after step k by the algorithm will be to the left of e_{in} by construction. All edges adjacent to v drawn before step k will be to the right of the edge e_{prev}. So, the edge to the right of e_{in} around v is precisely the one drawn by the algorithm, and thus it will be used to exit the vertex v.

In the case $k = \frac{p(p-1)}{2}$, the particle will end up at the vertex v_1, having just come in on the last edge drawn by the algorithm. The particle enters v_1 between the edges $\{v_1, v_2\}$ and $\{v_1, v_3\}$, and it will turn right. So, the edge $\{v_1, v_2\}$ must be used to exit v_1 since no other edge has a part inside the original cycle, except the one that was used to enter v_1 and the edge $\{v_1, v_3\}$, which is to the left. Thus, after tracing the last edge, the particle retraces the edge it started from for the first time (by inductive hypothesis). So, the orbit of the particle will consist of all edges of G_p.

Q.E.D.

In view of the above construction, there exist graphs of arbitrary size, on which the period of the non-flipping LGCA model is quadratic in the number of vertices. Consequently,

Corollary 3 *The bound of Proposition 1 on the period of a LGCA with fixed environment on general graphs is sharp.*

G_p is a complete graph on p vertices. There certainly exist other ways of drawing the same graph with the same initial state of the system in such a way that LGCA has a linear period on it (for example, make all edges go outside of the initial cycle,

and LGCA will proceed to move along the cycle with period p). Thus, for LGCA with fixed scatterers on non-planar graphs, the period of the particle is drawing-dependent. This is analogous to what was found in [34, 37] for the flipping-scatterer model.

3.5 Dynamics on Trees

Consider a LGCA with fixed environment on a tree $T = (V, E)$ with n vertices and m edges. We already mentioned that the period of the motion will be linear in n [34]. For trees we can describe the evolution in much more detail.

Proposition 4 *The particle of a LGCA with fixed environment on a tree T performs a depth-first search on T, where the order of visiting children at any vertex v is specified by $\phi(v)$. This order will be right-to-left if $\phi(v) = R$, and left-to-right if $\phi(v) = L$.*

Proof. Consider local behavior of the particle near some arbitrary vertex v in the tree. When visiting v for the first time, the particle will visit all children of v in order, one after another. This order will be right-to-left if $\phi(v) = R$, and left-to-right if $\phi(v) = L$. Finally, the particle will leave using the edge that was originally used to visit the vertex for the first time, i.e., towards v's parent in the tree. The global behavior of the particle, then, is to perform a depth-first search [1, 26] on the tree T, where the order of visiting children at every vertex is specified by the scatterer at that vertex.

Q.E.D.

This result shows that the only thing locally influenced by the state of the scatterer at any vertex is the order in which all of the children of that vertex are traversed. Hence, the resulting period is independent of the initial distribution of the scatterers and can be easily computed.

Corollary 5 *Let T be a tree with $n < \infty$ vertices and m edges. Each orbit of motion of a LGCA with fixed environment on T traces every edge of T exactly once in each direction in each period. This period equals $2m = 2n - 2$.*

CHAPTER IV

LGCA MODELS ON TREES

4.1 Models With Finite Rigidity on Finite Trees

Consider a particle of a LGCA is moving on a finite tree $T = (V, E)$, in an environment with rigidity r. At every $v \in V$ there is a scatterer that is always in one of two states: $\phi(v) \in \{L, R\}$. Every rth visit of the particle to v changes (flips) $\phi(v)$. One special feature of this system is that the scatterer at any vertex can be in one of $2r$ states. Let 0 through $r-1$ be the states of the scatterer corresponding to $\phi(v) = L$ and r through $2r-1$ be the states corresponding to $\phi(v) = R$.

4.1.1 Local Behavior

Suppose that our particle first visits some $v \in V$ using some edge e from the parent p of v. If $\phi(v) = R$, the particle will make a right turn towards a child of v. In the case $\phi(v) = L$, the particle will make a left turn. Let c_1 denote the first child of v visited by the particle.

The vertex v has been visited once so far. The particle will then browse the subtree rooted at c_1, and return to v, at which point it will proceed to make a turn in the same direction as the first turn, towards the child c_2. This behavior will be exhibited until one of two things happens: either we run out of children or $\phi(v)$ is flipped.

In the first case (i.e., we ran out of children), the scatterer is not flipped after the particle returns from the last child of v. The particle visited v precisely deg v times, so deg $v < r$. In the second case (i.e., the scatterer was flipped), the particle visits v precisely r times to flip the scatterer. Thus, deg $v \geq r$. We consider the cases

deg $v = r$ and deg $v > r$ separately.

Let deg $v < r$. Then, when the particle leaves v, the new state of the scatterer at v is deg v if $\phi(v) = L$ and $r + \deg v$ if $\phi(v) = R$. More generally, we have

Lemma 2 *Let* $\deg v < r$. *If the particle arrives at a vertex* v, *and the scatterer at* v *is in some state* $k \in \{0, 1, 2, \ldots, 2r-1\}$, *and* $\lfloor \frac{k+\deg\ v}{r} \rfloor = \lfloor \frac{k}{r} \rfloor$, *then it explores each subtree of* v *in order, from left to right (in the perspective of the particle) if* $k < r$ *and from right to left otherwise. When the particle leaves* v, *the scatterer at* v *is in the state* $k + \deg\ v$.

Now consider deg $v > r$.

Lemma 3 *Let* $\deg v > r$. *Suppose that the particle arrives at a vertex* v *that has been visited* k *times since the last flip, and* $\lfloor \frac{k+\deg\ v}{r} \rfloor > \lfloor \frac{k}{r} \rfloor$, *and* $(k + \deg\ v) \bmod r \neq 0$. *Then, the particle will flip the scatterer at* v *one time (or two times iff* $k = 0$*). If the initial state of the scatterer at* v *was* k *(or* $r+k$*), the particle will leave the scatterer in the state* $(2r-k) \bmod 2r$ *(or* $r-k$*). In this process, each of the subtrees* $1, 2, \ldots, r-1$ *of* v *will be visited twice and the* r*th subtree will be visited once.*

Proof. Suppose now $\deg v > r$. When $\phi(v)$ is flipped, the particle will still have at least one more child c_{r+1} to visit. After the particle explores the subtree of c_{r+1} and returns to v, $\phi(v)$ has been flipped. Then, the particle changes direction, and retraces the children of v in the reverse order from the way they were originally traced. This behavior is like performing a depth-first search right-to-left on a subtree of the original tree, rooted at v, and then doing it again left-to-right on the same subtree. Finally, when the particle leaves v towards p using the edge e, the vertex v has been visited precisely the same number of times on the way back as it was on the way forward. But on the way forward, it was visited r times, because the scatterer was flipped. Consequently, when the particle leaves v using e, the $\phi(v)$ will flip again.

Overall, the particle has visited the edge e twice, the rth child of v once and children $1, 2, 3, \ldots, r-1$ twice. In the case when we initially have $\phi(v) = L$ ($\phi(v) = R$), the particle will visit the left (right) children of v.

Q.E.D.

Finally, let $\deg v = r$. Then, when the particle comes back from the last child of v, right before it leaves using the edge e, the $\phi(v)$ is flipped. The next statement, summarizing this behavior, has a proof similar to Lemma 2.

Lemma 4 *Let* $\deg v = r$. *Whenever a particle visits a vertex* v *in some state* k *with* $(k + \deg\ v) \bmod\ r = 0$, *then the particle will perform a depth-first search, in some order, on each subtree, rooted at one of the children of* v, *leaving the scatterer in state* r *if* $0 \leq k < r$, *or* 0 *if* $r \leq k < 2r$, *flipping it exactly once.*

4.1.2 Complete d-Regular Trees

In this section, we apply the results on local behavior to analyze the LGCA model with arbitrary rigidity on complete d-regular trees. The particle will always start on the edge from the root of T towards one of its children, oriented away from the root. In a d-regular tree, every *non-leaf* vertex of the tree has degree d. Assume $d > 0$ and $r > 0$. Easy computation gives

Lemma 5 *Let* $T = (V, E)$ *be a complete* d*-regular tree with* n *vertices and* k *levels. Then,*

$$k = \log_{d-1}\left(1 + \frac{(n-1)(d-2)}{d}\right).$$

By the Division Algorithm, $\exists\ \alpha, \beta \in \mathbb{N}$ with $0 \leq \beta < d$, such that $r = \alpha d + \beta$. We will consider different cases, depending on the values of α and β.

Proposition 6 ($\alpha = 0, \beta \neq 0$) *Consider LGCA with rigidity* r *on a finite complete* d*-regular tree* $T = (V, E)$ *with* n *vertices and diameter* D. *Suppose that* $d > r$. *Then,*

the orbit of motion will have the period

$$\left\{\begin{array}{cc} 4D & r=1 \\ \frac{4r^2}{r-1}\left(\left(\frac{n(d-2)+2}{d}\right)^{\log_{d-1}(2r-1)}-1\right) & r\geq 2 \end{array}\right\|.$$

Proof. We consider the orbit of the particle during one period. Every non-leaf vertex of T has degree $d > r$. Therefore, locally, by Lemma 3, the particle will visit $r-1$ subtrees of each non-leaf vertex twice and one subtree exactly once. The root is an exception to this, because the particle visits *two* subtrees of the root once, and $r-1$ subtrees twice. This also follows from Lemma 3 because the edge towards the first subtree of the root to be browsed replaces the top edge e from the Lemma. Also, after the particle leaves any non-leaf vertex for the last time during one period, the scatterer at this vertex will remain in its initial state.

The root has $r+1$ identical subtrees that will get browsed. Of them, $r-1$ will be browsed twice. Then, one pass around the whole tree browses a total of $2(r-1)+2 = 2r$ root subtrees. Let t_k denote the time to complete one pass on a tree with k levels, and τ_k denote the number of edges visited in one root subtree during one pass (where a visit counts each time the particle traces the edge in both of the two directions). Let τ_k also include the edge from the root to the parent of the subtree. The particle never uses more than $r+1$ edges adjacent to any vertex. So, WMA $d = r+1$ for the purpose of calculating t_k and τ_k.

The time it takes to browse one subtree completely is $2\tau_k$, and therefore, it takes the time $t_k = 2r \cdot 2\tau_k = 4r\tau_k$ to complete one pass. Each orbit consists of $2r$ such passes, because every pass increments the state of the leaf scatterers by 1 and does not modify the state of the scatterers at non-leaf vertices. So, the period of LGCA on such a tree with k levels would be $8r^2\tau_k$. Now it remains to find τ_k and express k as a function of n.

Clearly, $\tau_1 = 1$. For $k > 1$, a root subtree on k levels consists of a root, whose

only child is a parent for r subtrees on $k-1$ levels. Of them, one will be browsed once, and the other $r-1$ will be browsed twice. That makes $2(r-1)+1 = 2r-1$ subtrees to be browsed, and one more edge from root to the parent of the smaller subtrees. Therefore, $\tau_k = 1 + (2r-1)\tau_{k-1}$. Also, $\tau_1 = 1$ implies $\tau_0 = 0$.

For $r = 1$, this reduces to $\tau_k = \tau_{k-1} + 1$ with $\tau_1 = 1$, which is the arithmetic series $\tau_k = k$. So, the period is $8k$, where k is the number of levels in the tree T (so the diameter of T is $D = 2k$ and the period is $4D$). This is precisely the result obtained by Gajardo, Goles and Moreira [34].

Solving the recurrence for $r \geq 2$, we obtain $\tau_k = \frac{(2r-1)^k - 1}{2(r-1)}$. So, one pass along the tree takes time

$$t_k = 4r\tau_k = 4r\frac{(2r-1)^k - 1}{2(r-1)} = \frac{2r((2r-1)^k - 1)}{r-1}.$$

Consequently, the orbit will be of size $2rt_k = \frac{4r^2((2r-1)^k - 1)}{r-1}$. Now we only have to express k as a function of n. We have $d > r \geq 2$, so $d > 2$. By Lemma 5,

$$k = \log_{d-1}\left(1 + \frac{(n-1)(d-2)}{d}\right) = \log_{d-1}\left(\frac{n(d-2)+2}{d}\right).$$

Finally, $\forall\ r \geq 2$, our orbit must have period

$$\frac{4r^2((2r-1)^{\log_{d-1}\left(\frac{n(d-2)+2}{d}\right)} - 1)}{r-1} = \frac{4r^2}{r-1}\left(\left(\frac{n(d-2)+2}{d}\right)^{\log_{d-1}(2r-1)} - 1\right).$$

Q.E.D.

For a fixed d, the period has length $\Theta\left(rn^{\log_{d-1}(2r-1)}\right)$. We are assuming $d > r \geq 2$; therefore, we have $\log_{d-1}(2r-1) < 2$. So we get a sub-quadratic estimate in n. In terms of r, this estimate is polynomial with degree depending linearly on the depth of the tree T.

We now consider the easier case of $r = \alpha d$.

Proposition 7 ($\beta = 0$) *Consider LGCA with rigidity r on a finite complete d-regular tree $T = (V, E)$ with n vertices. Suppose that $r = \alpha d$. Then, the orbit of the motion will have period $4r(n-1)$.*

Proof. Suppose that $r = \alpha d$. Let one *pass* denote the amount of time it takes for the particle to return to the edge it initially started from. During the first $\alpha - 1$ passes, the behavior is described by Lemma 2. The state of the scatterer at any vertex is not flipped. The particle visits each subtree of each non-leaf vertex exactly once during every pass, tracing each edge in the tree twice (once in each direction). So, each pass takes time $2(n-1)$.

During the αth pass, the dynamics is given by Lemma 4. The particle will flip the state of the scatterer at each non-leaf vertex before leaving, but it will still visit each subtree exactly once, so this pass also takes time $2(n-1)$. The next $\alpha-1$ passes behave just like the first ones, except the order of browsing vertices is reversed due to the flipped state of the scatterer at each internal vertex. The next pass will again flip the states of the scatterers at all non-leaf vertices of T, returning them to their original state.

So, we need a total of 2α passes to return the scatterers of the non-leaf vertices to their original states. Because each path visits each leaf of T exactly once, in $2r$ passes the scatterers at the leaves return to their original states. Hence, we need a total of $\text{lcm}\{2r, 2\alpha\} = 2r$ passes. Each pass takes $2(n-1)$ time, so the period has size $2r \cdot 2(n-1) = 4r(n-1)$.

Q.E.D.

This is very similar to a depth-first search behavior. In fact, every pass made by the particle on the tree is just a depth-first search, with the property that the order of browsing the children at a particular vertex is specified by the state of the scatterer at that vertex. Also, the size of the resulting orbit is linear in both n and r.

Our last result of this section concerns the case when $d < r$ and $d \nmid r$.

Proposition 8 ($\alpha \neq 0, \beta \neq 0$) *Consider LGCA with rigidity r on a finite complete d-regular tree $T = (V, E)$ with n vertices. Suppose that $r = \alpha d + \beta$, where $\alpha \neq 0$ and*

$0 < \beta < d$. *Then, the size of the resulting orbit will be at most*

$$\frac{4r^2}{r-2\alpha-1}\left[u^{\log_{d-1}(2r-2\alpha-1)} - u^{\log_{d-1}(2\alpha+1)}\right] \text{ where } u = 1 + \frac{(n-1)(d-2)}{d}.$$

Proof. Due to the symmetry of the problem, WMA that all scatterers at non-leaf sites start out in state 0. We say that the particle *descends on a vertex v using the edge e* if it enters v using the edge e, and leaves v using the same edge e. The particle may actually visit v more than once during a particular descent from the parent of v to v.

Let v be some non-leaf vertex of T. During the first α descents to v, by Lemma 2, the particle increases the state of the scatterer at v by d and leaves using the edge it came from. After these first α descents are complete, the scatterer at v is in the state αd. On the next descent, by Lemma 3, the particle will flip the state of the scatterer, and visit v precisely 2β times before leaving v using the edge it came from. This happens because once the state of the scatterer at v flips, the particle will retrace its path along the subtrees of v, as discussed in the previous section. The next α descents will behave just like the first ones, except the order of browsing vertices is reversed due to the flipped state of the scatterer at v. After the particle leaves v in the last of those descents, the scatterer at v will be in its original state 0.

So, we need $2\alpha + 1$ descents to any non-leaf vertex v from its parent in order to return the scatterer at v to its original state. The root of T is a special case of this, because we will descend on the root from our initial starting edge (note that the first descent onto the root occurs after the subtree of the first child has been already browsed once). To complete the descent on the root $2\alpha + 1$ times from our initial starting edge, we need to perform $2\alpha + 1$ passes on the tree. In that case, the state of the scatterer at the root will not change.

We will now analyze properties of special tree-like structures and then extend the analysis to the whole tree. The structures we consider are subtrees $k \geq 1$ levels deep

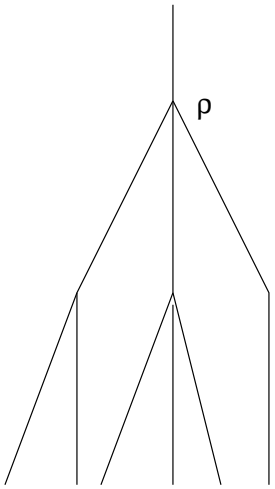

Figure 6: The Structure For Proof Of Proposition 8

(i.e., at least a root and its children that may be leaves), with the edge from the root ρ of the subtree to its parent included in the structure, as is pictured in Figure 6.

Let us examine how the time of browsal of such a structure S_k depends on k. Denote by τ_k the number of descents onto S_k that is necessary for all scatterers in S_k to return to their original states, and let T_k denote the time that these τ_k descents take. Consider S_1 (i.e., a root ρ with $d-1$ leaves, plus one edge going from ρ to its "supposed" parent, which is not a member of S). In a particular case of what we just examined above, the first α descents will increase the degree of ρ by d each. Every one of those passes will visit each edge in T precisely twice (once in each direction), and each descent will take time $2d$. The next pass will visit $\beta-1$ edges twice in each direction, two edges once in each direction (one of them is the top edge, and the other one is the edge to be visited immediately after the state of the scatterer at ρ flips), and the rest ($d-\beta-1$ of them) will not get visited at all. The total time for this descent is then $4(\beta-1)+4=4\beta$. Finally, the last α visits behave just like the first ones. So we need a total of $\tau_1=2\alpha+1$ descents to ρ from its parent to return the scatterer at ρ to its original state of 0. These descents comprise one complete period for the scatterer at ρ. Such a period takes a total time of $T_1=\alpha(2d)+4\beta+\alpha(2d)=4r$.

Now, we examine S_k. Every subtree of the root ρ forms S_{k-1}. We will need $2\alpha+1$ descents from the parent of ρ to ρ in order to return the scatter at ρ to its original state of 0. As before, the first and the last α descents behave similarly, descending onto each substructure exactly once per descent, and tracing the top edge exactly twice per descent. During the flipping descent, the particle descends to $\beta-1$ substructures twice, one substructure once and $d-\beta-1$ substructures are not descended to at all. Therefore, after one period of the root, we have substructures of the following kinds:

- $\beta-1$ substructures descended to $2\alpha+2$ times
- 1 substructure descended to $2\alpha+1$ times
- $d-\beta-1$ substructures descended to 2α times

Each substructure needs exactly τ_{k-1} descents to complete one period for all of its scatterers. Therefore, we need to complete a total of

$$\min\left\{x\in\mathbb{Z}^+\,\middle|\,\frac{(2\alpha+2)x}{\tau_{k-1}}\in\mathbb{Z},\frac{(2\alpha+1)x}{\tau_{k-1}}\in\mathbb{Z},\frac{2\alpha x}{\tau_{k-1}}\in\mathbb{Z}\right\}=\tau_{k-1}$$

periods of the scatterer of ρ. Thus, we need $\tau_k=(2\alpha+1)\tau_{k-1}$ descents onto ρ from its parent for the whole structure to complete one period. So, $\tau_k=(2\alpha+1)\tau_{k-1}$, with $\tau_1=2\alpha+1$. Thus, $\tau_k=(2\alpha+1)^k,\ \forall\ k\in\mathbb{Z}^+$.

We now compute T_k. Notice that in one period of our structure, we have

- $\beta-1$ substructures go through $2\alpha+2$ periods
- 1 substructure goes through $2\alpha+1$ periods
- $d-\beta-1$ substructures go through 2α periods

So, there is a total of $(\beta-1)(2\alpha+2)+(2\alpha+1)+2\alpha(d-\beta-1)=2r-2\alpha-1$ periods of lower substructures, each of which takes T_{k-1} time. In addition, the top edge is being browsed $\tau_k=(2\alpha+1)^k$ times in each direction. Thus,

$$T_k=(2r-2\alpha-1)T_{k-1}+2(2\alpha+1)^k,\quad \text{with } T_1=4r.$$

Therefore,

$$T_k = \frac{(2r-2\alpha-1)^{k+1} - (2\alpha+1)^{k+1}}{r-2\alpha-1}.$$

Hence, if the original tree T has k levels, then the structures under the root complete one period in $\tau_{k-1} = (2\alpha+1)^{k-1}$ descents that lasts a total time of

$$T_{k-1} = \frac{(2r-2\alpha-1)^{k} - (2\alpha+1)^{k}}{r-2\alpha-1}.$$

The behavior of the root is different than at the regular vertex, since there is no top edge to the parent. The first α passes on T descend into each substructure exactly once. During the flipping pass, $\beta - 1$ substructures get descended to twice, two (the first one and the last one visited on the pass) get visited once, and the rest don't get visited. The following α passes behave just like the first ones, except the order of browsal of the substructures is reversed. After these $2\alpha+1$ passes on T, the scatterer at the root of T completes exactly one period. Just as before, in this period, we have some structures that were descended to 2α times, some, $2\alpha+1$ times, and some, $2\alpha+2$ times. Each substructure needs precisely $\tau_{k-1} = (2\alpha+1)^{k-1}$ descents to complete its period, as we mentioned before. Thus, we need a total of $(2\alpha+1)^{k-1}$ periods of the root, or exactly $(2\alpha+1)^k$ passes on T to simultaneously return scatterers at all non-leaf vertices of T to their original states.

Now, let us calculate how much time this will take. We have

- $\beta - 1$ substructures go through $2\alpha + 2$ periods
- 2 substructures go through $2\alpha + 1$ periods
- $d - \beta - 1$ substructures go through 2α periods

In total, we have $(\beta-1)(2\alpha+2) + 2(2\alpha+1) + 2\alpha(d-\beta-1) = 2r$ periods, each one taking the time T_{k-1}. Therefore, one period of all non-leaf vertices of T takes total time $\frac{2r}{r-2\alpha-1}[(2r-2\alpha-1)^k - (2\alpha+1)^k]$. Thus, T will have an orbit of length at most $\frac{4r^2}{r-2\alpha-1}[(2r-2\alpha-1)^k - (2\alpha+1)^k]$.

By Lemma 5, $k = \log_{d-1}(1 + \frac{(n-1)(d-2)}{d})$. Thus, the orbit of T is of size

$$\frac{4r^2}{r - 2\alpha - 1}[u^{\log_{d-1}(2r-2\alpha-1)} - u^{\log_{d-1}(2\alpha+1)}], \text{ where } u = \frac{n(d-2)+2}{d}.$$

Q.E.D.

It is clear from the last proposition that LGCA with rigidity r on a finite complete d-regular tree $T = (V, E)$ with $r = \alpha d + \beta$ where $\alpha \neq 0$ and $\beta \neq 0$ evolves in an orbit of polynomial size in n for constant r and of polynomial size in r for constant n.

4.1.3 Arbitrary Trees

Now consider LGCA with rigidity r on an arbitrary tree $T = (V, E)$ with $n < \infty$ vertices. Recall that $\Delta(T)$ denotes the maximum degree of T, and let $\delta(T)$ denote the minimum *non-leaf* degree of T. The following corollary is a straight-forward generalization of Proposition 6.

Corollary 9 *Consider LGCA with rigidity $r \geq 2$ on a finite tree T with n vertices. Suppose that $\delta(T) > r$. Then, the orbit of the motion will have size $O(rn^{\log_{\delta(T)-1}(2r-1)})$.*

Observe that in the special case $r = 1$, which is just the flipping scatterer model (Langton's Ant), the upper bound established in our proof in the preceding section also holds [34].

The corollary holds because for a rigidity r we cannot use more than $r+1$ neighbors at each vertex. Since $\delta(t) > r$, the particle must use exactly $r+1$ subtrees at each non-leaf vertex, in exactly the same fashion as it did under the conditions of Proposition 6.

Generalization of Proposition 7 is also simple.

Corollary 10 *Consider LGCA with rigidity r on a finite tree $T = (V, E)$ with n vertices. Suppose that $\forall\ v \in V, \deg(v) \mid r$. Then, any orbit will have size $4r(n-1)$.*

Proof. Suppose $\forall\ v \in V, \deg(v) \mid r$. Then, during each pass, every subtree of each non-leaf vertex is browsed exactly once, just like in Proposition 7. So, each pass takes $2(n-1)$ time, since the particle traverses each edge twice (once in each direction). In addition, during each pass, the state of the scatterers at the leaves is incremented by 1 and the state of the scatterer at any non-leaf vertex v is incremented by $\deg(v)$. Thus, to return the leaves to their original state, we need $2r$ passes. After $2r$ passes each non-leaf vertex v will be returned to its original state because it will change state precisely $2 \cdot \frac{r}{\deg(v)}$ times, which is an even number because $\deg(v) \mid r$ by our assumption.

Q.E.D.

Now we will generalize Proposition 8. Consider a LGCA model on a tree T as described in the beginning of this section. In addition, assume that $\Delta(T) < r$. Let us try to measure the length of the resulting orbit. Just as before, we count the number of passes the particle needs to make on the tree in order to make sure that the scatterer at every node returns to its original state.

Consider a structure, similar to S_k that was examined in the proof of Proposition 8. The only difference will be that now the degrees of non-leaf vertices don't have to be the same. Now, if the structure has one level, and the root ρ has degree d_ρ, then the situation is just like in the analogous case of Proposition 8. Let α_ρ and $\beta_\rho < d_\rho$ be positive integers such that $r = \alpha_\rho d_\rho + \beta_\rho$. Then, for one-level structure to complete one period, we need $2\alpha_\rho + 1$ descents to ρ from the parent of ρ, and this period takes time $4r$.

The situation changes a little when we have $k > 1$ levels. Then, we must have $d_\rho - 1$ substructures, each of which needs $t_i, i = 1, 2, \ldots, d_\rho - 1$ descents from ρ to that substructure to go through one period (this quantity corresponds to τ in the proof of Proposition 8). The period of such a structure will take time $T_i, i = 1, 2, \ldots, d_\rho - 1$. We will now compute the total number t of descents from the parent of ρ to ρ,

necessary for the structure to go through one period, and the total time T this period would take.

As before, there exist positive integers α_ρ and $\beta_\rho < d_\rho$ such that $r = \alpha_\rho d_\rho + \beta_\rho$. Then, every $2\alpha_\rho + 1$ descents to ρ using the top edge, the scatterer at ρ goes through one period, which we call the *period of the scatterer at* ρ. In this one period of the scatterer at ρ,

- the substructures $1, 2, \ldots, \beta_\rho - 1$ have been visited $2\alpha_\rho + 2$ times,
- the substructure β_ρ has been visited $2\alpha_\rho + 1$ times,
- the substructures $\beta_\rho + 1, \beta_\rho + 2, \ldots, d_\rho - 1$ have been visited $2\alpha_\rho$ times.

To restore the scatterers for the whole subtree rooted at ρ to their original states, we need to make sure that $\frac{(2\alpha_\rho+2)x}{t_i}$, $\frac{(2\alpha_\rho+1)x}{\tau_{\beta_\rho}}$ and $\frac{2\alpha_\rho x}{t_j}$ are all integers for all $1 \le i < \beta_\rho$ and $\beta_\rho < j < d_\rho$. That means we need

$$X = \min\left\{ x \in \mathbb{Z}^+ \,\middle|\, \left\{\frac{(2\alpha_\rho+2)x}{t_i}\right\}_{i=1}^{\beta_\rho-1} \cup \left\{\frac{(2\alpha_\rho+1)x}{\tau_{\beta_\rho}}\right\} \cup \left\{\frac{2\alpha_\rho x}{t_j}\right\}_{j=\beta_\rho+1}^{d_\rho-1} \subset \mathbb{Z} \right\}$$

periods of the scatterer at ρ. So we need $t = (2\alpha_\rho + 1)X$ descents from the parent of ρ to ρ, necessary for the structure to go through one period. This takes a total time of

$$T = X\Big[\sum_{i=1}^{\beta_\rho-1} \frac{(2\alpha_\rho+2)T_i}{t_i} + \frac{(2\alpha_\rho+1)T_{\beta_\rho}}{t_{\beta_\rho}} + \sum_{i=\beta_\rho+1}^{d_\rho-1} \frac{2\alpha_\rho T_i}{t_i} + 2\Big].$$

Then, the average time per descent in a substructure is T/X.

To be able to use the above recurrences to compute T and t for the whole tree, these need to be slightly modified because the root does not have a top edge coming into it. We still have to have X passes on the tree for the scatterer at the root of T to complete one cycle. Now, however,

$$T = X\Big[\frac{(2\alpha_\rho+1)T_1}{t_1} + \sum_{i=2}^{\beta_\rho} \frac{(2\alpha_\rho+2)T_i}{t_i} + \frac{(2\alpha_\rho+1)T_{\beta_\rho+1}}{t_{\beta_\rho+1}} + \sum_{i=\beta_\rho+2}^{d_\rho} \frac{2\alpha_\rho T_i}{t_i}\Big]$$

and the average time per pass is T/X. In addition, the average time per pass and the average time per descent on any level are integers.

4.1.4 Examples.

Consider now some examples of trees of arbitrary degree. Our goal is to compute the length of the period that all orbits on T have.

Linear Growth of the Degree. Consider first an even number $r > 3$. The tree T will have $\frac{r}{2}+1$ children at the root, each of these will have $\frac{r}{2}+2$ children, and the degree will continue growing linearly at every level, until the vertices on level $\frac{r}{2}-1$ will have degree $r-1$ and their children will be leaves (i.e., have degree 1).

Let's examine a structure just like S_k in Proposition 8. For any degree of the root of the structure, $\alpha = 1$. In S_1, the root has degree $r-1$. Thus, $\beta = 1$. As in the proof of Proposition 8, we'll have $\tau_1 = 2\alpha + 1 = 3$ and $T_1 = 4r$.

For any other level i, $\deg\rho = r - i, \beta = i$. We always need $\tau_i = 3^i$ descents onto the root ρ from the top edge for the structure to complete one period. In this period, $i-1$ substructures will go through 4 periods, one substructure will go through 3 periods and the rest $(r-2i-1)$ of the substructures will go through 2 periods. Thus, the structure will go through $4(i-1)+3+2(r-2i-1) = 2r-3$ total periods of time T_{i-1} each. The top edge will get browsed τ_i times in each direction. Thus, $T_i = (2r-3)T_{i-1} + 2\cdot 3^i$. Solving this recurrence yields $T_i = \frac{(2r-3)^{i+1}-3^{i+1}}{r-3}$.

At the top level, this will be slightly different. The root has $\frac{r}{2}+1$ substructures of level $\frac{r}{2}-2$. We have to have $3^{r/2-1} = \frac{1}{3}\sqrt{3^r}$ passes on the tree. In summary, we will go through $2r$ substructure periods of time $T_{\frac{r}{2}-2}$ each. We need to repeat the procedure $2r$ times to make sure the leaves also return to their original state. Therefore, one period of the tree T will have size

$$4r^2 T_{\frac{r}{2}-2} = \frac{4r^2}{r-3}[(2r-3)^{\frac{r}{2}-1} - 3^{\frac{r}{2}-1}].$$

Linear Decay of the Degree. Now let $r > 3$ be even, but the tree T will have $r-1$ children at the root, each of these will have $r-2$ children, and the degree will

continue decaying linearly at every level, until the vertices on level $\frac{r}{2}-1$ will have degree $\frac{r}{2}+1$ and their children will be leaves (i.e., have degree 1).

As previously, we examine a structure like S_k in Proposition 8. For any degree of the root of the structure, $\alpha = 1$. In S_1, the root has degree $\frac{r}{2}+1$. Thus, $\beta = \frac{r}{2}-1$. As in the proof of Proposition 8, we'll have $\tau_1 = 2\alpha + 1 = 3$ and $T_1 = 4r$.

For any other level i, $\deg\rho = \frac{r}{2}+i, \beta = \frac{r}{2}-i$. We always need $\tau_i = 3^i$ descents onto the root ρ from the top edge for the structure to complete one period. In this period, $\frac{r}{2}-i-1$ substructures will go through 4 periods, one will go through 3 periods and the rest ($2i-1$ of them) will go through 2 periods. Thus, we will have exactly $4(\frac{r}{2}-i-1)+3+2(2i-1) = 2r-3$ total periods of time T_{i-1} each. The top edge will get browsed τ_i times in each direction. Thus, $T_i = (2r-3)T_{i-1} + 2\cdot 3^i$. This is the same recurrence as for the linear growth example. Solving this recurrence yields $T_i = \frac{(2r-3)^{i+1}-3^{i+1}}{r-3}$.

Again, the top level will be slightly different. The root has $r-1$ substructures of level $\frac{r}{2}-2$. We have to have $3^{r/2-1} = \frac{1}{3}\sqrt{3^r}$ passes on the tree. In total, we will go through $2r$ substructure periods of time $T_{\frac{r}{2}-2}$ each. We need to repeat the procedure $2r$ times to make sure the leaves also return to their original state. So, one period of the LGCA on the tree T with finite rigidity r will have length

$$4r^2 T_{\frac{r}{2}-2} = \frac{4r^2}{r-3}[(2r-3)^{\frac{r}{2}-1} - 3^{\frac{r}{2}-1}].$$

This period is the same for the linear growth model. Also, the number of vertices in the tree is exactly

$$n = \left(\frac{r}{2}+1\right)\times\left(\frac{r}{2}+2\right)\times\ldots\times(r-1) = \frac{(r-1)!}{(r/2)!}.$$

Since $(r/2+1)^{r/2-1} \le n \le (r-1)^{r/2-1}$ and the period of the orbit of the particle has size $\Theta(r(2r-3)^{r/2-1})$, the period is super-linear and sub-quadratic in the number of vertices of the tree in both the linear growth and linear decay cases.

4.2 Rigidity Models on Infinite Trees With Back-Scattering

Now we will consider a more general setting, with the particle moving on a tree possibly containing some rays. In the case when the underlying tree has no leaves, in the arbitrary rigidity model with right and left scatterers, the particle with each step propagates further and further away from the root in any initial configuration. This is the reason to consider a different type of scatterer. With the usual *to left* and *to right* states of the scatterer at any vertex of the tree, we will also allow back scatterers by introducing the state *back*. We will now have $\phi : V \to \{L, R, B\}$. If the particle enters a vertex v using the edge e, and the $\phi(v) = B$, the particle will leave the vertex v using the edge e, i.e., using precisely the edge that was originally used to enter v.

We discuss models of two types. In the first type, we will only allow the states of the scatterers *back* and *to right* (by symmetry, if we allow the states *back* and *to left*, the results would be identical). In the second type of the model, we will allow the scatterer at any vertex to be in one of the three states: *to left*, *to right* or *back*. For either kind of model, we consider models with fixed environment, flipping models and models with arbitrary finite rigidity.

4.2.1 The Fixed Scatterer Model

In this case, models of both type exhibit identical behavior, so we will analyze the more general system, allowing scatterers on vertices to be in any of the three states *to left*, *to right*, *back*.

Proposition 11 (Depth-First Search Behavior On Subtrees) *Consider the dynamics of a non-flipping LGCA model with right, left and back scatterers on an infinite tree $T = (V, E)$. Construct a new tree T' by removing from the subtrees of every vertex v with $\phi(v) = B$. Then, the particle will perform a depth-first search on the*

tree T', where the order of visiting children at every vertex v will be right-to-left if $\phi(v) = R$, and left-to-right if $\phi(v) = L$.

Proof. If for some $v \in V$ we initially have $\phi(v) = B$, this is equivalent to simply removing all of the subtree, rooted at v, from the tree T, and changing the state of the scatterer at the vertex v to the state *to right*. Thus, we can effectively eliminate all of the back-scatterers from consideration. We end up with a fixed-scatterer model on a (possibly infinite) tree. Then, by Proposition 4, the particle will perform a depth-first search on T.

If there are no rays (i.e., if T is a finite tree), we get exactly the behavior and the results of Section 3.5. However, if T is infinite, then over the course of time the particle will move farther and farther away from the root along the first ray that it encounters. The speed with which particle will be moving away from the root depends on how bushy the tree T is in the direction of that ray. For example, the maximum is unit velocity, i.e., one edge per unit time, and that occurs if the first subtree encountered by the particle has no leaves (i.e., paths in all directions of the subtree have infinite length). Otherwise, the speed may decrease.

Q.E.D.

Corollary 12 *Consider the dynamics of a LGCA with fixed environment with right, left and back scatterers on an infinite tree $T = (V, E)$ with some rays not containing any vertices with back-scatterers. Then, the particle will eventually propagate in the direction of the first such ray it encounters.*

This is a natural extension of the one-dimensional case [19]. There, the particle will propagate in one direction as long as no back-scatterers are encountered. A pair of back scatterers will make the one-dimensional integer lattice behave like a finite set of points, in the same way as in our case we can place back-scatterers to cover all possible rays, forcing the dynamics to be like the dynamics on a finite tree.

Also, it follows that if $\phi(v) = R, \forall\ v \in V$, then the particle will perform a depth-first search on the tree T.

4.2.2 The Flipping Scatterer Model

4.2.2.1 Two-State Scatterers

In this section, we consider the flipping scatterer model on the tree $T = (V, E)$ as in the previous section. First, we will examine the models with only two possible scatterer states, *back* and *to right*. The state of the scatterer $\phi : V \to \{R, B\}$ depends on time. So we denote the state of the scatterer at $v \in V$ at some time $t \in \mathbb{N}$ by $\phi_t(v)$.

Proposition 13 *Consider the dynamics of a flipping LGCA model with right and back scatterers on an infinite tree $T = (V, E)$. Then, due to a blocking pattern, the particle will eventually propagate along the first ray that it encounters.*

Proof. First we will analyze the local behavior of this model. Suppose the particle is moving on some edge e from the parent p to the child c, visiting c for the first time at time t. The scatterer at p can be either *back* or *to right*, and that is the opposite from what it was before p was entered immediately before proceeding to e. The state of the scatterer then could not have been *back* since the particle proceeded towards e instead of returning one level closer to the root of T. Thus, after the particle passed p, $\phi(p)$ flipped, and so now $\phi(p) = B$. Trivially, c is either a leaf or not. Also, either scatterer at c is in the state *back* or in the state *to right*.

Case I. c is a non-leaf vertex with a *to right* state of the scatterer.
Then, the particle proceeds to the right child of c, say v, and change the scatterer state at c to *back*. This is just like the situation we had before, except one level down in the tree T.

Case II. c is a non-leaf vertex with a *back* state of the scatterer.

Then, the particle goes back to p on the edge e, changing the state of the scatterer at c to $\phi(c) = R$. Since $\phi(p) = B$, after the particle hits p it has to re-trace e again, and now reach c with $\phi(c) = R$. As in the previous case, the particle changes the state of that scatterer to *back* and proceeds to the rightmost child of c. Thus, we again have the same situation, but now the particle propagates one level, recreating the preceding situation in three steps, instead of one step in the previous case.

Case IIIa. c is a leaf, but not the rightmost child of p.

Then, the particle will reach c and back-trace itself on the edge e, independently of the state of c. Now, the particle will reach p, where the scatterer is in the state *back*, and will have to again trace e towards c, changing the scatterer at p to the state *to right*. Finally, the particle will each c, re-trace the edge e towards p for the second time, and then turn to the edge, leading to the next to the right child of p, changing the scatterer at p to the state *back*. This is again a re-creation of the same situation, but this time, the particle propagated to the next to the right edge, outgoing from p.

Case IIIb. c is the rightmost child of p.

In this case, the dynamics will be identical to case IIIa, except instead of leaving towards the next to the right child of p, the particle leaves towards the parent of p, say π, on the tree T (in the special case when p is the root of T and has no parent, the particle propagates towards the left-most child of p). By a logic similar to the one we applied for p, the scatterer at π has to be in the state *back*. Thus, the particle goes from p to π, then back to p and then back to π, finally turning to the next to the right child of π, or proceeding up the tree towards the root in the case p is the rightmost child of π. This is a propagation up one level and to the right.

WLOG, we can to start the particle at the left-most edge of the root, and set the initial state of the root to be *back*. It is easy to see that the particle will start at the

left-most subtree of the root, and will explore all of the subtrees right-to-left, until it finds the one with a ray, and it will propagate on this ray with random velocity (depending only on the initial distribution of the scatterers and the structure of the underlying tree) due to a blocking pattern, described in the cases I and II above.

Q.E.D.

Like Corollary 12, this result is also similar to the corresponding one-dimensional model [42], where the blocking pattern leads to infinite propagation of the particle, as we proved for our more general case in Proposition refproposition:InfTreeRBPropag.

The evolution of this model is very similar to a depth-first search, with the exception that some edges may be repeated (this happens in Case II, where an edge must be traced three times instead of one, to take care of back scatterers at both ends of the edge). The result we get is in a sense similar to the one for models with fixed environment, containing scatterers of any type. However, here the particle always finds the rightmost ray, independently of the initial distribution of the scatterers and propagates along it at a slower pace than the propagation of the previous section, due to repetition necessary in Case II of the argument. In the preceding section, however, the ray along which propagation will occur depends on the initial distribution of the scatterers, and it is possible to consider a dynamics on an infinite tree and get a periodic trajectory (if all the rays have back-scatterers on them), while in the case we considered here, such situation cannot occur. In other words, if the underlying tree is infinite, the particle will propagate along the rightmost ray, independently of the distribution of the scatterers.

4.2.2.2 Three-State Scatterers

In this section, we consider the same dynamics as above, except the scatterers at the vertices of the underlying graph are allowed to be in one of the three states: $to\ left, to\ right$ and *back*. Due to symmetry, we may assume that transitions take

place in the same order, i.e., *to left* gets changed to *to right*, then *to right* changes to *back* and then *back* changes to *to left*. The motion of the particle in this case turns out to be similar to the case where no back-scatterers would be present. Recall that in this situation ($r = 1$ without back-scattering), the dynamics is time-reversible and the particle always stays on the same unique path between two leaves on both sides of the root. As it turns out, the back-scatterers prevent the dynamics from being time-reversible, but the second property holds.

Proposition 14 *Consider the dynamics of a flipping LGCA with left, right and back scatterers on a tree $T = (V, E)$ with some paths of infinite length. Then, the orbit of the particle is a path in T.*

Proof. It suffices to prove that for all non-leaf $v \in V$, there are at most two edges adjacent to v that are in the trajectory of the particle.

First let us look at the non-leaf non-root vertices visited by the particle. The first time such a vertex v is visited, say t, the particle comes along the unique root-to-v path in T, using the edge e from v to the parent of v in the tree. If $\phi_t(v) = B$, then the particle flips the state of the scatterer at v to $\phi_{t+1}(v) = L$ and leaves using the edge e it came from. In this case, only one edge adjacent to v was used.

If $\phi_t(v) = L$, the particle proceeds to the left child c of v. The scatterer at v is also changed to the state *to right*. When the particle returns to v, we see that it must return using the same edge $\{c, v\}$ that it used to leave v. When it arrives at v, the scatterer at v is in the state *to right* and the particle changes it to *back* and leaves using the edge e. At the next visit of the particle to v, it will come along e and leave along e, as described above, changing the scatterer at v to the state *to left*, thus returning v to its original position.

Finally, if we have $\phi_t(v) = R$, the particle proceeds to the right child c of v, and $\phi_{t+1}(v) = B$. Now when the particle returns to v, we see that it must return using

the same edge $\{c, v\}$ that it used to leave v. When it arrives at v, say at time τ, we have $\phi_\tau(v) = \phi_{t+1}(v) = B$. So, the particle changes it to *to left* and leaves using the edge $\{c, v\}$. At the next return of the particle to v, the particle flips the state of the scatterer from *to left* to the state *to right* and leaves using the edge e, thus returning v to its original position. Again, the particle used two edges adjacent to v, one of which coincides with the one used in the preceding case.

So it only remains to take care of the root. But exactly the same thing happens to the root as to the other non-leaf vertices, except the edge to the right-most child of the root plays the role of the edge e above. The only difference is, if the original path from the root is of infinite length, the particle may never visit the root except for the initial position of the particle.

Q.E.D.

Let S be the subtree of the root, in which the particle begins its motion. Rising from the subtree S towards the root, let S_R and S_L denote the next to the right and next to the left subtrees of the root. Suppose that the tree T has two leaves u, v, such that $u \in S$ and $v \in S_L$ and ancestors of u, v on all levels above 1 (grandchildren of the root and further) are either right-most or left-most children of their parents (if the scatterer states flip from *to right* to *to left* and then to *back*, let $v \in S_R$). Then, the probability that the trajectory of the particle is finite is strictly positive; such a situation happens when it will always stay on the unique $u \to v$ path in T.

Hence, even on a tree with infinitely many rays we can have a periodic orbit. This is very different from the model with only two scatterer types, where the existence of even one ray in T forces the particle to propagate.

4.2.3 The Case of Arbitrary Finite Rigidity

4.2.3.1 Two-State Scatterers

Lemma 6 *Consider the dynamics of a LGCA with* $1 \leq r < \infty$ *and with right and back scatterers on a tree* $T = (V, E)$*. Let* $v \in V$ *be such that the subtree of* T *rooted at* v *is finite. If the particle visits one child of* v*, then the particle will visit every child of* v*. If* v *is not the root of* T*, then every child of* v *is visited before the particle returns to the parent of* v*.*

Proof. Let $v \in V$ and suppose the particle at some time t visits one child c of v. Then $\phi_{t-1}(v) = R$ (otherwise we must have $\phi_{t-1}(v) = B$, which contradicts the fact that the particle was at c, a child of v, at time t). Then, the particle proceeds to c, which must be the right child of v. After returning from that subtree, it will again turn to the next child of v on the right, just like a depth-first search. This will continue until we either run out of children of v (so we are done) or until the scatterer at v flips to the state *back*. Since the subtree rooted at v is finite, the particle will return to v sufficiently many times to flip the scatterer at v to the state *to right*, and then again proceed to explore the next child of v to the right. Thus, eventually, every child of v will be explored.

Finally, it is clear that if v is not the root, then the parent of v will be visited only after all the children of v have been visited.

Q.E.D.

Proposition 15 *Consider the dynamics of a LGCA with finite rigidity and right and back scatterers on an infinite tree* $T = (V, E)$*. Then,* $\forall\ n \in \mathbb{N}\ \exists\ t \in \mathbb{N}$ *such that at time* t *the particle will be further from the root than* n*.*

Proof. Let $\mathcal{O}$ denote the orbit of the particle. It suffices to show that $|\mathcal{O}| = \infty$. Suppose that $|\mathcal{O}| < \infty$. Then, it has a (not necessarily unique) vertex with smallest

positive distance to the root, say u. Because u is in the orbit, it is visited by the particle infinitely often. Hence, if u has a parent in the tree, say p, then p is also visited infinitely often. If p is not the root of T, this contradicts u being the vertex in $\mathcal{O}$ with the smallest distance to the root, since $p \in \mathcal{O}$ and it is closer. So, p must be the root of T. Hence, the root of T is in $\mathcal{O}$.

By Lemma 6, $\mathcal{O}$ contains the root and all of its children. Also, every vertex in $\mathcal{O}$ will be visited infinitely often, so all of the paths from the root of T down along $\mathcal{O}$ terminate in the leaves of T.

We know T is infinite, so it contains at least one ray, say L. Because $\mathcal{O}$ contains all of the children of the root, and vertices of $\mathcal{O}$ maximally away from the root of T are all leaves, there has to be the vertex $v^* \in \mathcal{O} \cap L$ that is furthest away from the root of T. Then, since $v^* \in L$, we know v^* has children in T. So at least one of the children of v^* must be in $\mathcal{O}$. But by Lemma 6, we know that all children of v^* are in $\mathcal{O}$. This contradicts the maximality of v^*, since there is a child of v^* lying in L.

Q.E.D.

4.2.3.2 Three-State Scatterers

We consider the cases of arbitrary rigidity r of the system, where the scatterers can be in one of the three states: $to\ right, to\ left, back$. The situation here, just as in the finite case we studied above, will depend on the number of children at each node. We will first discuss the local behavior. We allow any cyclic kind scheme for changes in the states of the scatterers. For example, $to\ left \rightarrow to\ right \rightarrow back$ is a valid scheme, and $back \rightarrow to\ left \rightarrow back \rightarrow to\ right$ is not a valid scheme. Let I_v be the indicator variable of the event "if the scatterer at v flips, it's next state is *back*." (i.e., in that case $I_v = 1$ and otherwise $I_v = 0$.)

Lemma 7 *Suppose a particle descends into the vertex v of a finite tree T, with the scatterer at v in the state $to\ left$ or $to\ right$. Suppose in addition that v in its current*

state has been visited less than $r - \deg v$ *times. Then, every child of* v *will get visited and the state of the scatterer at* v *will not get flipped.*

Proof. Consider a particle moving away from the root of the tree to some vertex v. If the scatterer at v is in the state $to - back$, the particle undergoes a reflection at v, increasing the number of visits to v by one until the scatterer state flips. If the scatterer at v is $to\ right$ or $to\ left$, the particle proceeds to the subtree, rooted at v and explores the subtrees rooted at the children of v. Now, the analog of Lemma 2 is the same as the original, in other words, the scatterer is not flipped and the particle visits all subtrees, rooted at the children of v.

Q.E.D.

Similarly, an analog of Lemma 4 holds in almost the same fashion.

Lemma 8 *Suppose a particle descends into the vertex* v *of a finite tree* T*, with the scatterer at* v *in the state to* $left$ *or to* $right$*. Suppose in addition that* v *in its current state has been visited exactly* $r - \deg v$ *times. Then, every child of* v *will get visited and the state of the scatterer at* v *will get flipped.*

Finally, our next result will be similar to Lemma 3. Here, if there is sufficient number of children to flip the scatterer state, and the vertex v was visited k times in its current scatterer state, then the particle will visit $r - k + 1$ children of v twice, one child of v exactly $1 + I_v r$ times, and will not visit any other child of v, since the direction of exploration of children of v will be reversed once the scatterer at v flips state. Lastly, the particle will leave the scatterer at v in the state opposite to the one it was found in.

Lemma 9 *Suppose a particle descends into the vertex* v *of a finite tree* T*, with the scatterer at* v *in the state to* $left$ *or to* $right$*. Suppose in addition that* v *in its current*

state has been visited exactly $k > r - \deg v$ *times. Then, the particle will visit* $r - k + 1$ *children of* v *twice, one child of* v *exactly* $1 + I_v r$ *times, and will not visit any other child of* v*. After the particle has left from* v *to the parent of* v*, the scatterer at* v *will be in the opposite state from the one originally seen by the particle.*

Either way, if every vertex of T satisfies the conditions of Lemma 7 or Lemma 8, then clearly every root-to-leaf path will be found and traced, and so if there is one of infinite length, then eventually the particle will be at an infinite distance from the root of T.

Corollary 16 *Consider the dynamics of a LGCA on a tree* T *with some paths of infinite length, such that* $\Delta(T) \leq r$*. In that case,* $\forall\ n \in \mathbb{N}, \exists\ t \in \mathbb{N}$*, such that at time* t *the particle will be further from the root of* T *than* n*.*

CHAPTER V

RIGIDITY MODELS ON $\mathbb{Z}$

5.1 Background

5.1.1 Notation And Basic Definitions

Even though the models discussed in this chapter are more general than Langton's ant [52], we will adopt the terminology of that model, and sometimes will refer to the moving particle in LLGCA as the "ant." Following [37], we define the ant as an arrow over a cell, pointing in some direction. The position of the ant at time t is denoted $X(t)$. If the arrow points to the right, we have $v(t) = +1$. Otherwise, we have $v(t) = -1$. The state of the scatterer at the cell affects the ant position and velocity (pointing direction of the arrow). This state is indicated by a either white or black color of the cell. We write $\phi(n)$ for the state of the scatterer at the site n. We have four different possible scattering rules for each vertex.

Recall that a collection of states of the scatterers over the entire $\mathbb{Z}$ lattice at any fixed time is called a *configuration*. Any configuration, in which some color is encountered only on a finite amount of cells is said to have *finite support*. Any initial distribution of colors that results in an initial configuration with finite support with positive probability is called a *degenerate distribution*. For each cell n, we assume that the initial distribution of $\phi(n)$ is Bernoulli denoting

$$p = Prob[\text{a cell is white}] \quad \text{and} \quad q = 1 - p = Prob[\text{a cell is black}]$$

Finally, a sequence of alternating black and white cells is called a *checkered pattern*, and a sequence of cells of the same color of length at least 2 is called a *block*.

5.1.2 Definitions of Scattering Rules

We illustrate how the scattering rules work by an example. Suppose $X(t) = n$. In the case $\phi(n) = 0$, we have $X(t+1) = n + v(t)$ and $v(t+1) = v(t)$. This is called a *forward scattering rule*. In the case $\phi(n) = 1$ (*back scattering rule*), we have $X(t+1) = n - v(t)$ and $v(t+1) = -v(t)$. Next, if $\phi(n) = 2$ (*delayed back scattering rule*) we have $X(t+1) = n+v(t)$ and $v(t+1) = -v(t)$. Finally, if $\phi(n) = 3$ (*pushback scattering rule*), $X(t+1) = n - v(t)$ and $v(t+1) = v(t)$. The graphic description of motion is represented in Table 5.1.2.

Table 1: Motion Under Various Scattering Rules

	-1	0	1
$\phi(n)$ at $t = 0$		$\leftarrow$	
0	$\leftarrow$		
1			$\rightarrow$
2	$\rightarrow$		
3			$\leftarrow$

This definition is invariant under reflection, so if the ant initially heads to the right, the movement will be analogous. This leads to the representation of the basic rules of dynamics for the ant, given in Table 5.1.2.

Table 2: Representing Scattering Rules

old color	**new color**	**scattering rule**
black	a	c
white	b	d

In the representation of scattering rules, $a, b \in \{0, 1\}$, with 1 if and only if the ant changes the color of the cell; $c, d \in \{0, 1, 2, 3\}$ represent the scattering rule associated with cells of the specified color. In other words, whenever n is black we have $\phi(n) = c$, and whenever n is white we have $\phi(n) = d$. For example, the usual flipping model

of the LLGCA, studied by Grosfils et al [42], is represented as $\begin{pmatrix} 1 & 0 \\ 1 & 1 \end{pmatrix}$. The motion under this rule is illustrated in Figure 7.

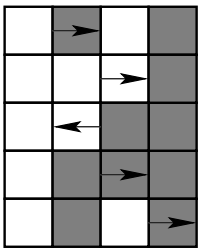

Figure 7: Dynamics Under The Flipping Model

5.1.3 Classification of Scattering Rules

Gajardo [37] studied the situations with $\phi(0) \in \{0, 1, 2\}$ and classified the corresponding rules into classes. The class B includes all models, where the trajectory is bounded with probability 1. In other words, setting any finite amount of cells in the initial configuration will still result in a bounded trajectory. This class is subdivided into two subclasses. $B1$ contains all models, where the particle eventually ends up in a period of 2 or 4, while $B2$ contains models that admit periodic motion of any even cycle.

The class U contains all other models. This way, the models in the class U are always unbounded. If the ant eventually engages in repetitive motion for some finite configuration, this will fall in class $U1$. The class $U2$ contains the rest of the models.

We will keep the same classes, completing the classification of possible scattering rules for our model on the one-dimensional integer lattice.

5.1.4 Equivalence of Scattering Rules

Basically, a complete description of an LLGCA model on $\mathbb{Z}$, consists of the initial position and velocity of the ant, as well as of the type and rigidity of the scatterers

involved. We will call two LLGCA models on $\mathbb{Z}$ *equivalent* if for any initial state of one model, there will be a corresponding initial state in the other model, such that the position of the ant in both models will coincide at every point in time.

Fix any LLGCA model on $\mathbb{Z}$ and consider constructing an equivalent model. It is easy to notice that the only difference between back scatterers and delayed back scatterers, as well as between the forward and the pushback scatterers, is the progression of the ant (either in the direction of $v(t)$ or in the direction of $-v(t)$). Thus, changing a back scatterer into a delayed back scatterer, or a forward scatterer into a pushback scatterer, will preserve the velocity of the ant, but scatter it in the opposite direction. To take care of this difference, we can flip the initial velocity of the particle. So, we have the following result.

Theorem 17 (Construction of Equivalent Models) *Given an initial state of any model of LLGCA on $\mathbb{Z}$, replace all back scatterers with delayed back scatterers (or vice versa), replace all forward scatterers with pushback scatterers (or vice versa) and flip the initial velocity of the ant. The resulting model is equivalent to the original model.*

This limits the total number of models that need to be studied. There are 64 possible model choices. In 16 of them the dynamics is independent of cell color. Then the ant propagates indefinitely or cycles with period two between a pair of consecutive cells. In the remaining 48 models, when the rows of the matrix are interchanged, the new rule has the same behavior as the old one, except with the colors interchanged. Such models are called *dual*, and only one model in the dual pair needs to be studied. Of the remaining 24, we have 4 variations (both fixed scatterers, white flipping and black fixed, black flipping and white fixed, and both flipping scatterers) for each of the 6 possible selections of scatterer types (as there are 6 ways to choose 2 necessary types from 4 available types). Of these choices, there are 4 that result in equivalent models (so only half of them needs to be considered), and

2 that don't (since the construction of the Theorem will result in the same model, e.g., the model with forward and pushback scatterers). Hence, we need to study 4 distinct choices. Effectively, we will need to study only 16 different rules, of which Bunimovich [42] described one and Gajardo [37] considered 12.

5.1.5 How The Logic Gates Are Constructed

We have four different scattering rules, but only two colors are possible for each vertex. So, we will need to select a pair of rules to examine together. For each such selection of two rules on the $\mathbb{Z}$ lattice, we give a construction of AND and NOT logic gates, the minimum gates required to construct Boolean circuits. Thus, for the possibility of using more colors in our system (i.e., allowing more types of scatterers to be present simultaneously on the lattice), the existence of such gates will follow automatically.

The constructions are as follows. The gates will receive input in the form of states of the scatterers at the cell 0 and, if necessary, at the cells ± 1. In the initial state of the system, the ant begins at the cell 0 (i.e., $X(0) = 0$) with $v(0) = +1$. Then, the system is run (i.e., we let the ant travel according to its rules of dynamics) for a fixed period of time, also specified in the construction. This period of time will depend on the selection of the two rules that we are using. The gate will either accept or reject its input. This decision will be based on whether the ant visited or did not visit a certain cell, specified in the construction. At the end of the simulation, the question can be answered by keeping track of the orbit of the ant, so the problem is decidable.

5.2 Forward and Back Scatterers

5.2.1 Construction of Logic Gates

For the construction of the gates, we will use white color for back scatterers and black color for forward scatterers.

For the NOT gate, the input is indicated by the state of the scatterer at 0 in the initial configuration: $\phi(0) = 0$ means the input variable is $TRUE$ and $\phi(0) = 1$ means

the input variable is $FALSE$. All other scatterers are set to be forward scatterers. Now we will simulate the ant's behavior for exactly one step, which is shown in Figure 8 for each possible value of the input variables. We will ask the question *does the ant ever visit cell* -1? In other words, the gate accepts its input if and only if the ant visits cell -1 at some point during the simulation of ant's dynamics.

Observe that $X(1) = -1$ if and only if the scatterer at 0 was a back scatterer (otherwise, $X(1) = 1$). Hence the gate accepts its input if and only if the input variable had value $FALSE$, as desired.

For the AND gate, the input is indicated by the state of the scatterers at 0 and 1 in the initial configuration. All other cells contain forward scatterers. We run the system for 2 steps and ask the question *does the ant ever visit cell* 2? The dynamics of the system for both gates is illustrated in Figure 8.

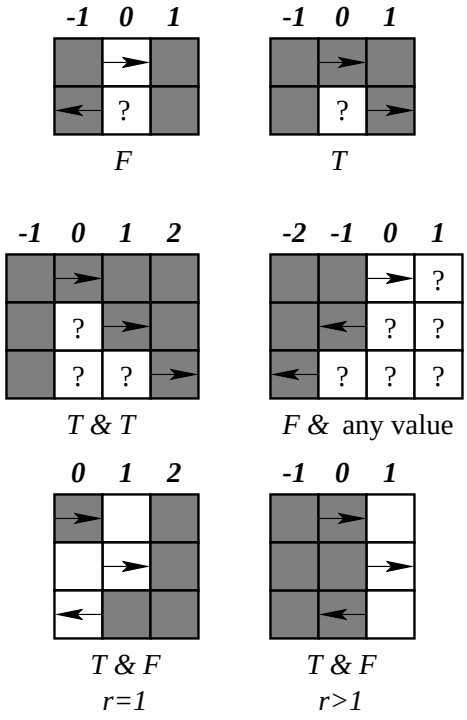

Figure 8: Dynamics Of The Logic Gates For Black Forward And White Back Scatterers

Observe that if both scatterers are forward scatterers, $X(t) = t \forall\ t \in \mathbb{N}$, hence the

gate will accept its input. If $\phi(0) = 1$, then $X(t) = -t \forall\ t \in \mathbb{N}$ and so the input will be rejected since $\mathbb{Z}^+$ is never visited. Lastly, if $\phi(0) = 0$ and $\phi(1) = 1$, the orbit of the particle will look like $(0, 1)$ for any rigidity. Consequently, the gate will reject its input. In summary, the gate accepts its input if and only if both input variables have value $TRUE$, as desired.

5.2.2 Dynamics For Fixed Scatterers

5.2.2.1 Description of Dynamics

This $\begin{pmatrix} 0 & 0 \\ 0 & 1 \end{pmatrix}$ model is also known as the *non-flipping scatterer model* and as the *fixed-scatterer model*. It belongs to the class $B2$ [37]. The local dynamics of this model are pictured in Figure 9.

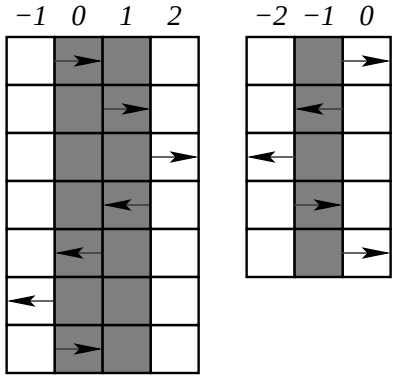

Figure 9: Dynamics Of The Black Fixed Forward Scatterer and White Fixed Back Scatterer Model

Basically, the particle moves in the direction of $v(0)$ until a white cell is encountered at some z_1. Then, the particle moves in the direction of $-v(0)$ until another white cell is encountered at some z_2. Afterwards, the particle oscillates between z_1 and z_2 with unit velocity. This dynamics, as well as the next two results are an easy consequence of Lemma 6 in [37].

Corollary 18 (Periodic Oscillation) *A particle of LLGCA moving on* $\mathbb{Z}$ *according*

to the rule $\begin{pmatrix} 0 & 0 \\ 0 & 1 \end{pmatrix}$ *will end up in a periodic trajectory with probability* 1*, always oscillating with the same amplitude.*

Corollary 19 *Under the conditions of the preceding corollary, assume in addition that* $v(0) = +1$*. Then, the particle does not end up in a periodic orbit if and only if either all* $\mathbb{N}$ *is black or all* $\mathbb{Z}^-$ *is black. In this case, the particle will eventually propagate in one direction (along the black block) with unit speed.*

5.2.2.2 Statistical Properties

Assume $v(0) = +1$. Let $\mathcal{O}$ denote the orbit of the particle. Then,

$$Prob[n \in \mathcal{O}] = \begin{cases} q^n, & n \geq 0 \\ q^{n-1}, & n \leq -1 \end{cases}.$$

Observe that we always have $0, -1 \in \mathcal{O}$, and $1 \in \mathcal{O}$ with probability q. Moreover,

$$\begin{aligned} Prob[n \in \mathcal{O}, (n+1) \notin \mathcal{O}] &= Prob[0, 1, \ldots, n-1 \text{ are black}, n \text{ is white}] \\ &= q^n p, \quad n \geq 0. \\ Prob[-n \in \mathcal{O}, -(n+1) \notin \mathcal{O}] &= Prob[-1, -2, \ldots, -(n-1) \text{ are black}, -n \text{ is white}] \\ &= pq^{n-1}, \quad n \geq 1. \end{aligned}$$

Using these, it is easy to see that the length of the interval to the right of 0 (and to the left of -1, due to symmetry of the problem) is $N - 1$, where N a random variable with a geometric distribution. Hence, the expected length to the right of zero is $1/p - 1$. Therefore, we expect the particle to oscillate between $-1/p$ and $1/p - 1$. Clearly, for $0 \leq p \leq 1$, this interval becomes at most the non-negative grid $\mathbb{N}$ when $p = 0$ (i.e., if all cells are black, then the orbit is the non-negative part of the grid, and we move with unit speed to the right forever), and the minimum expected length occurs at $p = 1$ (i.e., when all cells are white, then particle oscillates between -1 and 0).

Proposition 20 *Under the conditions of the corollary, with probability* 1*, the particle will end up oscillating with constant amplitude. The particle will oscillate in* $[-N, M-1]$*, where* N *and* M *are both independent geometric random variables with mean* $1/p$*.*

Corollary 21 *The expected orbit of the particle is the interval* $[-1/p, 1/p-1]$*.*

5.2.3 Black Flipping Forward Scatterer And White Fixed Back Scatterer

5.2.3.1 Description of Dynamics

This $\begin{pmatrix} 1 & 0 \\ 0 & 1 \end{pmatrix}$ model belongs to the class $B1$ [37]. The dynamics in the case of $r = 1$ is illustrated in Figure 10.

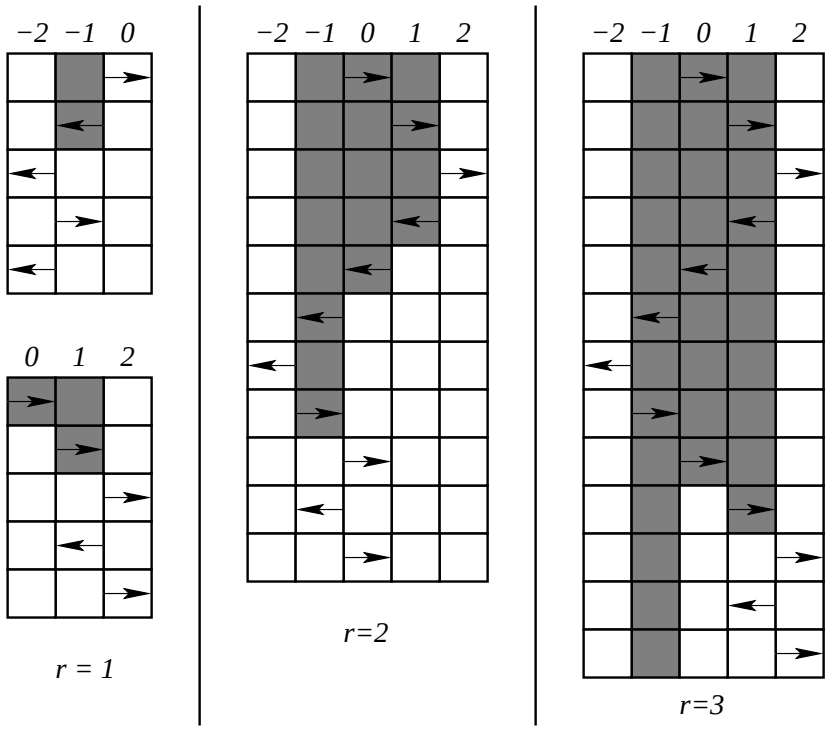

Figure 10: Dynamics Of The Black Flipping Forward Scatterer And White Fixed Back Scatterer Model With $r = 1, r = 2$, and $r = 3$

In the case 0 is black, the particle moves in the direction of $v(0)$ until a white cell $z \geq 1$ is encountered. At this point, the site $z - v(0)$ must be white since it was flipped on the way towards z. Thus, the particle will oscillate with period 2 between

the sites $z-v(0)$ and z. In the case 0 is white, the particle moves once in the direction of $-v(0)$. Now, if the next cell encountered $(-v(0))$ is white, the particle will oscillate between this cell $-v(0)$ and 0 (call this orbit $\mathcal{O}_1$). Otherwise, the particle will move in the direction of $-v(0)$ until a white cell is encountered at some site z. At this point, the particle will oscillate between z and $z+v(0)$.

5.2.3.2 Effects of Odd Rigidity

The effects of odd rigidity on a similar situation (the model $\begin{pmatrix} 1 & 0 \\ 1 & 1 \end{pmatrix}$ on the $\mathbb{Z}$ lattice) have been explored by Bunimovich [17]. Just as in Theorem 1 of [17], the particle will oscillate between the two nearest white cells (one in the direction of $v(0)$, z_+, and one in the opposite direction, z_-), visiting all cells in the direction of $-v(0)$ exactly $r-1$ times, and visiting all cells in the direction of $v(0)$ (including the 0 cell) r times. Eventually, the particle will reach z_+, changing all cells between z_+ and z_- to white. Finally, the particle will oscillate between z_+ and $z_+ - v(0)$, just like in the case of $r=1$ discussed above. This is illustrated for $r=3$ in Figure 10.

Proposition 22 (Periodic Oscillation) *A particle of LLGCA moving on $\mathbb{Z}$ according to the rule $\begin{pmatrix} 1 & 0 \\ 0 & 1 \end{pmatrix}$ with odd rigidity, will eventually end up in a periodic trajectory with period 2 with probability 1. If 0 is white (respectively, black), the particle will oscillate between the extreme site in the direction $-v(0)$ (respectively, $v(0)$) and the site that was visited immediately preceding to it.*

Proof. For $r=1$, the argument is essentially the same as the proof in the first part of Lemma 5 of [37]. If initially $\phi(0)=0$ ($\phi(0)=1$), then the particle moves in the direction of $v(0)$ $(-v(0))$, building behind it a trail of white cells, until the first white cell is encountered. At this point, the particle will oscillate between the first white encountered cell and the cell, visited immediately before it.

in the case $r = 2k + 1$ for some $k \in \mathbb{Z}^+$, the particle will travel in the direction of $v(0)$ until the first white cell is encountered at some z_+, and then will reflect from it, travel until it reaches the 0 cell, and repeat the same process on the other side of the integer lattice, discovering the first white cell at some z_-, and again coming back to 0. On this route, the particle visits every vertex in its orbit exactly two times. The particle will proceed to repeat this route exactly k times. Now, the situation reduces to the analogous case of $r = 1$. In addition, if initially $\phi(0) = 1$, we also know $z_+ = 0$.

Q.E.D.

The set of exceptions, as previously, has measure zero. It is characterized by the following result.

Corollary 23 *Under the conditions of the proposition, assume that $v(0) = +1$. The particle does not end up in a periodic orbit if and only if either all $\mathbb{N}$ is black or all $\mathbb{Z}^-$ is black. In this case, the particle will eventually propagate in one direction with unit speed.*

5.2.3.3 Effects of Even Rigidity

The effects of even rigidity on a similar situation (the model $\begin{pmatrix} 1 & 0 \\ 1 & 1 \end{pmatrix}$ on the $\mathbb{Z}$ lattice) also have been explored by Bunimovich [17]. Just like in Theorem 2 of [17], the particle will oscillate between the two nearest white cells (one in the direction of $v(0)$, z_+, and one in the opposite direction, z_-), visiting all cells between z_+ and z_- exactly r times. Eventually, the particle will reach 0, changing all cells between z_+ and z_- to white. Finally, the particle will oscillate between cells 0 and $-v(0)$. This is pictured in Figure 10 for the case of $r = 2$.

Proposition 24 (Periodic Oscillation) *A particle of LLGCA moving on $\mathbb{Z}$ according to the rule $\begin{pmatrix} 1 & 0 \\ 0 & 1 \end{pmatrix}$ with even rigidity, with probability 1 will eventually end*

up in a periodic trajectory with period 2*, oscillating between* 0 *and* $v(0)$ *(between* 0 *and* $-v(0)$*) if initially* 0 *was black (white).*

Proof. Just like in the dynamics with odd $r > 1$ in the preceding proposition, the particle will travel in the direction of $v(0)$ until the first white cell is encountered at some z_+, and then will reflect from it, travel until it reaches the 0 cell, and repeat the same process on the other side of the integer lattice, discovering the first white cell at some z_-, and again coming back to 0. On this route, the particle visits every vertex in its orbit exactly two times. The particle will proceed to repeat this route exactly k times. At this point, all cells in the orbit have been visited a total of $2k = r$ times (2 times per oscillation for k oscillations), and so all cells in the orbit are now white, meaning that the particle will now oscillate between 0 and 1 (between 0 and -1) if initially 0 was black (white).

Q.E.D.

The set of exceptional initial distributions is common to both even and odd rigidity.

Corollary 25 *Under the conditions of the proposition, assume that* $v(0) = +1$*. The particle does not end up in a periodic orbit if and only if either all* $\mathbb{N}$ *is black or all* $\mathbb{Z}^-$ *is black. In this case, the particle will eventually propagate in one direction with unit speed.*

5.2.3.4 Statistical Properties

Assume $v(0) = +1$. Let $\mathcal{O}$ denote the orbit of the particle.

In the case of rigidity $r = 1$,

$$Prob[n \in \mathcal{O}] = \begin{cases} q^n, & \forall\ n \in \mathbb{N} \\ pq^{n-1}, & \forall\ n \in \mathbb{Z}^- \end{cases} \Bigg\| .$$

Moreover,

$$Prob[n \in \mathcal{O}, (n+1) \notin \mathcal{O}] = pq^n, \quad n \geq 0$$

$$Prob[-n \in \mathcal{O}, -(n+1) \notin \mathcal{O}] = p^2 q^{n-1}, \quad n \geq 1.$$

Therefore, $Prob[\mathcal{O} = \mathcal{O}_1] = p^2$.

Now we calculate the extreme points in the orbit of the particle after it starts traveling in one of the directions. The situation in the positive and negative directions is symmetric. So for simplification, in addition to $v(0) = +1$, assume that 0 is black. Now, the length of the walk of the particle to the right is a geometrically distributed random variable with parameter p. Hence the expected length of this walk is $1/p$. Therefore, we expect the particle to oscillate between $1/p - 1$ and $1/p$. Clearly, over $0 \leq p \leq 1$, the minimum occurs at $p = 1$. In that case, all initial cells are white (except 0, which is black by assumption) – then the particle eventually oscillates between 0 and 1. The maximum occurs at $p = 0$. In that case, all cells are black initially, and the particle moves to the right with unit speed forever.

If we have the case of $r > 1$, then the orbit is the exactly like the orbit for the case of the non-flipping model with the same scatterers, $\begin{pmatrix} 0 & 0 \\ 0 & 1 \end{pmatrix}$. The dynamics, however, is very different. As mentioned in the results above, the particle will eventually always end up in an oscillation of period 2 between consecutive white cells.

5.2.4 Black Flipping Back Scatterer And White Fixed Forward Scatterer

5.2.4.1 Description of Dynamics

The $\begin{pmatrix} 1 & 1 \\ 0 & 0 \end{pmatrix}$ model belongs to the class $U1$ [37]. It is very similar to the model studied quite extensively by Bunimovich [17] and Grosfils, et al [42]. The particle moves in the direction of $v(0)$ until the first black cell is encountered. At the point, the particle reflects off the black cell (flipping it to white) and continues in the direction of $-v(0)$

until the next black cell. The particle continues to oscillate about the origin in this fashion forever, each time increasing the amplitude of oscillation.

5.2.4.2 Effects of Rigidity

In this model, the rigidity of the environment will not make any changes in the overall dynamics of the particle, except influencing the amount of oscillations of the particle between two black cells necessary to flip them. This is contrary to what was found [17] in the case when both types of scatterers are allowed to flip (in the model $\begin{pmatrix} 1 & 1 \\ 1 & 0 \end{pmatrix}$). The dynamics of the model for $r = 1$ and $r = 2$ is pictured in Figure 11.

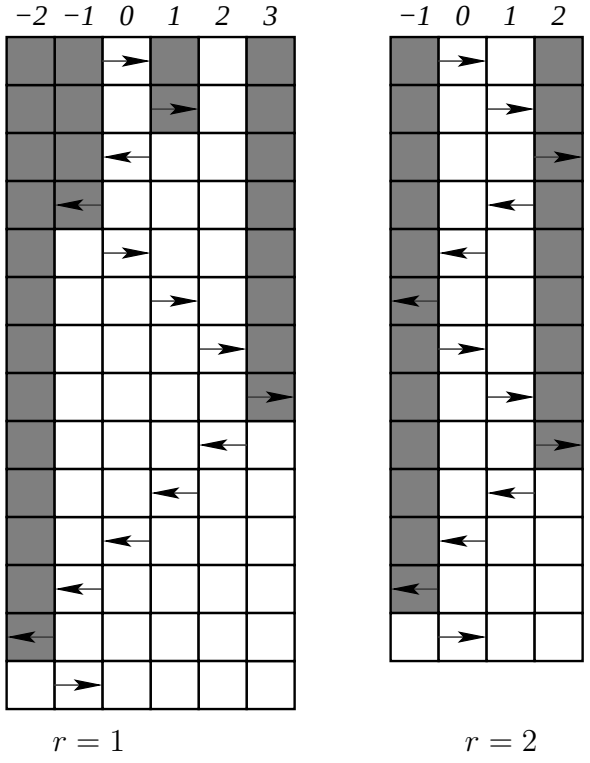

Figure 11: Dynamics Of The Black Flipping Back Scatterer And White Fixed Forward Scatterer Model With $r = 1$ And $r = 2$

Proposition 26 (Oscillation) *If the particle moves on the* $\mathbb{Z}$ *lattice according to the rule* $\begin{pmatrix} 1 & 1 \\ 0 & 0 \end{pmatrix}$ *with arbitrary rigidity, then with probability* 1*, the particle will oscillate*

with non-decreasing amplitude, visiting every site of the lattice infinitely many times.

Proof. Whenever the particle encounters a block of forward scatterers, it moves through them with unit speed. Hence, the particle moves in the direction of $v(0)$ until a back scatterer is encountered. Then, the particle reflects off of the back scatterer, and travels in the direction of $-v(0)$ until a back scatterer is encountered. Since the forward scatterers are fixed in this model, and the back scatterers flip after r visits, the particle will oscillate between the two back scatterers until it will flip them, converting them to forward scatterers. Then, the amplitude of oscillations will increase. Thus, the particle oscillates with always increasing amplitude, provided that the amount of back scatterers on both sides of 0 is initially infinite. This happens with probability 1. In this case, the particle must eventually visit each site of $\mathbb{Z}$, as desired.

Q.E.D.

It is also clear from the proof of Proposition 26that if a particle visits any site of the lattice $\mathbb{Z}$ infinitely many times, then it visits all site of $\mathbb{Z}$ infinitely many times. This condition yields a set of the exceptional environments to Proposition 26.

Corollary 27 *Suppose that the particle moves according to the rule* $\begin{pmatrix} 1 & 1 \\ 0 & 0 \end{pmatrix}$. *Then the particle will not oscillate if and only if* $\exists\ n_+ \in \mathbb{Z}^+$ *and/or* $n_- \in \mathbb{Z}^-$ *such that in the initial configuration at all sites* $z > n_+$ *and/or* $z < n_-$ *there are only white cells.*

Moreover, if the above conditions are satisfied, then the particle will eventually propagate in one direction with unit velocity. If $v(0) = +1$, *the direction of propagation will be positive (negative) if, in the initial configuration, the number of black cells on* $\mathbb{Z}^-$ *is at least (strictly smaller than) the number of black cells on* $\mathbb{N}$.

Finally, it is obvious that if the initial configuration contains a finite number of white cells, then the particle will proceed to visit every site of the lattice. This is

precisely the Lemma from [37], describing the dynamics of this rule.

The case of $v(0) = -1$ is similar, and is omitted for the sake of brevity.

5.2.4.3 Statistical Properties

We will now calculate the expected time τ_M of reaching some site $M \in \mathbb{Z}$ for the first time, such that M is white. Observe that every pair of black cells $\alpha_j \geq 0 > -\beta_j$ bounding the particle in exactly $2r(\alpha_j + \beta_j)$ steps returns the lattice to its original state, except the scatterers at α_j and β_j are flipped (i.e., these cells are now white). Therefore, if $0 \leq \alpha_1 < \alpha_2 < \ldots < \alpha_\nu \leq M$ are the only initial black cells between 0 and M, and $0 > -\beta_1 > \ldots > -\beta_\nu$ are the first ν black cells to the left of 0, then

$$\tau_M = E\left[M + \sum_{j=1}^{\nu} 2r(\alpha_j + \beta_j)\right] = M + 2rE\left[\sum_{j=1}^{\nu}(\alpha_j + \beta_j)\right].$$

Note that ν is a binomial random variable with parameters $M+1, q$. Also, if $\nu = 0$ then α_j, β_j do not contribute anything, as they are not defined. Also, β_j is independent of ν. In fact, β_j is a random variable that has a negative binomial distribution with parameters q and j. Thus, $E[\beta_j] = pj/q$.

At the same time, α_j depends on ν in the following way. Suppose that $\nu = N$. Then, $\alpha_j = k$ when in the sites 0 through $k-1$, we have exactly $j-1$ blocks, and in the sites $k+1$ up to M we have exactly $N-j$ blocks. Thus,

$$Prob[a_j = k | \nu = N] = \frac{\begin{pmatrix} k \\ j-1 \end{pmatrix}\begin{pmatrix} M-k \\ N-j \end{pmatrix}}{\begin{pmatrix} M+1 \\ N \end{pmatrix}},$$

for $1 \leq j \leq N$ and $j - 1 \leq k \leq M + 1 - N + j$. The probability is zero for every other k. In fact, when $k = M + 1 - N + j$, the probability is also zero because $\begin{pmatrix} M-k \\ N-j \end{pmatrix} = 0$. Thus, $j - 1 \leq k \leq M - N + j$.

Consequently,

$$E\left[a_j|\nu=N\right]=\sum_{k=j-1}^{M-N+j}k\frac{\binom{k}{j-1}\binom{M-k}{N-j}}{\binom{M+1}{N}}.$$

This distribution is a special case of the equation (5.25) in [41]. We will use generating functions to evaluate this sum. Let $[x^n]\,f(x)$ denote the coefficient of x^n in a generating function $f(x)$. Observe that

$$\frac{x^{j-1}}{(1-x)^j}=\sum_{k=j-1}^{\infty}\binom{k}{j-1}x^k.$$

Hence,

$$x\frac{\mathsf{d}}{\mathsf{d}x}\left(\frac{x^{j-1}}{(1-x)^j}\right)=\sum_{k=j-1}^{\infty}k\binom{k}{j-1}x^k.$$

Also,

$$\frac{1}{(1-x)^{N-j+1}}=\sum_{t=0}^{\infty}\binom{N-j+t}{N-j}x^t.$$

Thus,

$$\begin{aligned}K&=\left[x^{M-N+j}\right]\frac{1}{(1-x)^{N-j+1}}\cdot x\frac{\mathsf{d}}{\mathsf{d}x}\left(\frac{x^{j-1}}{(1-x)^j}\right)\\&=\left[x^{M-N+j}\right]\left(\left(\sum_{k=j-1}^{\infty}k\binom{k}{j-1}x^k\right)\left(\sum_{t=0}^{\infty}\binom{N-j+t}{N-j}x^t\right)\right)\\&=\sum_{k=j-1}^{M-N+j}k\binom{k}{j-1}\binom{M-k}{N-j}.\end{aligned}$$

On the other hand,

$$\begin{aligned}
K &= \left[x^{M-N+j}\right] \frac{1}{(1-x)^{N-j+1}} \cdot x\frac{\mathsf{d}}{\mathsf{d}x}\left(\frac{x^{j-1}}{(1-x)^{j}}\right) \\
&= \left[x^{M-N+j}\right] \frac{x^{j-1}\,(j+1-x)}{(1-x)^{N+2}} \\
&= (j-1)\left[x^{M-N+1}\right] \frac{1}{(1-x)^{N+2}} + \left[x^{M-N}\right] \frac{1}{(1-x)^{N+2}} \\
&= \binom{M+1}{N} \frac{jM+2j-N-1}{N+1}.
\end{aligned}$$

Consequently,

$$E\left[a_j|\nu=N\right] = \frac{K}{\binom{M+1}{N}} = \frac{jM+2j-N-1}{N+1} = \frac{j(M+2)}{N+1} - 1.$$

Now we will use these to find τ_M.

$$\begin{aligned}
\tau_M &= M + 2rE\left[\sum_{j=1}^{\nu}(\alpha_j+\beta_j)\right] \\
&= M + 2r\sum_{N=0}^{M+1} Prob[\nu=N]E\left[\sum_{j=1}^{N}(\alpha_j+\beta_j)\middle|\,\nu=N\right] \\
&= M + 2r\sum_{N=0}^{M+1}\binom{M+1}{N} q^N p^{M+1-N}\sum_{j=1}^{N}\left(E\left[\alpha_j|\,\nu=N\right]+E\left[\beta_j\right]\right) \\
&= M + 2r\sum_{N=0}^{M+1}\binom{M+1}{N} q^N p^{M+1-N}\sum_{j=1}^{N}\left(\frac{jM+2j-N-1}{N+1}+\frac{pj}{q}\right) \\
&= M + \frac{r}{q}\sum_{N=0}^{M+1}\binom{M+1}{N} q^N p^{M+1-N} N\left(Mq+(N+1)p\right) \\
&= M + Mr\sum_{N=0}^{M+1} N\binom{M+1}{N} q^N p^{M+1-N} + \frac{rp}{q}\sum_{N=0}^{M} N(N+1)\binom{M+1}{N} q^N p^{M+1-N} \\
&= M + Mr(M+1)q + \frac{rp(M+1)q(2+Mq)}{q} \\
&= M^2rq(2-q) + M(1+2r-rq^2) + 2r(1-q).
\end{aligned}$$

This implies the following result.

Proposition 28 *Under the conditions of the corollary, assume* $v(0) = +1$. *Let* τ_M *be the expected time to hit a cell* $M > 0$ *for the first time with* M *being white. Then,*

$$\tau_M = M^2 rq(2-q) + M(1 + 2r - rq^2) + 2r(1-q)$$

and the average velocity $\bar{v}$ *of moving to the right is*

$$\bar{v} = \frac{M}{\tau_M} = \frac{M}{M^2 rq(2-q) + M(1 + 2r - rq^2) + 2r(1-q)}.$$

5.3 Forward and Delayed Back Scatterers

5.3.1 Construction of Logic Gates

The scheme for the gates here is similar to the preceding case. Again, we use black color to indicate forward scatterers and white color for delayed back scatterers.

For the NOT gate, the input is indicated by the state of the scatterer at 0 in the initial configuration: $\phi(0) = 0$ means the input variable is $TRUE$ and $\phi(0) = 2$ means the input variable is $FALSE$. All other scatterers are set to be forward scatterers. Now we will simulate the ant's behavior for exactly 2 steps. The dynamics of this gate is pictured in Figure 12. We will ask the question — *does the ant never visit cell* 2? In other words, the gate accepts its input if and only if the ant never visits cell 2 during the simulation of ant's dynamics.

Observe that after the first step, the ant is at 1 always, so $X(1) = 1$. After the second step, the ant is at 2 if and only if the scatterer at 0 was a forward scatterer (otherwise, the ant is at 1). Hence the gate rejects its input if and only if the input variable had value $TRUE$, as desired.

For the AND gate, the input is indicated by the state of the scatterers at 0 and 1 in the initial configuration. All other cells contain forward scatterers. The dynamics of the logic gates for this model are pictured in Figure 12. We run the system for 3 steps and ask the questions *does the ant ever visit cell* 3?

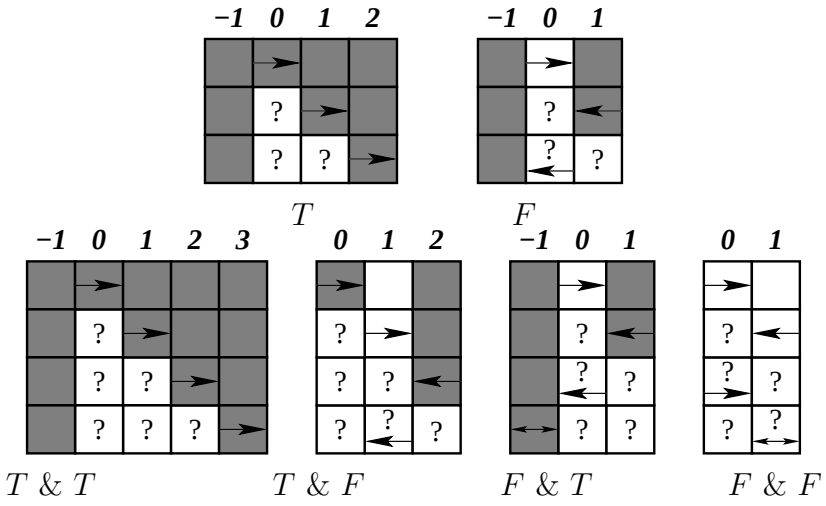

Figure 12: Dynamics Of The Logic Gates For Black Forward And White Delayed Back Scatterers

Note that if both scatterers are forward scatterers, then $X(t) = t \forall\ t \in \mathbb{N}$, hence the gate will accept its input. However, if $\phi(0) = 2$ then at time 1 the ant's velocity will flip, and if $\phi(0) = 0, \phi(1) = 2$ then at time 2 the ant's velocity will flip. As a result, the ant will turn back within the first three steps and will never reach cell 3 during the simulation. Consequently, the gate will reject its input. In summary, the gate accepts its input if and only if both input variables have value $TRUE$, as desired.

5.3.2 Dynamics For Fixed Scatterers

5.3.2.1 Description of Dynamics

This $\begin{pmatrix} 0 & 0 \\ 0 & 2 \end{pmatrix}$ model belongs to the class $B1$ [37]. The local dynamics of this model is pictured in Figure 13.

The ant will travel in the direction of $v(0)$ until a white cell is encountered. Then, the ant will cycle around this white cell either with period 2 or with period 4.

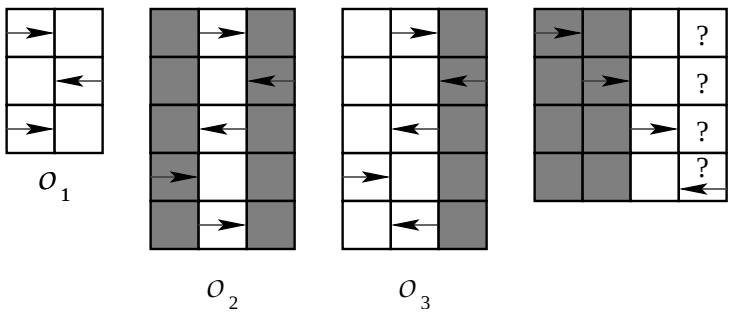

Figure 13: Dynamics Of The Black Fixed Forward Scatterer And White Fixed Delayed Back Scatterer Model

Proposition 29 (Periodic Oscillation) *A particle of LLGCA moving on* $\mathbb{Z}$ *according to the rule* $\begin{pmatrix} 0 & 0 \\ & \\ 0 & 2 \end{pmatrix}$ *will end up in a periodic trajectory with probability* 1. *The period will be* 2 *if the first white site encountered by the particle is a part of a block, and will be* 4 *otherwise.*

Proof. Suppose initially $\phi(0) = 2$. If 1 is white, then the particle will cycle between 0 and 1 as in the dynamics for the previously-discussed rule $\begin{pmatrix} 0 & 1 \\ & \\ 0 & 2 \end{pmatrix}$. Call this orbit $\mathcal{O}_1$. Alternatively, $1, -1$ are both black, so the particle will cycle between $-1, 0$ and 1 with period 4, along the orbit $\mathcal{O}_2 = (0, 1, 0, -1, 0, \ldots)$. Otherwise, 1 is black and -1 is white. In this case, the particle will reflect off 1, visiting it exactly once, and will oscillate between 0 and -1 with period 2. Call this orbit $\mathcal{O}_3$.

in the case 0 is black, the particle will move in the direction of $v(0)$ until a white cell $z \geq 0$ is encountered. At this point, if $z+1$ is white, the particle will cycle between z and $z+1$ with period 2 (this motion is similar to the orbit $\mathcal{O}_1$), and if $z+1$ is black, the particle will cycle between $z-1, z, z+1$, with trajectory $(z-1, z, z+1, z, z-1, \ldots)$, resulting in a period of 4 (this motion is similar to the orbit $\mathcal{O}_2$).

Q.E.D.

The set of exceptions to this result is evident from its proof. It is also evident

that this set has measure 0.

Corollary 30 *Under the conditions of the proposition, assume in addition that* $v(0) = +1$. *The particle does not end up in a periodic orbit if and only if* $\mathbb{N}$ *are all black. In this case, the particle always propagates in the direction of the black block with unit speed.*

The case of $v(0) = -1$ is symmetric, and therefore omitted for the sake of brevity.

5.3.2.2 Statistical Properties

Assume now $v(0) = +1$. Let $\mathcal{O}$ denote the orbit of the particle. Then, $Prob[\mathcal{O} = \mathcal{O}_1] = p^2, Prob[\mathcal{O} = \mathcal{O}_2] = pq^2$, and $Prob[\mathcal{O} = \mathcal{O}_3] = p^2q$. Also,

$$Prob[n \in \mathcal{O}] = \left\{ \begin{array}{cc} 0, & \forall\ n \leq -2 \\ pq, & n = -1 \\ 1, & n \in \{0, 1\} \\ q^{n-1}, & n \geq 1 \end{array} \right\| .$$

The last case happens since $n \geq 1$ is in the orbit $\mathcal{O}$ if and only if initially $\phi(k) = 0 \forall\ k \in [0, n-2] \cap \mathbb{Z}$, i.e., if and only if all of the cells $0, 1, \ldots, n-2$ initially are black. This happens with probability q^{n-1}. Moreover,

$$\begin{aligned} Prob[n \in \mathcal{O}, (n+1) \notin \mathcal{O}] &= Prob[0, 1, \ldots, (n-2) \text{ are black}, (n-1) \text{ is white}] \\ &= pq^{n-1}, \quad n \geq 1. \end{aligned}$$

Thus, the rightmost point in the orbit of the particle is a geometric random variable that has a mean of $1/p$. Clearly, for $0 \leq p \leq 1$, we see that the minimum of 1 occurs at $p = 1$ and a maximum of $+\infty$ occurs at $p = 0$. So, the minimum expected stopping point is 1 (in the case all cells are white), and the maximum expected stopping point is infinite (in the case where all cells of $\mathbb{N}$ are black, as we pointed out in the Corollary above).

Finally, we calculate the probability that particle ends up in the orbit of period 2. We have

$$\begin{aligned} Prob[\text{period is } 2] &= Prob[\mathcal{O} = \mathcal{O}_3] + Prob[\mathcal{O} = \mathcal{O}_1] + \sum_{n=2}^{\infty} Prob[\text{particle cycles at} \{n-1, n\}] \\ &= Prob[\mathcal{O} = \mathcal{O}_3] + Prob[\mathcal{O} = \mathcal{O}_1] + \sum_{n=2}^{\infty} Prob[n \in \mathcal{O}, (n+1) \notin \mathcal{O}, n \text{ is white}] \\ &= qp^2 + p^2 + \sum_{n=2}^{\infty} p^2 q^{n-1} \\ &= qp^2 + p^2 \sum_{n=0}^{\infty} q^n = p + qp^2 = p(1+qp). \end{aligned}$$

Also, the probability that a particle ends up in an orbit of period 4 is

$$Prob[\text{period is } 4] = 1 - p(1+qp) = q^2(p+1) = q^2(2-q).$$

These results are summed up in the following proposition.

Proposition 31 *Assume the conditions of the corollary. Then, the rightmost point in the orbit of the particle is a geometric random variable that has a mean of* $1/p$. *Thus, the minimum expected rightmost point is* 1 *(for* $p = 1$*) and the maximum expected rightmost point is* ∞ *(for* $p = 0$*).*

Finally, the particle end up in an orbit of period 2 *with probability* $p(1+qp)$, *and in an orbit of period* 4 *with probability* $q^2(2-q)$.

5.3.3 Black Flipping Forward Scatterer And White Fixed Delayed Back Scatterer

5.3.3.1 Description of Dynamics

This $\begin{pmatrix} 1 & 0 \\ 0 & 2 \end{pmatrix}$ model belongs to the class $B1$ [37]. The dynamics for the case of $r = 1$ is shown in Figure 14.

in the case 0 is black, the particle moves in the direction of $v(0)$ until a white cell $z \geq 1$ is encountered. At this point, the site $z - v(0)$ must be white since it was flipped on the way forward. Thus, if $z + v(0)$ is black, it will be visited once, and

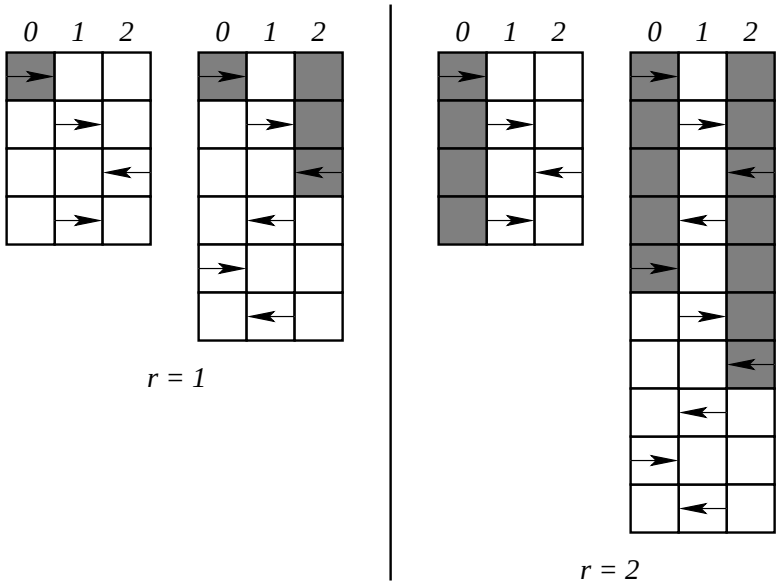

Figure 14: Dynamics Of The Black Flipping Forward Scatterer And White Fixed Delayed Back Scatterer Model With $r = 1$ and $r = 2$

then the particle will oscillate with period 2 between the sites $z - v(0)$ and z. On the other hand, if $z + v(0)$ is white, the particle will cycle with period 2 between z and $z + v(0)$.

in the case 0 is white, the particle moves once in the direction of $v(0)$ and changes direction. Now, if the next cell encountered (namely, site $v(0)$) is white, the particle will oscillate between this cell $v(0)$ and 0. Otherwise, the particle will return to 0, flipping $v(0)$, and proceed to $-v(0)$. Again, if $-v(0)$ is white, then the particle will oscillate between $-v(0)$ and 0. If not, the particle proceeds to oscillate between 0 and $v(0)$, which is now white since it was flipped on the way back.

5.3.3.2 Effects of Rigidity

Suppose now the environment has rigidity r. in the case 0 is black, the particle proceeds at unit speed in the direction of $v(0)$ until it hits the first white cell at some site z. Now, the particle will oscillate between $z+1, z$, and $z-1$ until either $z+1$ or $z-1$ becomes white. At this point, the particle will oscillate strictly between the first

cell to turn white and the cell z. in the case 0 is white, similar behavior is exhibited in $-1, 0, 1$ as in the case of $z-1, z, z+1$ above. The dynamics for the case of $r = 2$ is pictured in Figure 14.

Proposition 32 (Periodic Oscillation) *A particle of LLGCA moving on* $\mathbb{Z}$ *according to the rule* $\begin{pmatrix} 1 & 0 \\ 0 & 2 \end{pmatrix}$ *with arbitrary rigidity, with probability* 1 *will eventually end up in a periodic trajectory with period* 2*, oscillating between the first white site encountered by the particle and one of the sites adjacent to it.*

Proof. If 0 is initially white, the statement of the proposition is trivially true. In this case, the particle will oscillate along the orbit $(0, v(0), 0, -v(0))$ until $v(0)$ becomes white. At this point, the particle will oscillate strictly between 0 and $v(0)$ with period 2 forever.

in the case 0 is initially black, the particle proceeds to travel in the direction of $v(0)$ until the first white cell is encountered at some z. The behavior of the particle around z is similar to the above case where 0 is initially white. Namely, if $z + v(0)$ is white, then the particle will oscillate with period 2 between z and $z+v(0)$. Otherwise, the particle will oscillate in the orbit $(z - v(0), z, z + v(0), z)$ until $z - v(0)$ becomes white (it will become white faster than $z + v(0)$, since it was visited first earlier). Then the particle oscillates between z and $z - v(0)$ with period 2 forever.

Q.E.D.

Corollary 33 *Assume the conditions of the proposition, and assume in addition that* $v(0) = +1$*. The particle does not end up in a periodic orbit if and only if all cells of* $\mathbb{N}$ *are initially black. In this case, the particle will always propagate in the direction of* $v(0)$ *with unit speed.*

This rule is interesting in that the parity of r plays no role in the behavior of the

particle. This is very different from the rule $\begin{pmatrix} 1 & 0 \\ 0 & 1 \end{pmatrix}$, where we could see that the parity of the rigidity influences the dynamics of the system. Bunimovich [17] also found a similar effect in his analysis of the rule $\begin{pmatrix} 1 & 0 \\ 1 & 1 \end{pmatrix}$.

5.3.3.3 Statistical Properties

Assume $v(0) = +1$. Let $\mathcal{O}$ denote the orbit of the particle. Then,

$$Prob[n \in \mathcal{O}] = \left\| \begin{cases} 1, & n = 0 \\ q^{n-1}, & \forall\ n \in \mathbb{Z}^+ \\ pq, & n = -1 \\ 0, & n \leq -2 \end{cases} \right\|$$

Moreover,

$$Prob[n \in \mathcal{O}, (n+1) \notin \mathcal{O}] = pq^{n-1}, \quad n \geq 1.$$

Clearly, the first white site to be encountered by the particle is $N - 1$, where N is a geometric random variable with mean $1/p$.

5.3.4 Black Flipping Delayed Back Scatterer And White Fixed Forward Scatterer

5.3.4.1 Description of Dynamics

The model $\begin{pmatrix} 1 & 2 \\ 0 & 0 \end{pmatrix}$ belongs to the class $U1$ [37]. It is quite similar to the model analyzed in [17] and [42]. It is also somewhat similar to the preceding model $\begin{pmatrix} 1 & 2 \\ 0 & 0 \end{pmatrix}$.

The particle moves in the direction of $v(0)$ until the first black cell is encountered at some cell z. If the particle encounters a stand-alone black cell (i.e., it is not the first cell of a black block), the particle changes speed to $-v(0)$ in 2 steps (flipping it to white) and continues in the direction of $-v(0)$ until the next black cell. in the

case the particle meets a block of black cells, in 2 steps the first two cells are flipped to white and the particle does not change position or velocity.

5.3.4.2 Effects of Rigidity

To flip a block of 2 black cells now takes $2r$ steps. When we have a stand-alone black cell, and r is even, then the particle flips it in $2r$ steps without altering the direction of the particle. If r is odd, the black cell is still flipped in $2r$ steps, but the direction of the particle is reversed. This is pictured in Figure 15 for the cases of $r = 2$ and $r = 3$.

in the case of even rigidity, the particle always propagates in its initial direction, and in the case of odd rigidity, the particle oscillates with probability 1. In the latter situation, the propagation occurs if and only if it eventually encounters black blocks of only even size. Therefore, we get the following results.

Proposition 34 (Propagation) *Suppose that the particle moves according to the rule* $\begin{pmatrix} 1 & 2 \\ & \\ 0 & 0 \end{pmatrix}$ *with even rigidity. Then the particle always propagates in the direction of* $v(0)$.

Proof. Clearly, the particle will propagate in the direction of $v(0)$ while moving through a white block. When a stand-alone black cell is encountered, the particle will oscillate around this cell, and since rigidity is even, once the scatterer in this cell changes its state, the particle will visit the cell again, retaining the original velocity $v(0)$. Hence, the propagation in the direction of $v(0)$ will continue. Finally, when a black block is encountered, the particle will oscillate between consecutive pairs of cells in the block, converting them to white cells. e.g., first the particle will oscillate between the first and the second cells in the block, convert them to white, and proceed to the next pair. Thus, if the block is even, the propagation will continue, and if the block is odd, it will eventually be reduced to a stand-alone cell, which we have already

covered. Thus, the particle always propagates in the direction of $v(0)$, in all possible initial distributions.

Q.E.D.

Proposition 35 (Oscillation) *If the particle moves according to the rule* $\begin{pmatrix} 1 & 2 \\ 0 & 0 \end{pmatrix}$ *with odd rigidity, then the particle will visit every site of the lattice* $\mathbb{Z}$ *infinitely many times with probability* 1*.*

Proof. The local dynamics here is very similar to the previous result, except since the rigidity is odd, once a stand-alone black cell is encountered, while it is flipped to a white cell, the velocity of the particle is reversed. Hence, the result is oscillation. Upon encountering a stand-alone black cell, or a black block of odd size, the particle flips the encountered black cells to white, but changes its direction after the flipping is done.

Hence, unless the particle encounters neither stand-alone black cells nor black blocks of odd size, the particle continues oscillating with the always increasing amplitude. Then, all sites of $\mathbb{Z}$ will be eventually visited.

Q.E.D.

A set of the exceptional environments to this result is also evident from the description of the dynamics of the particle. The dynamics in this case is very similar to the model $\begin{pmatrix} 1 & 1 \\ 0 & 0 \end{pmatrix}$ with arbitrary rigidity, so it is natural to expect the same set of exceptions.

Corollary 36 *Suppose that the particle moves according to the rule* $\begin{pmatrix} 1 & 2 \\ 0 & 0 \end{pmatrix}$ *with odd rigidity. Then the particle will not oscillate if and only if* $\exists\ n_+ \in \mathbb{Z}^+$ *and/or*

$n_- \in \mathbb{Z}^-$ such that in the initial configuration at all sites $z > n_+$ and/or $z < n_-$ there are only even blocks of black cells or no black cells at all.

If these conditions are satisfied, then the particle eventually propagates in one direction. If $v(0) = +1$, the direction of propagation will be positive (negative) if, in the initial configuration, the number of odd blocks of black cells on $\mathbb{Z}^-$ is at least (strictly smaller) than the number of odd blocks of black cells on $\mathbb{N}$.

The case of $v(0) = -1$ is similar, and is omitted for the sake of brevity.

5.3.4.3 Statistical Properties

Assume that the rigidity is even and $v(0) = +1$. As evident from Proposition 34, the particle propagates in the direction of $v(0)$. We calculate the average velocity of propagation $\bar{v}$, as well as τ_M, the expected time of arriving at the cell $M \geq 0$ with M being white and the particle moving with velocity of $v(0)$.

in the case M was originally white, when the particle moves from some $M-1$ to M, M is still white at this point, and the particle does not change velocity. Therefore, we only require 1 step.

in the case M was originally black, we have two possibilities. Recall that when the particle hits a black block, it takes $2r$ steps to flip a block of 2 cells, and then the particle proceeds to the next pair of cells in the same block, if one exists. If M was an odd cell in a block of black cells, it will take additional $2r$ steps to flip the site M into white, after the particle hits M for the first time. So, in total we need $2r+1$ steps. A similar case happens if M is either a stand-alone black cell, or the last cell in a block of odd size (i.e., we still need $2r+1$ steps). However, in the case M was originally an even cell in a block of black cells, M was flipped along with the cell preceding it, so it again only takes one step.

In summary, if M was originally an odd cell inside a black block, or a stand-alone black cell, we have $\tau_M - \tau_{M-1} = 2r+1$. Otherwise, $\tau_M - \tau_{M+1} = 1$. Let $\mathcal{P}$ denote the

probability that M was originally an odd cell inside a black block, or a stand-alone black cell. Then, we clearly have

$$\tau_M - \tau_{M-1} = 1 + 2r\mathcal{P}, \quad \tau_0 = 0.$$

Now, it remains to compute the desired probability $\mathcal{P}$ for $M \neq 0$. First, suppose $M = 2k$ for some $k \in \mathbb{Z}$. Then, our probability is

$$\begin{aligned}
\mathcal{P} &= q^{2k+1} + qp \sum_{j=0}^{k-1} \left(q^2\right)^j \\
&= q^{2k+1} + \frac{qp\left(1-q^{2k}\right)}{1-q^2} \\
&= q^{M+1} + \frac{q\left(1-q^{M}\right)}{1+q} \\
&= \frac{q+q^{M+2}}{1+q} \\
&= \frac{q\left(1+q^{M+1}\right)}{1+q}.
\end{aligned}$$

in the case $M = 2k+1$, we have

$$\mathcal{P} = qp \sum_{j=0}^{k} \left(q^2\right)^j = \frac{qp\left(1-q^{2k+2}\right)}{1-q^2} = \frac{q\left(1-q^{M+1}\right)}{1+q}$$

Consequently, $\mathcal{P} = \frac{q}{1+q}\left(1+(-1)^M q^{M+1}\right)$. Therefore, we find

$$\tau_M - \tau_{M-1} = 1 + \frac{2rq}{1+q}\left(1+(-1)^M q^{M+1}\right) = 1 + \frac{2rq}{1+q}\left(1+(-q)^M q\right).$$

Solving this recurrence relation with the initial condition $\tau_0 = 0$ we find

$$\tau_M = \frac{M(q+1)(q+1+2rq) - 2rq^3\left(1-(-q)^M\right)}{(q+1)^2}.$$

Consequently, the average velocity is given by

$$\bar{v} = \frac{M}{\tau_M} = \frac{M(q+1)^2}{M(q+1)(q+1+2rq) - 2rq^3\left(1-(-q)^M\right)}.$$

We proved the following.

Proposition 37 *Under the conditions of Proposition 34, assume* $v(0) = +1$. *Then, the particle propagates with an average velocity of*

$$\bar{v} = \frac{M}{\tau_M} = \frac{M(q+1)^2}{M(q+1)(q+1+2rq) - 2rq^3\left(1-(-q)^M\right)}.$$

5.3.5 Dynamics For Two Flipping Scatterer Types

5.3.5.1 Description of Dynamics

This $\begin{pmatrix} 1 & 2 \\ 1 & 0 \end{pmatrix}$ model belongs in the class $U1$ [37].

5.3.5.2 Effects of Even Rigidity

For the purposes of this section, assume $v(0) = +1$. in the case $v(0) = -1$, the situation is symmetric; we omit it for the sake of brevity.

Suppose that 0 is white. In that case, the particle will continue traveling in the direction of $v(0)$ until a black cell is encountered. Then, if the particle encounters a block (at least 2 in a row) of black cells, the first pair will be converted to white in $2r$ steps, while the particle will retain it's velocity and position, without modifying any other cells in the lattice. If a checkered pattern is encountered, starting and ending with white cells, the particle will also eventually proceed through the pattern. The first time the particle leaves the pattern, it retains its original velocity. The latter case is illustrated in the left part of Figure 16 for $r = 2$.

Because the particle eventually propagates through every possible structure it encounters and retains its original velocity from before entering the structure, we have the following result.

Proposition 38 (Propagation) *Suppose that the particle moves on the* $\mathbb{Z}$ *lattice with even rigidity according to the rule* $\begin{pmatrix} 1 & 2 \\ 1 & 0 \end{pmatrix}$. *Then, the particle will eventually propagate in the direction of* $v(0)$.

5.3.5.3 Effects of Odd Rigidity

As in the previous case of even rigidity, even blocks of black cells can be converted pair by pair to white cells by the particle. However, the case of a black block of odd size or a stand-alone black cell will result in change of direction for the particle, while the barrier is being flipped. Hence, it makes sense that the particle should oscillate.

Proposition 39 (Oscillation) *Suppose that the particle moves on the $\mathbb{Z}$ lattice with odd rigidity according to the rule* $\begin{pmatrix} 1 & 2 \\ & \\ 1 & 0 \end{pmatrix}$. *Then, with probability* 1*, the particle will oscillate.*

Proof. The particle should still propagate through blocks of forward scatterers, as well as through even blocks of delayed back scatterers. In addition, all odd blocks of delayed back scatterers will be converted by the particle to even blocks of forward scatterers, followed by one delayed back scatterer. We would like to show that the particle eventually propagates through every possible structure it encounters. Thus, it suffices to prove that the particle will eventually propagate through any checkered pattern of length three. There are only two of them – either two forward scatterers at n and $n+2$ with a delayed back scatterer at $n+1$ (call this primal configuration), or its dual, with delayed back scatterers at n and $n+2$ and a forward scatterer at $n+1$ (call this the dual configuration).

We will first prove this result for $r = 1$. Notice that the particle converts even blocks of delayed back scatterers to forward scatterers, and goes through them, always leaving behind a trail with only delayed back scatterers. Until a block of odd size of delayed back scatterers is encountered, this motion will go on. An odd block of delayed back scatterers will reverse the motion of the particle, converting the last forward scatterer to a delayed back, and now similar motion will happen in the reverse direction. Thus, the delayed back scatterer block on the right of zero grew by at least

one cell (if there is another such block after the cell that was just converted, the block could have grown by more than one cell). Same will happen in the other direction. Thus, particle oscillates and this block grows with every oscillation. This can be seen in the right part of Figure 16.

Now we consider $r = 2k + 1$, for some integer $k \geq 1$. Let us look at the first time a particle visits the dual configuration. In the case the particle came from a black cell, $n - 1$ and n is a black block, which is a case we discussed above. In the case the particle came from a white cell, $n-1, n, n+1$ form the first checkered pattern. Thus, the only case left to consider is when $n = 0$ and the particle starts its dynamics from this configuration.

In that case, -1 is either black or white. If -1 is white, the particle will take $2r$ steps to flip the cell 0, leaving -1 and 1 as forward scatterers. Hence, the next time the particle will visit cell 1, it will proceed to 2, and will eventually propagate through the pattern to visit 3. On the other hand, if -1 is black, the particle will proceed to 1 with flipped velocity, return to 0 at time 2 with $v = -1$, and proceed to alternate between 0 and -1 until 0 flips. Now we have a similar situation to the case when -1 was white – next visit through the structure will result in the particle visiting 3, i.e., propagating through the structure.

Thus, it suffices to consider the primal checkered pattern, where $\phi(n) = 0 = \phi(n + 2)$ and $\phi(n + 1) = 2$ for any n. WLOG, assume $n = 0$. In $4k + 5$ steps, the particle will be located at -1, visiting it for the first time. The state of the checkered pattern will be as follows. Cell 0 would be visited $k + 2$ times (remember, $r = 2k + 1$ from above), 2 would be visited $k + 1$ times, and 1 will contain a forward scatterer, visited exactly once. Thus, for any $k \geq 2$ (i.e., for $r \geq 5$), this becomes a pattern of forward scatterers, which will be passed through the next time the particle enters this configuration. This only leaves the case $r = 3$ and $k = 1$. This case is illustrated in Figure 17.

In that situation, we are left with $\phi(0) = 2$ and $\phi(1) = \phi(2) = 0$, where 2 was visited twice and 1 was visited once. The next time the particle enters the configuration, if $\phi(-1) = 0$, the particle will proceed to 0 then to 1, reversing its velocity, then to 0 and to -1, again, reversing its velocity. At this point, $\phi(1) = \phi(2) = 0$, and both have been visited once. So if -1 changed its scatterer because of the last visit, 0 will be converted to a forward scatterer and we have a pattern of 3 forward scatterers at $0, 1, 2$. If not (i.e., if we still have $\phi(-1) = 0$, the particle makes another pass, and we end up with $\phi(0) = \phi(2) = 0$ and $\phi(1) = 2$, but 0 is visited once and 2 is visited twice. The next time around, if the particle comes from a white cell, it will reach 3, as desired. But if it comes from a black cell, 0 may be converted to a black cell. In that case, 0 and 1 will form a black block, eventually causing the particle to propagate forward through it towards 2.

If originally -1 is a delayed back scatterer, it will only contribute to converting 0 to a forward scatterer. This will create a block of delayed back scatterers at 0 and 1, also eventually causing the particle to propagate through the desired blocks and reach 3.

In summary, any configuration of the scatterers will be eventually traversed by the particle. Because there exist configurations of the scatterers that reverse the velocity of the particle, it must oscillate.

Q.E.D.

5.4 Back and Delayed Back Scatterers

An interesting feature of these models is that the velocity here flips with every movement of the particle. In other words, $v(2k) = -v(2k+1) \forall\ k \in \mathbb{N}$.

5.4.1 Construction of Logic Gates

We will use white to indicate back scatterers and black to indicate delayed back scatterers.

For the NOT gate, the input is indicated by the state of the scatterer at 0 in the initial configuration: $\phi(0) = 2$ means the input variable is $TRUE$ and $\phi(0) = 1$ means the input variable is $FALSE$. All other scatterers are set to be delayed back scatterers. Now we will simulate the ant's behavior for exactly 1 step. The resulting dynamics can be found in Figure 18. We will ask the question — *does the ant ever visit cell* -1? In other words, the gate accepts its input if and only if the ant visits cell -1 during the simulation of ant's dynamics.

Observe that $X(1) = -1$ if and only if $\phi(0) = 1$. Hence the gate rejects its input if and only if the input variable had value $TRUE$, as desired.

For the AND gate, the input is indicated by the state of the scatterers at 0 and 1 in the initial configuration. All other cells contain delayed back scatterers. The dynamics for logic gates of this model is given in Figure 18. We run the system for 2 steps and ask the questions *does the ant never visit cells* 2 *and* -1? Equivalently, we may ask *does the orbit of the ant consist only of cells* $0, 1$? In other words, the gate accepts its input if and only if the only cells visited by the ant were 0 and 1.

Observe that if both scatterers are delayed back scatterers, the ant will have trajectory $(0, 1, 0)$ and the input will be accepted. On the other hand, if $\phi(0) = 1$ then the ant visits -1 at step 1 and the input is rejected. Similarly, if $\phi(0) = 2, \phi(1) = 1$ then the ant visits 1 at time 1 and 2 at time 2. Thus, the input is again rejected. Hence, the input is accepted if and only if both input variables evaluate to $TRUE$.

5.4.2 Dynamics For Fixed Scatterers

5.4.2.1 Description of Dynamics

This is the $\begin{pmatrix} 0 & 1 \\ & \\ 0 & 2 \end{pmatrix}$ model that belongs to the class $B1$ [37]. The local dynamics of the particle is pictured in Figure 19.

The particle moves in the direction of $v(0)$ $(-v(0))$ if the vertex 0 is white (black), until it passes over two consecutive cells of the same color. At this point, the particle will cycle over the two consecutive cells of the same color it just encountered. Once the particle passes over a cell z and goes to $z+1$ with $v(z+1) = +1$, or, alternatively, goes to $z-1$ with $v(z-1) = -1$, it will never come back to z. We end up with the following result.

Proposition 40 (Periodic Oscillation) *A particle of LLGCA moving on the* $\mathbb{Z}$ *lattice according to the rule* $\begin{pmatrix} 0 & 1 \\ & \\ 0 & 2 \end{pmatrix}$ *with probability* 1 *ends up in a periodic trajectory of period* 2*. This trajectory consists of the first consecutive cells of the same color, encountered by the particle.*

Proof. As soon as the particle passes over two consecutive cells of the same color, it will oscillate between them forever with period 2. Observe that in the contrary case (i.e., if such oscillation is not to happen), we must have no two adjacent cells of the same color encountered by the particle. Consequently, in that case, the particle must be moving through a checkered pattern.

Suppose the particle is positioned over a black cell at some time t. Then, the particle has to move in the direction $-v(t)$ and change the direction. So, as long as 0 is black, the ant will move in the direction of $-v(0)$. If the ant now encounters a checkered pattern, it will continue moving at unit speed through the pattern until it hits a block of the same color. This will happen with probability 1. As we said

above, at that point the ant will oscillate with period 2 between the first two cells in this block of the same color.

Q.E.D.

The exceptional conditions to the proposition occur when there are no two adjacent cells of the same color in the direction that the ant is moving. In that case, the ant moves along the checkered pattern forever, so the set of exceptional conditions has measure 0 and the behavior of the ant in that case is also easy to analyze.

Corollary 41 *Assume the conditions of the proposition. If the particle does not end up in an orbit of period* 2*, then the particle propagates with unit speed forever. This propagation occurs in the direction of* $v(0)$ *(*$-v(0)$*) if and only if the scatterers from* 0 *to* ∞ *(*$-\infty$*) form a checkered pattern and* 0 *is white (black).*

5.4.2.2 Statistical Properties

Assume $v(0) = +1$. Let $\mathcal{O}$ denote the orbit of the particle. Then,

$$Prob[(2n) \in \mathcal{O}] = p^n q^n, \quad n \geq 0$$

$$Prob[(2n+1) \in \mathcal{O}] = p^{n+1} q^n, \quad n \geq 0$$

Assume in addition now that 0 is white. Then,

$$\begin{aligned} Prob[(2n) \in \mathcal{O}, (2n+1) \notin \mathcal{O}] &= Prob[(2n) \in \mathcal{O}] \cdot Prob[(2n) \text{ is white}] \\ &= p^{n-1} q^{n+1}, \quad n \geq 1 \\ Prob[(2n+1) \in \mathcal{O}, (2n+2) \notin \mathcal{O}] &= Prob[(2n+1) \in \mathcal{O}] \cdot Prob[(2n+1) \text{ is black}] \\ &= p^{n+1} q^n, \quad n \geq 0. \end{aligned}$$

Using these, we can calculate the expected stopping point of the particle.

$$\begin{aligned}
&\sum_{m=0}^{\infty}(2m+1)p^{m+1}q^m + \sum_{m=1}^{\infty}2mp^{m-1}q^{m+1} \\
&\qquad = \sum_{m=0}^{\infty}p^m q^m\left((2m+1)p + 2(m+1)q^2\right) \\
&\qquad = (p+2q^2)\sum_{m=0}^{\infty}p^m q^m + 2(p+q^2)\sum_{m=0}^{\infty}mp^m q^m \\
&\qquad = \frac{p+2q^2}{1-pq} + \frac{2(p+q^2)pq}{(1-pq)^2} = \frac{p+2q^2+p^2q}{(1-pq)^2} = \frac{1+q^3}{(1-pq)^2} \\
&\qquad = \frac{2-p}{1-pq} = \frac{2-p}{p^2-p+1}.
\end{aligned}$$

Finding the extrema of the right hand side for $0 \leq p \leq 1$, we see that the minimum of 1 occurs at $p = 1$ and a maximum of $\frac{1}{2\sqrt{3}-3} = \frac{2\sqrt{3}+3}{3} \approx 2.1547$ occurs at $p = 2-\sqrt{3} \approx 0.267949$. So, the minimum expected stopping point is 1, and the maximum expected stopping point is between 2 and 3.

Proposition 42 *Suppose a particle of LLGCA moves on the $\mathbb{Z}$ lattice according to the rule* $\begin{pmatrix} 0 & 1 \\ 0 & 2 \end{pmatrix}$ *with 0 initially white and $v(0) = +1$. Then, the expected rightmost site that the particle will reach will be $\frac{2-p}{p^2-p+1}$.*

The minimum (over all $p \in [0,1]$) such site is 1, which occurs at $p = 1$; the maximum such site is $\frac{2\sqrt{3}+3}{3} \approx 2.1547$, which occurs at $p = 2-\sqrt{3} \approx 0.267949$.

5.4.3 Black Back Scatterer And White Delayed Back Scatterer – Dynamics For One Flipping Scatter Type

This section will discuss the models $\begin{pmatrix} 1 & 1 \\ 0 & 2 \end{pmatrix}$ and $\begin{pmatrix} 0 & 1 \\ 1 & 2 \end{pmatrix}$. Note that the models are, actually, equivalent, and so all results done for one model will apply to the other one as well.

5.4.3.1 Description of Dynamics

Both $\begin{pmatrix} 1 & 1 \\ 0 & 2 \end{pmatrix}$ and $\begin{pmatrix} 0 & 1 \\ 1 & 2 \end{pmatrix}$ models belong to the class $B1$ [37] and have identical properties. From Lemma 4 of [37] we know that in both models, the particle proceeds along a checkered pattern until it reaches two cells of the same color (which happens with probability 1), and shortly after ends up oscillating with period 2 around one of the cells of the block that had just been discovered. The dynamics of both models for $r = 1$ is illustrated in Figure 20.

5.4.3.2 Effects of Rigidity

The dynamics of the particle under the rules considered in this section is only affected by the rigidity of the environment in the amount of time it will take for the consecutive cells, between which the particle might oscillate, to change their color, if necessary. We represent the case of $r = 2$ for both models in Figure 21.

As a result, we end up with the following corollary of Lemma 4 of [37].

Corollary 43 (Periodic Oscillation) *Consider a particle of LLGCA moving on the $\mathbb{Z}$ lattice according to the rule $\begin{pmatrix} 1 & 1 \\ 0 & 2 \end{pmatrix}$ or according to the rule $\begin{pmatrix} 0 & 1 \\ 1 & 2 \end{pmatrix}$. Then, with probability 1, the particle will eventually oscillate with period 2 around one of the two adjacent cells of the same color that it encounters.*

The exceptional condition occurs if the particle can proceed along the checkered pattern forever. As previously, this condition has measure 0.

Corollary 44 *Consider a particle of LLGCA moving on the $\mathbb{Z}$ lattice according to the rule $\begin{pmatrix} 1 & 1 \\ 0 & 2 \end{pmatrix}$ or according to the rule $\begin{pmatrix} 0 & 1 \\ 1 & 2 \end{pmatrix}$. Assume in addition that $v(0) = +1$. Then, the particle does not end up oscillating with period 2 if and only if either 0 is black and all cells of $\mathbb{Z}^-$ form a checkered pattern, or if 0 is white and all cells of $\mathbb{Z}^+$*

form a checkered pattern. In either of these cases, the particle always propagates with unit speed in the direction of the checkered pattern.

5.4.3.3 Statistical Properties

Statistical properties of these models are analogous to the model $\begin{pmatrix} 0 & 1 \\ & \\ 0 & 2 \end{pmatrix}$ with non-flipping scatterers, which we have considered before.

5.4.4 Dynamics For Two Flipping Scatterer Types

5.4.4.1 Description of Dynamics

This $\begin{pmatrix} 1 & 1 \\ & \\ 1 & 2 \end{pmatrix}$ model belongs in the class $U2$ [37]. The particle uses checkered pattern to move in either direction with unit speed.

If 0 is white (black), the particle will move in the direction of $v(0)$ $(-v(0))$ with unit speed, following a checkered pattern and leaving the dual checkered pattern as its trail, until a block of any color is encountered. At that point, the particle will take 1 step to flip the newly-encountered barrier. In this process, the velocity of the particle will flip, and the particle will travel across the checkered pattern in the opposite direction with unit speed, until meeting another block on the other side of 0. Thus, a particle proceeds to oscillate with an always increasing amplitude. Thus, with probability 1, the particle visits all cells of the underlying lattice $\mathbb{Z}$.

5.4.4.2 Effects of Rigidity

Note that rigidity did not play an important role in the dynamics under the rules $\begin{pmatrix} 1 & 1 \\ & \\ 0 & 2 \end{pmatrix}$ and $\begin{pmatrix} 0 & 1 \\ & \\ 1 & 2 \end{pmatrix}$. Hence, it is reasonable to expect that under the rule $\begin{pmatrix} 1 & 1 \\ & \\ 1 & 2 \end{pmatrix}$ the rigidity will not play a significant role either. We illustrate the dynamics of this model in Figure 22.

Before we proceed, we need a lemma on local dynamics under this rule.

Lemma 10 (Conversion Of Blocks) *We discuss a couple of local dynamics properties under the rule* $\begin{pmatrix} 1 & 1 \\ 1 & 2 \end{pmatrix}$ *with rigidity* $r > 1$.

(i) *Suppose* $X(t) = n \geq 0$ *and this is the first visit of the particle to* n *during the current state of the scatterer. If* $\phi(n) = \phi(n+1) = 2, v(t) = 1$, *then* $X(t+2r) = n, v(t+2r) = 1, \phi(n) = \phi(n+1) = 1$ *and no other cells have been affected by the dynamics.*

(ii) *Suppose* $X(t) = n \geq 0$ *and this is the first visit of the particle to* n *during the current state of the scatterer. If* $\phi(n) = \phi(n+1) = 1, v(t) = +1$, *then* $X(t+2r) = n, v(t+2r) = -1, \phi(n) = \phi(n+1) = 2$ *and no other cells have been affected by the dynamics.*

(iii) *Suppose* $X(t) = n \leq 0$ *and this is the first visit of the particle to* n *during the current state of the scatterer. If* $\phi(n) = \phi(n-1) = 1, v(t) = -1$, *then* $X(t+2r) = n, v(t+2r) = -1, \phi(n) = \phi(n+1) = 2$ *and no other cells have been affected by the dynamics.*

(iv) *Suppose* $X(t) = n \leq 0$ *and this is the first visit of the particle to* n *during the current state of the scatterer. If* $\phi(n) = \phi(n-1) = 2, v(t) = -1$, *then* $X(t+2r) = n, v(t+2r) = -1, \phi(n) = \phi(n+1) = 1$ *and no other cells have been affected by the dynamics.*

Proof. It suffices to consider the dynamics of the particle for $2r$ steps. In all four cases, the particle oscillates between the two cells in question exactly r times. Thus, at the end of $2r$ steps, both cells flip color, and no other cells are affected.

Q.E.D.

Now we prove another lemma on local dynamics that we will need later.

Lemma 11 (Return Through Checkered Pattern) *We discuss a couple of local dynamics properties under the rule* $\begin{pmatrix} 1 & 1 \\ 1 & 2 \end{pmatrix}$ *with rigidity* $r > 1$.

(i) *Suppose* $X(t) = n > 0$ *and this is the first visit of the particle to* n *during the current state of the scatterer. Also suppose that the cell* $n-1$ *has been visited exactly once during the current state of the scatterer at* $n-1$*. Also suppose that* $\phi(n) = \phi(n-1) = v(t) = 1$*. Then,* $v(t+2r-1) = -1, \phi(n) = \phi(n-1) = 2, X(t+2r-1) = n-1$*, the current visit to* $n-1$ *is the first during the current state of the scatterer at* $n-1$*, and the site* n *has not been visited during the current state of its scatterer.*

(ii) *Suppose* $X(t) = n > 0$ *and this is the first visit of the particle to* n *during the current state of the scatterer. Also suppose that the cell* $n-1$ *has been visited exactly once during the current state of the scatterer at* $n-1$*. Also suppose that* $\phi(n) = \phi(n-1) = 2, v(t) = -1$*. Then,* $v(t+2r-1) = 1, \phi(n) = \phi(n-1) = 1, X(t+2r-1) = n-1$*, the current visit to* $n-1$ *is the first during the current state of the scatterer at* $n-1$*, and the site* n *has not been visited during the current state of its scatterer.*

(iii) *Suppose* $X(t) = n < 0$ *and this is the first visit of the particle to* n *during the current state of the scatterer. Also suppose that the cell* $n+1$ *has been visited exactly once during the current state of the scatterer at* $n+1$*. Also suppose that* $\phi(n) = \phi(n+1) = 1, v(t) = -1$*. Then,* $v(t+2r-1) = 1, \phi(n) = \phi(n-1) = 2, X(t+2r-1) = n+1$*, the current visit to* $n-1$ *is the first during the current state of the scatterer at* $n-1$*, and the site* n *has not been visited during the current state of its scatterer.*

(iv) *Suppose* $X(t) = n < 0$ *and this is the first visit of the particle to* n *during the current state of the scatterer. Also suppose that the cell* $n+1$ *has been visited*

exactly once during the current state of the scatterer at $n+1$*. Also suppose that* $\phi(n) = \phi(n+1) = 2, v(t) = 1$*. Then,* $v(t+2r-1) = -1, \phi(n) = \phi(n-1) = 1, X(t+2r-1) = n+1$*, the current visit to* $n-1$ *is the first during the current state of the scatterer at* $n-1$*, and the site* n *has not been visited during the current state of its scatterer.*

The proof of this result is similar to the Conversion Of Blocks Lemma, as the particle oscillates between the two cells in question. Now we are ready to examine the dynamics of this rule.

Proposition 45 (Oscillation) *A particle of LLGCA moving on the* $\mathbb{Z}$ *lattice under the rule* $\begin{pmatrix} 1 & 1 \\ 1 & 2 \end{pmatrix}$ *visits all sites of the underlying lattice infinitely many times with probability* 1.

Proof. Because of symmetry, WMA $v(0) = 1$. Let us examine what happens to the underlying lattice $\mathbb{Z}$ between the consecutive visits of the particle to 0. If 0 is initially white (black), the particle proceeds along a checkered pattern to the right (left), until it encounters a block of two cells. This happens with probability 1.

If these cells are white, the particle overturns them by case (i) (or case (iv) if 0 was initially black) of the Conversion of Blocks Lemma. The resulting situation is precisely the hypothesis of case (i) (or case (iii)) of the Return Through Checkered Pattern Lemma. Hence, after the blocks get overturned, so does the next pair of cells. Notice that the rightmost (leftmost) cell was overturned once with respect to its original state, but the one preceding to it was overturned twice. Now the situation fits again as a hypothesis for case (ii) (or case (iv)) of the Return Through Checkered Pattern Lemma. Now this Lemma can be repeatedly applied, until the particle reaches 0 and flips its color. At this point, the rightmost (leftmost) cell encountered by the particle was flipped once, also 0 was flipped once, and all cells in between were flipped twice

(hence, they retain their original states).

in the case the encountered block is black, it is overturned by case (ii) (or case (iii)) of the Conversion of Blocks Lemma. Similarly, the Return Through Checkered Pattern Lemma can be applied with the same conclusions. Now the particle will exhibit similar behavior on the other side of 0. Once it comes back to zero, we have the following.

- The checkered pattern on both sides of 0 grew by at least 1 cell.
- Only one cell has been modified on either side of 0 (i.e., 2 cells total)

Therefore, with probability 1, the particle ends up oscillating with always increasing amplitude. Hence, with probability 1, the particle will visit every cell of the underlying lattice $\mathbb{Z}$.

Q.E.D.

We conclude the discussion of dynamics with the obvious set of exceptional conditions. They have measure 0, as all previous exceptional conditions we have analyzed.

Corollary 46 *Under the conditions of the Oscillation Proposition, assume* $v(0) = +1$. *Then, the particle does not oscillate if and only if either*

(i) $n > 0$, *and initially* $\phi(n) = 2$ *and all of the cells* $\{k\}_{k \geq n}$ *form a checkered pattern, or*

(ii) $n < 0$, *and initially* $\phi(n) = 2$ *and all of the cells* $\{k\}_{k \leq n}$ *form a checkered pattern.*

In such a case, the particle will eventually propagate along the direction of the checkered pattern with unit speed.

5.5 Forward and Pushback Scatterers

An interesting feature of all models in this section is the fact that the velocity of the particle stays constant throughout the dynamics. None of these models were studied by Gajardo, so in addition to the usual construction of gates and complete statistical behavior, we classify these models as well.

5.5.1 Construction of Logic Gates

We will use white to indicate forward scatterers and black to indicate pushback scatterers.

For the NOT gate, the input is indicated by the state of the scatterer at 0 in the initial configuration: $\phi(0) = 3$ means the input variable is $FALSE$ and $\phi(0) = 0$ means the input variable is $TRUE$. All other scatterers are set to be forward scatterers. Now we will simulate the ant's behavior for exactly 1 step. The resulting dynamics can be found in Figure 23. We will ask the question — *does the ant ever visit cell* -1? In other words, the gate accepts its input if and only if the ant visits cell -1 during the simulation of ant's dynamics.

Observe that $X(1) = -1$ if and only if $\phi(0) = 3$. Hence the gate accepts its input if and only if the input variable had value $FALSE$, as desired.

For the AND gate, the input is indicated by the state of the scatterers at 0 and 1 in the initial configuration. All other cells contain forward scatterers. The dynamics for logic gates of this model is given in Figure 23. We run the system for 2 steps and ask the question *does the ant ever visit cell* 2? In other words, the gate accepts its input if and only if the ant visited cell 2.

Clearly, the ant visits the cell 2 after 2 steps if and only if initially $\phi(0) = \phi(1) = 0$. In other words, the gate accepts its input if and only if both input variables have the value $TRUE$, as desired.

5.5.2 Dynamics For Fixed Scatterers

5.5.2.1 Description of Dynamics

This is the $\begin{pmatrix} 0 & 3 \\ 0 & 0 \end{pmatrix}$ model. The local dynamics of the particle is pictured in Figure 24.

The particle moves in the direction of $v(0)$ $(-v(0))$ if the vertex 0 is white (black), until it passes over a cell of different color. At this point, the particle will cycle over the last pair of cells it visited.

Proposition 47 (Periodic Oscillation) *A particle of LLGCA moving on the* $\mathbb{Z}$ *lattice according to the rule* $\begin{pmatrix} 0 & 3 \\ 0 & 0 \end{pmatrix}$ *ends up in a periodic trajectory of period* 2 *with probability* 1. *This trajectory consists of the first consecutive cells of distinct color, encountered by the particle.*

Proof. Assume WLOG that $v(0) = +1$. Clearly, as soon as particle passes over two consecutive cells of different color it will oscillate between them forever with period 2. Observe that in the contrary case (i.e., if such oscillation is not to happen), we must have no two adjacent cells of different color encountered by the particle. In other words, either $\mathbb{N}$ is all white or $\mathbb{Z}^- \cup \{0\}$ is black.

Q.E.D.

The exceptional conditions to the proposition occur when there are no two adjacent cells of different color in the direction that the ant is moving. In that case, the ant moves along the infinite-size block of one color forever, so the set of exceptional conditions has measure 0 and the behavior of the ant in that case is also easy to analyze.

Corollary 48 *Under the conditions of the proposition, assume* $v(0) = +1$. *If the ant does not end up in an orbit of period* 2, *then the ant propagates with unit speed*

forever. This propagation occurs in the direction of $v(0)$ $(-v(0))$ *if and only if the scatterers from* 0 *to* ∞ $(-\infty)$ *form a white (black) block.*

Corollary 49 *The model* $\begin{pmatrix} 0 & 3 \\ & \\ 0 & 0 \end{pmatrix}$ *belongs to the class B1.*

5.5.2.2 Statistical Properties

Assume that initially $\phi(0) = 0$. Clearly then, $0, 1 \in \mathcal{O}$ and $Prob[n \in \mathcal{O}] = p^{n-1}$, for all $n \in \mathbb{Z}^+$. Hence, $Prob[n \in \mathcal{O}, (n+1) \notin \mathcal{O}] = qp^{n-1}$, for all $n \in \mathbb{Z}^+$.

Consequently, the rightmost point of the orbit in this model is a geometric random variable $N \geq 1$ with probability q of success. The cells visited by the particle infinitely often will be N and $N-1$, while the cells $0, 1, \ldots, N-2$ will be visited exactly once.

Proposition 50 *Under the conditions of the corollary, assume that initially* $\phi(0) = 0$. *Then, the rightmost point of the orbit in this model is a geometric random variable* $N \geq 1$ *with probability* q *of success. Thus, the expected sites that will be visited infinitely often are* $1/q$ *and* $1/q - 1 = p/q$. *So, the minimum expected rightmost site is* 1 *(for* $q = 1$*), and the maximum expected rightmost site is* ∞ *(for* $q = 0$*).*

5.5.3 Dynamics For One Flipping Scatterer Type

In this section, we will discuss the models $\begin{pmatrix} 1 & 3 \\ & \\ 0 & 0 \end{pmatrix}$ and $\begin{pmatrix} 0 & 3 \\ & \\ 1 & 0 \end{pmatrix}$. It is easy to notice that these models are actually equivalents of each other, and so mimic each other's properties. Hence, we only provide the results for the $\begin{pmatrix} 1 & 3 \\ & \\ 0 & 0 \end{pmatrix}$ model.

5.5.3.1 Description of Dynamics

We will analyze the model $\begin{pmatrix} 1 & 3 \\ & \\ 0 & 0 \end{pmatrix}$. The local dynamics of the particle is pictured in Figure 24.

The particle moves in the direction of $-v(0)$ until it encounters a white scatterer. Then the particle will proceed in the direction of $v(0)$, oscillating between each consecutive black cell it encounters and between the last visited white cell until the black cell flips and changes to a forward scatterer. Afterwards, the particle proceeds in the direction of $v(0)$. This results in infinite propagation of the particle.

5.5.3.2 Effects of Rigidity

The only effect rigidity has is in slowing down the propagation speed, as it takes more oscillations to flip the state of the scatterer at each initially black cell. Other than that, the behavior of the particle stays exactly the same as in the $r = 1$ case, and results in infinite propagation in the direction of $v(0)$ with probability 1.

Proposition 51 (Propagation) *Suppose that the particle of LLGCA is moving on* $\mathbb{Z}$ *in accordance with the rule* $\begin{pmatrix} 1 & 3 \\ & \\ 0 & 0 \end{pmatrix}$ *with any rigidity. Then, with probability* 1*, the particle will eventually propagate in the direction of* $v(0)$*.*

Proof. The particle will initially move in the negative direction until it encounters a white cell at some z. At this point, it will oscillate between z and $z + v(0)$ until $z + v(0)$ becomes white, and then the particle proceeds to $z + v(0)$, repeating this process, and never returning to z again. Hence, the particle eventually propagates in the direction of $v(0)$, unless no white cell can be found going from 0 in the direction of $-v(0)$, which occurs with probability of 0.

Q.E.D.

The exceptional conditions are obvious from the proof of the proposition.

Corollary 52 *Under the conditions of the proposition, the particle does not propagate in the direction of* $v(0)$ *if and only if initially all cells from* 0 *in the direction of* $-v(0)$ *are black. In this case the particle propagates with unit speed in the direction* $-v(0)$*.*

Corollary 53 *The model* $\begin{pmatrix} 1 & 3 \\ 0 & 0 \end{pmatrix}$ *belongs to the class U1.*

5.5.3.3 Statistical Properties

Assume $v(0) = +1$. Here we will attempt to compute the expected time τ_M that the particle will visit some site $M \geq 0$ for the first time, such that $\phi(M) = 0$ at the time of the visit. Clearly, $\tau_{M+1} - \tau_M = 1 + 2rq$, so it only remains to compute τ_0. Clearly, the length of the black block to the left of 1 is a geometric random variable with parameter q. For each additional cell in this black block, we add $2r$ steps to convert that cell. Hence,

$$\tau_0 = \sum_{n=0}^{\infty} \left(pq^n\right)(2rn) = \frac{2rpq}{(1-q)^2} = \frac{2rq}{p}.$$

Using this as an initial condition, we solve the recurrence for τ_M to get

$$\tau_M = M + 2rqM + \frac{2rq}{p}, \quad M \in \mathbb{N}.$$

Hence, the long-term speed of propagation is

$$\lim_{M\to\infty} \frac{M}{\tau_M} = \frac{1}{1+2rq}.$$

Proposition 54 *Assume the conditions of the previous proposition. Then, with probability* 1*, the particle eventually propagates with speed of* $(1 + 2rq)^{-1}$ *in the direction of* $v(0)$*. Precisely, the expected time* τ_M *that the particle will visit some site* $M \in \mathbb{N}$ *for the first time, such that* $\phi(M) = 0$ *at the time of the visit, is given by* $\tau_M = M + 2rqM + \frac{2rq}{p}$*.*

5.5.4 Dynamics For Two Flipping Scatterer Types

5.5.4.1 Description of Dynamics

This is the model $\begin{pmatrix} 1 & 3 \\ 1 & 0 \end{pmatrix}$. The local dynamics of the particle is pictured in Figure 24.

The particle will move in the direction of $v(0)$ with speed 1, leaving behind a trail of black cells, until a black cell is encountered. At that point, the particle will move in the opposite direction, leaving behind a white block, until a white cell is encountered. Then, the particle will oscillate this way forever, always increasing the size of its amplitude, eventually visiting all the sites of the underlying integer lattice.

5.5.4.2 Effects of Rigidity

For this particular model, with the introduction of rigidity, the basic behavior stays the same. The particle slows down, but continues oscillating with always increasing amplitude.

For the purpose of our analysis, we assume $v(0) = +1$ (which means that $v(t) = +1 \forall\ t \in \mathbb{N}$, as we remarked before). It turns out that there are two special local configurations, essential to understanding the behavior of the particle. They are as follows.

Suppose the particle is in a white cell that was never visited before, and to the right of the particle is a block of black cells, not visited before, followed by a block of unvisited white cells. Call such a configuration C_0. On the other hand, if the particle is in a black cell, and to the left of it is a block of white cells visited once, followed by an unvisited black block, then we call such configuration C_1.

Proposition 55 *Suppose a particle of LLGCA is moving on $\mathbb{Z}$ according to the model* $\begin{pmatrix} 1 & 3 \\ 1 & 0 \end{pmatrix}$. *Also assume $v(0) = +1$. Then, the particle ends up oscillating with increasing amplitude. Eventually the particle visits each site of $\mathbb{Z}$ infinitely many times.*

Proof. We will prove that the particle must end up in either of configurations C_0, C_1, and that C_0 evolves into C_1, while C_1 evolves into C_0.

First, assume that configuration C_0 occurs. The particle oscillates between the white cell z and the first black cell $z+1$ exactly $2r-1$ times. At this point, z is black

and is as if it was never visited, particle is at $z+1$ and $z+1$ is white and visited once. This is repeated until the end of the black block. Then, the particle browses through the white block at unit speed until it encounters some black cell. At this point, the white block that was never visited became a white block that was visited once; the black block that was visited once, now is a black block that was not visited at all, and it grew by one cell on the left; finally, the particle is in a black cell to the right of the structure. In summary, we have precisely C_1.

Now assume we are in C_1 and the particle is at some black cell z. In $2r-1$ steps, z becomes white as if it was not visited before and the particle is at $z-1$ that now turned black. This repeats until the end of the white block, and the particle proceeds to traverse the black block at unit speed. It's easy to see we end up in C_0 again, except the white block grew by at least one cell (could be more if there was a white block to the right of z).

Hence, C_0 and C_1 evolve into each other, increasing with each evolution. Now, if initially 0 is black, the particle proceeds to the left until it hits a white cell, and this is configuration C_0 (it's possible that the unvisited white block has size 0 at this point). Now suppose initially 0 is white. The particle proceeds to the right until it hits a black cell. Now we are in configuration C_1 (though if -1 was originally white it is possible to have the unvisited black block of size 0). Hence, one of C_0, C_1 must occur.

Q.E.D.

The set of exceptional condition is evident from the proof as well. As in other cases, it has measure 0 considering our initial distribution of the scatterers.

Corollary 56 *Under the conditions of the proposition, the particle does not end up oscillating if and only if either* $\mathbb{N}$ *is initially white (then the particle propagates with unit speed in the positive direction) or if* $\mathbb{Z}^- \cup \{0\}$ *is initially black (then the particle propagates with unit speed in the negative direction).*

Corollary 57 *The model* $\begin{pmatrix} 1 & 3 \\ 1 & 0 \end{pmatrix}$ *belongs to the class* $U1$.

5.5.4.3 Statistical Properties

Assume the conditions of the proposition. Fix some $M \in \mathbb{N}$. We will compute τ_M — the expected time of first visit to M so that M is white. The argument is strikingly similar to the situation in Section 5.2.4.3, which described the statistical properties of the model $\begin{pmatrix} 1 & 1 \\ 0 & 0 \end{pmatrix}$. Just as there, we let $0 \leq \alpha_1 < \ldots < \alpha_\nu \leq M$ denote the positions of all initially black scatterers in $[0, M] \cap \mathbb{Z}$ and let $0 > -\beta_1 > \ldots > -\beta_\nu$ denote the positions of the first ν initially white scatterers in $\mathbb{Z}^-$. Clearly, from the proof of proposition, it is evident that to travel from 0 to 0, in the process flipping the first black cell on the right and the first white cell on the left, takes exactly $2r(\alpha_1+\beta_1)$ time. Applying this principle, it is easy to see that just as in Section 5.2.4.3, we have

$$\tau_M = M + 2rE\left[\sum_{j=1}^{\nu}(\alpha_j + \beta_j)\right],$$

with

$$Prob\left[a_j = k | \nu = N\right] = \frac{\begin{pmatrix} k \\ j-1 \end{pmatrix}\begin{pmatrix} M-k \\ N-j \end{pmatrix}}{\begin{pmatrix} M+1 \\ N \end{pmatrix}},$$

for $1 \leq j \leq N$ and $j - 1 \leq k \leq M + 1 - N + j$. The probability is zero for every other k. Moreover, β_j is still distributed negative binomial. However, this time the parameters are j and p, so $E\left[\beta_j\right] = qj/p$, and our results will be a bit different. Repeating the argument from Section 5.2.4.3, we just plug in a different value for

$E[\beta_j]$, and do similar modifications. We obtain

$$\begin{aligned}
\tau_M &= M + 2rE\left[\sum_{j=1}^{\nu}(\alpha_j+\beta_j)\right] \\
&= M + 2r\sum_{N=0}^{M+1}\binom{M+1}{N}q^N p^{M+1-N}\sum_{j=1}^{N}\left(\frac{jM+2j-N-1}{N+1}+\frac{qj}{p}\right) \\
&= M + \frac{r}{p}\sum_{N=0}^{M+1}\binom{M+1}{N}q^N p^{M+1-N}N\left(Mp+(N+1)q\right) \\
&= M + Mr\sum_{N=0}^{M+1}N\binom{M+1}{N}q^N p^{M+1-N} + \frac{qr}{p}\sum_{N=0}^{M}N(N+1)\binom{M+1}{N}q^N p^{M+1-N} \\
&= M + Mr(M+1)q + \frac{qr(M+1)q(2+Mq)}{p} \\
&= M^2rq\left(1+\frac{q^2}{p}\right) + M\left(1+\frac{rq(1+q^2)}{p}\right) + \frac{2rq^2}{p}.
\end{aligned}$$

We have just established the following

Proposition 58 *Under the conditions of the proposition, assume $v(0) = +1$. Let τ_M be the expected time to hit a cell $M \in \mathbb{N}$ for the first time with M being white. Then,*

$$\tau_M = M^2rq\left(1+\frac{q^2}{p}\right) + M\left(1+\frac{rq(1+q^2)}{p}\right) + \frac{2rq^2}{p}.$$

5.6 Simulating Boolean Circuits With LLGCA

In a recent paper, Gajardo, Goles and Moreira considered the so-called Langton's ant model on $\mathbb{Z}^2$ [36]. They were able to construct logic gates and simulate a Boolean network, thus proving that predicting whether Langton's ant on the square lattice will visit a certain site is a **P**-hard problem (see above or [58] for the definition).

Langton's Ant is a particular restriction of our model to rigidity 1. This implies that if the rigidity models are extended from one dimension to the two-dimensional square lattice, predicting whether or not the particle will visit a certain site of $\mathbb{Z}^2$ will also be **P**-hard.

However, we are concerned with such systems in one dimension. Due to the inherent two-dimensionality of the binary tree of the Boolean network, if we are to successfully simulate it, we must have the particle repeatedly browse through the gates, re-using the output of the previous pass of the particle as the input for its next pass. In our models, there are only two things that change with time – the characteristics of the particle (position, velocity) and states of the scatterers. Therefore, if we wish to simulate a Boolean network, there are only two choices for the variables, which we explain below.

The first choice, which has been used in [36], picks the states of the scatterers to be the Boolean variables in the network. If we follow this choice, we must exclude any analysis of the fixed-environment models. Additionally, among the models with changing environment, many result in propagation or end up in a periodic orbit, neither of which is acceptable for construction of a Boolean network, because with such models it is impossible to browse repeatedly through the gates. This leaves us with a few models that end up visiting each site of the lattice infinitely many times (see, e.g., $\begin{pmatrix} 1 & 2 \\ & \\ 1 & 0 \end{pmatrix}$ with odd rigidity). Finally, even among these models, we must have the particle pass a configuration and always get scattered in the same direction on exit, which is impossible in one dimension. This is precisely how the gates were constructed in [36]. There, the ant always passes left to right over a configuration of gates, and always exits on the right. Thus, the bottom layer of cells of the previous configuration, which is the output, becomes the top layer of cells of the lower configuration, which is its input. This uses the two-dimensionality of the square lattice.

Alternatively, if we let the characteristics of the particle define the Boolean variables in the network, it becomes impossible to reuse the output of one layer of the gates as the input to the next layer. In fact, since the output is defined in terms of

the characteristics of the particle, and the input is still defined as states of the scatterers, it is impossible to use the output of one layer of gates as an input to the next layer. Consequently, there is no adequate choice of variables to be able to simulate the Boolean network with LLGCA on $\mathbb{Z}$. Thus, we have proved the following

Theorem 59 *It is impossible to simulate a Boolean network with LLGCA models on* $\mathbb{Z}$.

In this work, the gates are constructed using the characteristics of the particle to define the output of the gates, and using the settings of the scatterers to define the input to the gates. Compared to the other alternative, this avoids the problem of having a fixed environment.

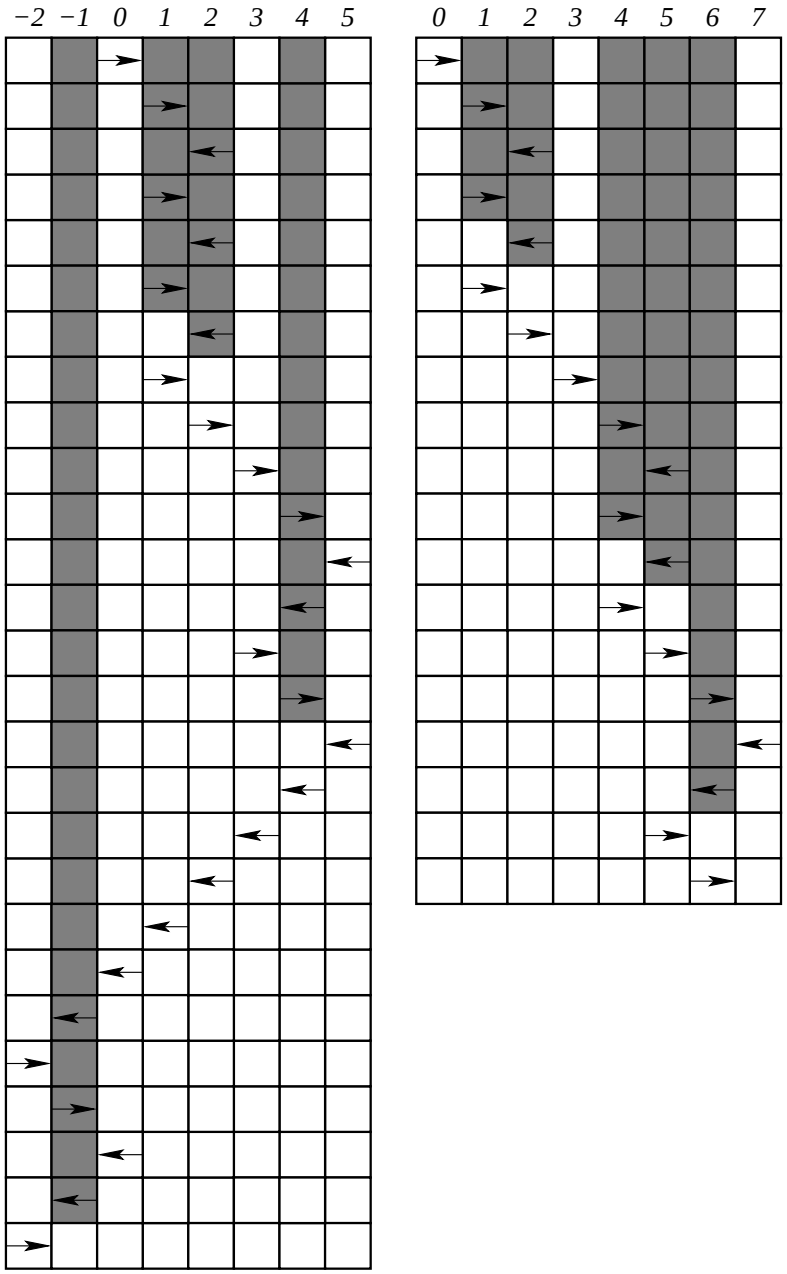

Figure 15: Dynamics Of The Black Flipping Delayed Back Scatterer And White Fixed Forward Scatterer Model With $r = 1$ And $r = 2$

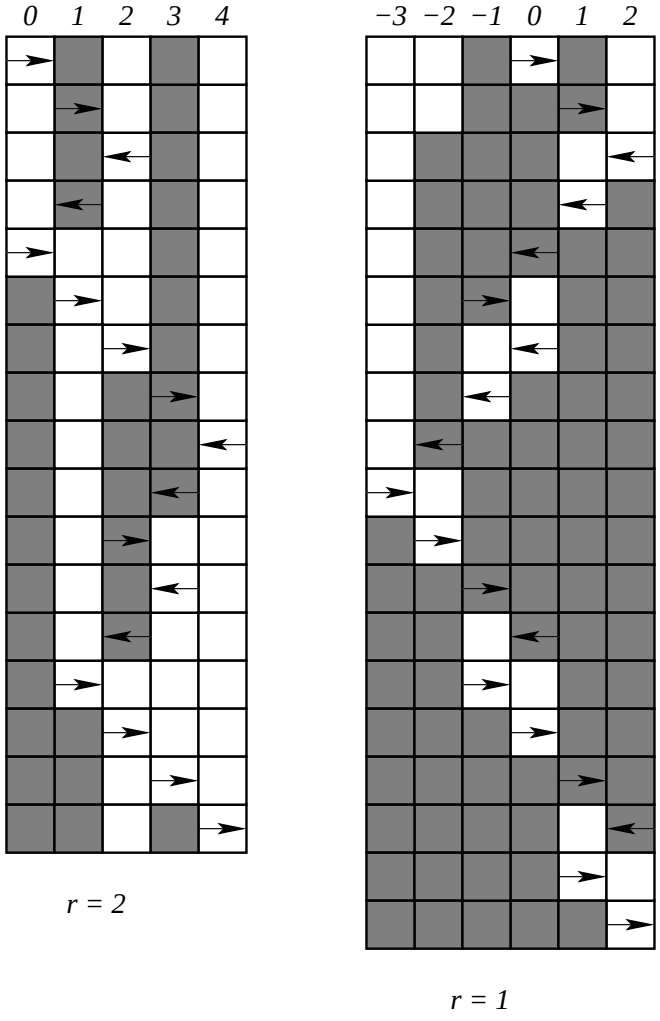

Figure 16: Dynamics Of The Black Flipping Delayed Back Scatterer And White Flipping Forward Scatterer Model With $r = 1$ and $r = 2$

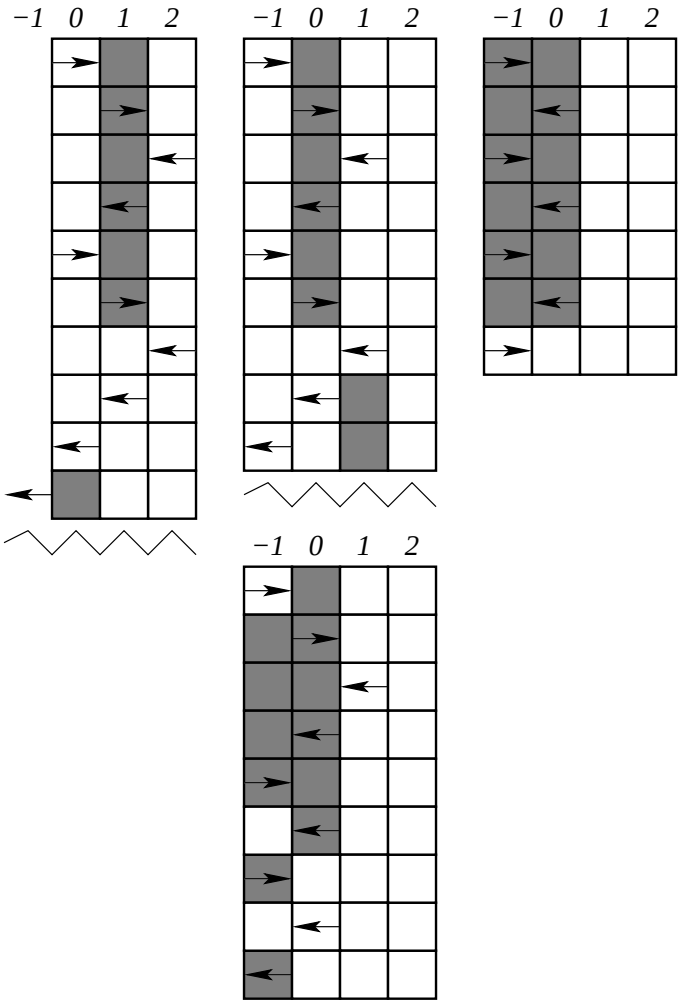

Figure 17: Dynamics Of The Black Flipping Delayed Back Scatterer And White Flipping Forward Scatterer Model With $r = 3$

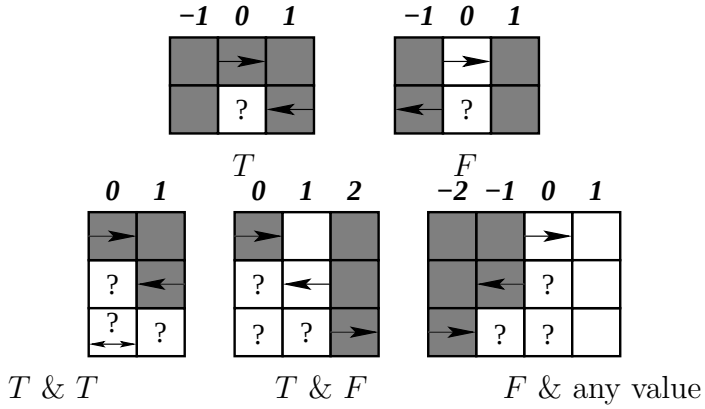

Figure 18: Dynamics Of The Logic Gates For White Back And Black Delayed Back Scatterers

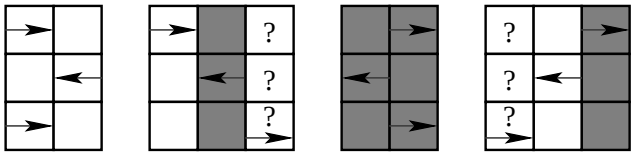

Figure 19: Dynamics Of The Black Fixed Back Scatterer and White Fixed Delayed Back Scatterer Model

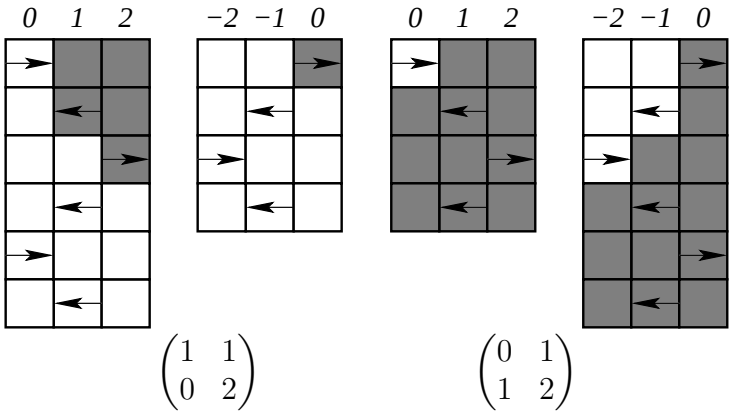

Figure 20: Dynamics Of The Black Back Scatterer And White Delayed Back Scatterer Models With $r = 1$

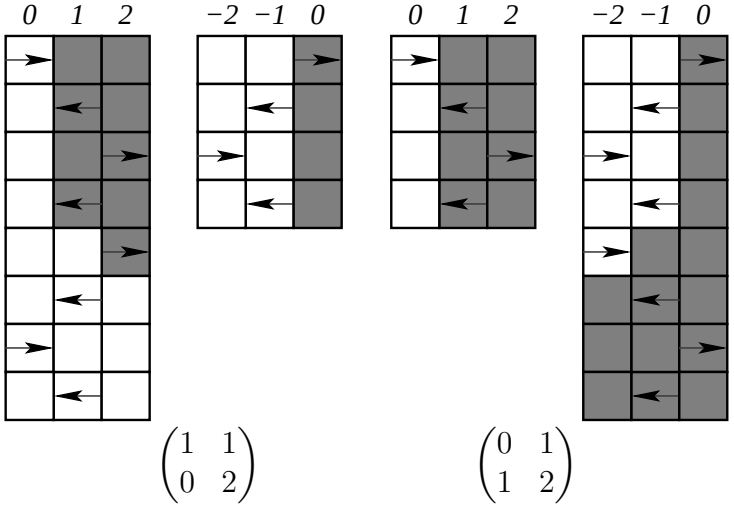

Figure 21: Dynamics Of The Black Back Scatterer And White Delayed Back Scatterer Models With $r = 2$

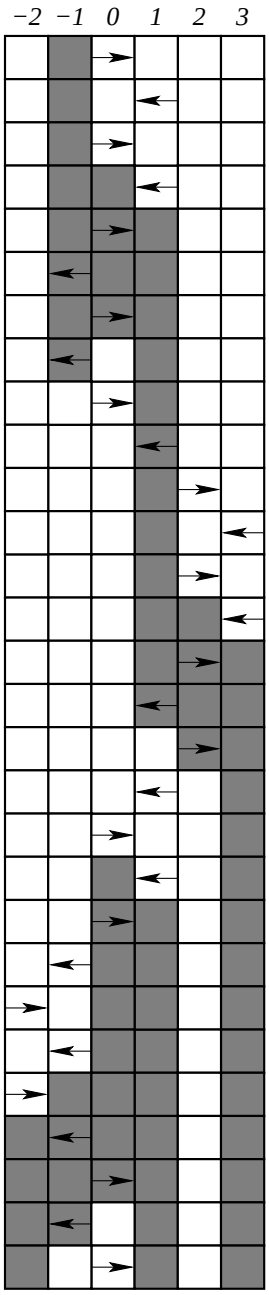

Figure 22: Dynamics Of The Black Flipping Back Scatterer And White Flipping Delayed Back Scatterer Model With $r = 2$

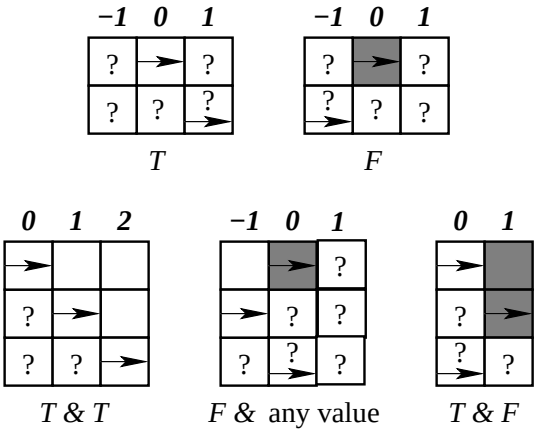

Figure 23: Dynamics Of The Logic Gates For White Forward And Black Pushback Scatterers

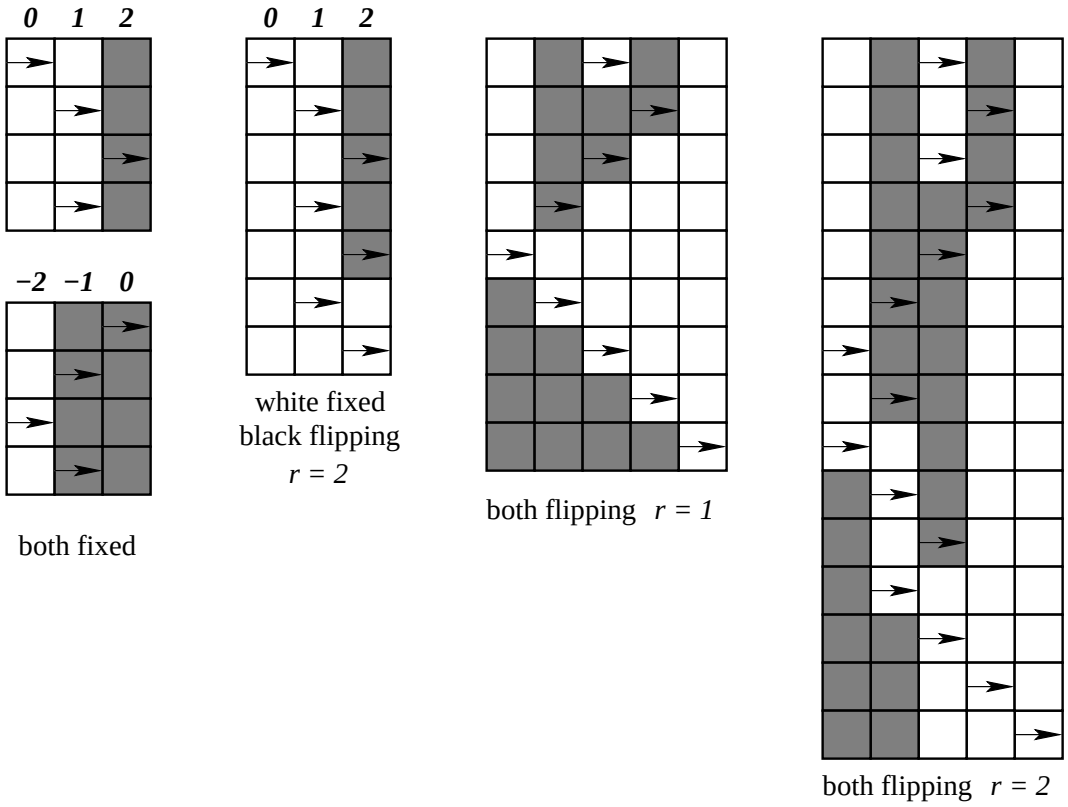

Figure 24: Dynamics Of The Models With White Forward And Black Pushback Scatterers

CHAPTER VI

PARTITIONING TSS LINES

6.1 TSS Production Lines Model

6.1.1 Introduction

The TSS line works as follows. Consider an assembly line in which each set of items (e.g., coats, fish nets, etc.) requires processing in the same sequence on m workstations. A station can process at most one item at a time, and exactly one worker is required to accomplish the processing. All items are identical, and so each one requires the same total processing time, which we will normalize to one "time unit."

Each worker carries an item from station to station, processing it on each of the stations. If this is the last worker, he continues processing until he finishes the item. Otherwise, the processing continues until he passes it on to a subsequent worker. According to the sequence of workers on the line, each worker can be labeled by a number from 1 to n in the direction of the product flow. To implement the above behavior, we require each worker to follow the TSS rule:

The Forward Part. The worker will remain devoted to a single item and will process it on successive work stations. At any station the worker of higher index has higher priority. If the worker's item is taken over by his successor, or, if the last worker completes processing the item, then he should relinquish the item and begin to follow the Backward Part.

The Backward Part. The worker will walk back and take over the item of his predecessor. If he is the first worker, he will pick up raw materials to start a new item. He will then begin to follow the Forward Part.

When compared to standard zone manufacturing, the TSS rule has at least two drawbacks. The first is that a worker following the Forward Part may be blocked if the machine he needs to operate on is used by the subsequent worker. In such a case, the TSS rule requires the worker to wait until the machine becomes available.

The second drawback is the interruption caused while following the Backward Part of the TSS rule, when one worker is attempting to take over the work of his predecessor on the line. A great deal of effort is invested to avoid this delay. For instance, Aisin-Seiki sells workstations that have been specifically configured to support TSS-style processing. In addition, the production line is U-shaped to reduce walking time.

Nevertheless, TSS production lines have proven to be effective. In apparel, they allowed simplification of the management of the flow lines. Additionally, introduction of TSS methodology increased the production rate of such lines by more than 30% compared to zone manufacturing [8].

6.1.2 Mathematical Model of TSS Production

We will represent the production line by the unit segment $[0, 1] \subset \mathbb{R}$. Each worker can be completely characterized by his velocity $v_i(z) : [0, 1] \to \mathbb{R}^+$, which we assume to be constant. In other words, $v_i(z) = v_i \forall\ 1 \leq i \leq n, z \in [0, 1]$. The state of the system at any time t can be captured by the vector $(x_i(t))_{i=1}^n$, where $0 \leq x_1(t) \leq x_2(t) \leq \ldots \leq x_n(t) \leq 1$ are the positions of workers at time t. Finally, the same setup can be considered in discrete time by looking at the Poincaré section of the underlying dynamical system. We will choose the Poincaré section as $\{x_1(t) = 0\}$.

Assume that worker velocities satisfy $v_1 \leq v_2 \leq \ldots \leq v_n$. Then, there are no blockage points during production. Also WMA that the walk during the backward part of the rule happens with infinite speed. This assumption is supported by the studies in [6] where all examined lines required just a few seconds to walk back to the preceding worker.

Hence, the map generating the corresponding dynamical system is linear and has the form

$$x_k^{(t+1)} = x_{k-1}^{(t)} + \frac{v_{k-1}}{v_n}\left(1 - x_n^{(t)}\right). \tag{1}$$

We can change variables, setting

$$a_n^{(t)} = \frac{1 - x_n^{(t)}}{v_n} \quad \text{and} \quad a_k^{(t)} = \frac{x_{k+1}^{(t)} - x_k^{(t)}}{v_k}, 1 \leq k \leq n-1.$$

The map (1) becomes

$$a_1^{(t+1)} = a_n^{(t)} \quad \text{and} \quad a_k^{(t+1)} = \frac{v_{k-1}}{v_k} a_{k-1}^{(t)} + \left(1 - \frac{v_{k-1}}{v_k}\right) a_n^{(t)}, 2 \leq k \leq n. \tag{2}$$

It is clear that (2) is describing a Markov chain with transition matrix

$$T = \begin{bmatrix} 0 & 0 & \dots & 0 & 1 \\ \frac{v_1}{v_2} & 0 & \dots & 0 & 1 - \frac{v_1}{v_2} \\ 0 & \frac{v_2}{v_3} & \dots & 0 & 1 - \frac{v_2}{v_3} \\ \dots 0 & 0 & \dots & \frac{v_{n-1}}{v_n} & 1 - \frac{v_{n-1}}{v_n} \end{bmatrix}. \tag{3}$$

The corresponding characteristic polynomial is

$$p_T(\lambda) = (\lambda - 1)\left(\lambda^{n-1} + \frac{v_{n-1}}{v_n}\lambda^{n-2} + \ldots + \frac{v_2}{v_n}\lambda + \frac{v_1}{v_n}\right). \tag{4}$$

T is stochastic, with all entries between 0 and 1. Consequently, the largest eigenvalue of T, corresponding to the vector $(1, \ldots, 1)^T$ is 1. In addition, this system must also have a unique fixed point that is stable and is a global attractor. The speed of convergence of our dynamical system to its fixed point is dependent on the second largest eigenvalue of T, say Λ_T.

We will now consider partitioning workers into groups to work on TSS production lines. We will always assume that in each group the workers will be sequenced from slowest (in the beginning) to fastest (at the end).

6.2 Partitioning According To Rate Of Production

6.2.1 Reduction to Multiprocessor Scheduling

The first practical type of partitioning to consider is attempting to split the pool of workers into groups $\{G_i\}_{i=1}^{m}$ that will work at approximately the same rate. In other words, we are interested in minimizing the maximal production rate among the resulting groups. It is easy to see that this is equivalent to synchronizing these groups.

To formulate this *Equal Worker Partitioning Problem* (EWPP) precisely, let Ω denote the set of all possible assignments into groups. For each particular assignment $\omega \in \Omega$, let each group G_i be assigned the workers $\left\{v_{i_j}\right\}_{j=1}^{k}$, where $k = k(i)$. The optimal rate of production in each group is just the sum of the speeds of the workers: $r_i = \sum_{j=1}^{k(i)} v_{i_j}$. We need to find the optimal assignment ω^* that will minimize the largest r_i. Therefore, we must find

$$\omega^* = \arg\min_{\Omega} \max_{1 \le i \le m} r_i = \arg\min_{\Omega} \max_{1 \le i \le m} \sum_{j=1}^{k(i)} v_{i_j}.$$

Let us consider the following decision problem (e.g., see [39, 44, 63].)

Multiprocessor Scheduling Problem (MSP). Given m processors and n tasks, with each task j requiring a processing time p_j, we seek to allocate each task to a processor so as to minimize the total processing time allocated to any one processor.

Observe that if we let Ψ denote the set of all possible assignments, then for any particular assignment $\psi \in \Psi$, processor i will be assigned jobs with running times $\left\{v_{i_j}\right\}_{j=1}^{k}$, where $k = k(i)$. We are basically aiming to

$$\min_{\Psi} \max_{1 \le i \le m} \sum_{j=1}^{k(i)} p_{i_j}.$$

Clearly, our EWPP problem is just the MSP in disguise. This can be revealed by renaming workers v_{i_j} to jobs p_{i_j}, groups to processors, and Ω to Ψ. In other words,

not only does our EWPP reduce to the MSP, but the reverse is also true, since they are, in fact, the same problem.

The MSP has been proven to be **NP**-hard [44, 63]. Consequently, our EWPP is also **NP**-hard. This means that the most efficient way to find the correct partitioning is to sift through all possible orderings, examining each one.

6.2.2 Approximation Algorithms

MSP is a special case of scheduling, which is a classical **NP**-hard problem. A lot of research has been done on designing approximation algorithms to solve the various versions of the scheduling problem. Such research seeks to come up with algorithms that will quickly reach an answer, guaranteed to be at most α-factor optimal. In other words, if T is the processing time needed by the assignment produced by the algorithm and T^* is time needed by the optimal assignment, then $T/T^* \leq \alpha$.

In particular, the most intuitive algorithm is as follows. We order the jobs arbitrarily. Then, we schedule each successive job on the next machine that has been assigned the least amount of work so far. This algorithm runs in linear time. Graham [39] proved that this is a 2-factor approximation algorithm. To prove the tightness of the bound, he forced the algorithm to schedule a very long job last.

To take care of this difficulty, we may pre-sort the jobs by required processing time p_j. The resulting algorithm would run in time $O(n \log n)$. Alternatively, we could sort in linear time if we assume that the required processing times p_j are integers. This modification was also analyzed by Graham [40], who showed that it results in a 4/3-factor algorithm.

In 1987, Hochbaum and Shmoys [48] came up with a polynomial time approximation scheme that runs in $O(n^{2k}\lceil \log_2 \frac{1}{\epsilon} \rceil)$ where $k = \lceil \log_{1+\epsilon} \frac{1}{\epsilon} \rceil$. This polynomial scheme is a $(1+\epsilon)^2$-factor solution.

Hence, for a person who is interested in solving a particular instance of the problem, many approximation algorithms are available. The preciseness of the answer will depend on the computing resources that the client wishes to invest.

6.2.3 Variations of the Problem

One may desire to simplify the problem by considering only the partitions into groups of the same size (i.e., let $k \neq k(i)$), which greatly reduces the size of Ω. However, if in the MSP we consider jobs large enough, the partitions must work out to be of equal size. This may be achieved by adding the same big constant (say, $\sum_j p_j$) to each p_j. Thus, the complexity of the problem does not reduce.

Alternatively, one may want to formulate different optimality constraints. For example, in EWPP we may want to partition the pool of workers so that all average group speeds will be as close as possible to the average worker speed. In other words, letting $\bar{V} = \frac{1}{n}\sum_{j=1}^{n} v_j$, we will seek

$$\hat{\omega} = \arg\min_{\Omega} \max_{1\leq i\leq m} \left| \frac{\sum_{j=1}^{k(i)} v_{i_j}}{k(i)} - \bar{V} \right| = \arg\min_{\Omega} \max_{1\leq i\leq m} \left(\frac{\sum_{j=1}^{k(i)} v_{i_j}}{k(i)} - \bar{V} \right)^2 .$$

Intuitively, it should be clear that the optimal assignment $\hat{\omega}$ will not change from ω^* in the preceding formulation. The reason is that $\hat{\omega}$ minimizes the largest deviation from the average. Such deviation is minimum precisely when the speed of the fastest group is minimal among all possible distributions $\omega \in \Omega$. Hence, we should expect $\hat{\omega} = \omega^*$.

This analysis is particularly simple for $k \neq k(i)$ (i.e., for constant k). Then, addition or subtraction of a constant $\bar{V}$ will not affect the optimal solution, and neither will squaring the resulting difference, since x^2 is monotone increasing for $x > 0$. Thus, the new optimality criterion is just a reformulation of the preceding one.

6.3 Partitioning According To Speed Of Convergence

6.3.1 Partitioning Into Pairs

Given the worker velocities $v_1 \leq v_2 \leq \ldots v_{2n}$, we can subdivide them into n pairs $\{\{v_{i_1}, v_{i_2}\}_{i=1}^{n}\}$, where $v_{i_1} \leq v_{i_2}$. The transition matrix (3) for each such pair will be given by

$$T_i = \begin{bmatrix} 0 & 1 \\ \frac{v_{i_1}}{v_{i_2}} & 1 - \frac{v_{i_1}}{v_{i_2}} \end{bmatrix}.$$

We seek to achieve convergence to the optimal production stage with the fastest rate. This optimal production stage occurs at the fixed point of the corresponding dynamical system. T_i clearly has two eigenvalues, 1 and $-\frac{v_{i_1}}{v_{i_2}}$. Consequently, the rate of convergence to the fixed point for each such pair $\{v_{i_1}, v_{i_2}\}$ is determined by the absolute value of the second largest eigenvalue of the corresponding transition matrix. This eigenvalue is $\Lambda_{T_i} = \frac{v_{i_1}}{v_{i_2}} < 1$. Hence, the rate of convergence is the fastest when Λ_{T_i} is the smallest possible. We will therefore seek to minimize Λ_{T_i}.

Call the set of all such assignments Ω. We can characterize a particular assignment $f \in \Omega$ of the workers into actual pairs by the rate of convergence to the fixed point of the slowest pair in the assignment, say $X(f)$. Clearly,

$$X(f) = \max_{1 \leq i \leq n} \left\{ \frac{v_{i_1}}{v_{i_2}} \right\}.$$

So, we now have a way of identifying the optimal assignment:

$$f^* = \arg\min_{f \in \Omega} X(f) = \arg\min_{f \in \Omega} \max_{1 \leq i \leq n} \left\{ \frac{v_{i_1}}{v_{i_2}} \right\}.$$

In other words, we seek an assignment that will minimize the second largest eigenvalue of the slowest pair, thus maximizing the rate of convergence to the fixed point.

Theorem 60 *The optimal assignment is given by* $f^*\left(v_{i_j}\right) = v_{i+n(2-j)}$ *where* $1 \leq i \leq n$ *and* $1 \leq j \leq 2$.

Proof. We define the index-distance δ on the worker speeds as follows

$$\delta(v_i, v_j) = |i - j|.$$

Basically, we are claiming that if $v_1 \leq \ldots \leq v_{2n}$ are the worker speeds, then the optimal pairings f^* preserve the maximum possible index-distance between worker speeds in the sequence $\{v_i\}_{i=1}^{2n}$, i.e.,,, the pairings are $\{v_i, v_{n+i}\}_{i=1}^{n}$.

We proceed by induction on n. For the base case, let $n = 2$ and consider a system with $2n = 4$ workers. There are three ways of pairing them up. These are as follows:

$$\begin{aligned} f_1 = &\quad \{\{v_1, v_2\}, \{v_3, v_4\}\} \\ f_2 = &\quad \{\{v_1, v_3\}, \{v_2, v_4\}\} \\ f_3 = &\quad \{\{v_1, v_4\}, \{v_2, v_3\}\} \end{aligned}$$

Clearly, $X(f_3) = \frac{v_2}{v_3}$. We have $\frac{v_2}{v_3} \geq \frac{v_1}{v_3}$ and $\frac{v_2}{v_3} \geq \frac{v_2}{v_4}$. Thus, $X(f_2) \leq X(f_3)$. Moreover, $\frac{v_1}{v_2} \geq \frac{v_1}{v_3}$ and $\frac{v_3}{v_4} \geq \frac{v_2}{v_4}$. Consequently, $X(f_1) \geq X(f_2)$.

In summary, we have $X(f_2) \leq X(f_1)$ and $X(f_2) \leq X(f_3)$. So, $f^* = f_2$, as desired.

□

Now for the inductive step, assume that we are working with $n \geq 3$ pairs and $2n \geq 6$ total workers. Each assignment $f \in \Omega$ clearly must pair up the worker v_1 with some worker v_k where $2 \leq k \leq 2n$. For any fixed k, denote the set of all such assignments Ω_k. Clearly, $\{\Omega_k\}_{k=2}^{2n}$ is a partition of Ω. Let

$$f^k = \arg\min_{f \in \Omega_k} X(f) = \arg\min_{f \in \Omega_k} \max_{1 \leq i \leq n} \left\{ \frac{v_{i_1}}{v_{i_2}} \right\}.$$

All assignments in Ω_k at the same time have exactly one pair assigned identically, namely $\{v_1, v_k\}$. Hence, this pair can be removed from every assignment in Ω_k, then the Inductive Hypothesis can be applied to yield the actual optimal assignments, and then the pair $\{v_1, v_k\}$ will be attached to the conclusions of the Inductive Hypothesis, to obtain the actual f^k. This way,

$$f^k = \left\{ \begin{array}{ll} \left\{\{v_1, v_k\}, \{v_i, v_{n+i}\}_{i=2}^{k}, \{v_i, v_{n+i-1}\}_{i=k+1}^{2n}\right\}, & 2 \leq k \leq n+1 \\ \left\{\{v_1, v_{n+m}\}, \{v_i, v_{n+i-1}\}_{i=2}^{m}, \{v_i, v_{n+i}\}_{i=m+1}^{n}\right\}, & k = n+m \geq n+1 \end{array} \right\|.$$

It suffices to prove that $f^* = f^{n+1}$.

In the case $k = n + m \geq n + 1$, f^k and f^{k+1} only differ in two pairs. Under f^k we have the assignments $\{v_1, v_{n+m}\}, \{v_{m+1}, v_{n+m+1}\}$, while under f^{k+1} we pair up $\{v_1, v_{n+m+1}\}, \{v_{m+1}, v_{n+m}\}$. Since $v_1 \leq v_{m+1} \leq v_{n+m} \leq v_{n+m+1}$, the base case implies $X(f^k) \leq X(f^{k+1})$. So, $X(f^{n+1}) \leq X(f^{n+2}) \leq \ldots \leq X(f^{2n})$.

Similarly, in the case $k \leq n + 1$, f^k and f^{k+1} also differ only in two pairs. Under f^k we assign $\{v_1, v_k\}, \{v_{k+1}, v_{n+k}\}$, while under f^{k+1} we pair up $\{v_1, v_{k+1}\}, \{v_k, v_{n+k}\}$. Again, the base case implies $X(f^k) \geq X(f^{k+1})$. So, $X(f^2) \geq X(f^3) \geq \ldots \geq X(f^{n+1})$. Hence, $f^{n+1} = \arg\min_{f \in \Omega} X(f) = f^*$, as desired.

Q.E.D.

6.3.2 Partitioning Into Triples

Given the worker speeds $v_1 \leq v_2 \leq \ldots v_{3n}$, we can subdivide them into n triples $\{\{v_{i_1}, v_{i_2}, v_{i_3}\}_{i=1}^n\}$, where $v_{i_1} \leq v_{i_2} \leq v_{i_3}$. The transition matrix (3) for each such pair will be given by

$$T_i = \begin{bmatrix} 0 & 0 & 1 \\ \frac{v_{i_1}}{v_{i_2}} & 0 & 1 - \frac{v_{i_1}}{v_{i_2}} \\ 0 & \frac{v_{i_2}}{v_{i_3}} & 1 - \frac{v_{i_2}}{v_{i_3}} \end{bmatrix}.$$

The corresponding characteristic polynomial (4) becomes

$$p_{T_i}(\lambda) = (\lambda - 1)\left(\lambda^2 + \lambda \frac{v_{i_2}}{v_{i_3}} + \frac{v_{i_1}}{v_{i_3}}\right).$$

So, T_i has three eigenvalues: 1, corresponding to the eigenvector $\vec{1}$, and

$$\lambda_{\pm} = \frac{-\frac{v_{i_2}}{v_{i_3}} \pm \sqrt{\frac{v_{i_2}^2}{v_{i_3}^2} - \frac{4v_{i_1}}{v_{i_3}}}}{2} = \frac{-v_{i_2} \pm \sqrt{v_{i_2}^2 - 4v_{i_1}v_{i_3}}}{2v_{i_3}}.$$

If $\sqrt{v_{i_2}^2 - 4v_{i_1}v_{i_3}}$ is imaginary, then both λ_+ and λ_- will yield the same modulus of the resulting complex number, namely $\sqrt{v_{i_1}/v_{i_3}}$. However, when $\sqrt{v_{i_2}^2 - 4v_{i_1}v_{i_3}}$ is

real, we have $|\lambda_-| > |\lambda_+|$. Hence, the speed of each such pair, which is the absolute value of the second largest eigenvalue of the corresponding transition matrix, will be

$$\Lambda_{T_i} = \left\| \begin{cases} \sqrt{\frac{v_{i_1}}{v_{i_3}}}, & v_{i_2}^2 \leq 4v_{i_1}v_{i_3} \\ \frac{v_{i_2}+\sqrt{v_{i_2}^2-4v_{i_1}v_{i_3}}}{2v_{i_3}}, & v_{i_2}^2 \geq 4v_{i_1}v_{i_3} \end{cases} \right\|.$$

Define $\Omega, X(f)$ and f^* as in the preceding section, and denote the optimal second largest eigenvalue corresponding to f^* by Λ^*. It would be logical to assume that an analog of Theorem 60 holds for splitting into triples as well. In other words, we would suspect that

$$f^* = \arg\min_{f\in\Omega} \max_{1\leq i\leq n} \{\Lambda_{T_i}\}$$

can be achieved by a splitting that, as in the preceding section, will maintain the biggest possible index-distance inside all triples. The resulting assignment would be $\{\{v_1, v_{n+1}, v_{2n+1}\}, \ldots, \{v_n, v_{2n}, v_{3n}\}\}$.

However, this is not the case. Using a computer simulation, a wide range of counter-examples was discovered. Grouping a set of six workers intuitively (having in mind Theorem 60 for grouping workers into pairs), we would form the triples as $\{\{v_1, v_3, v_5\}, \{v_2, v_4, v_6\}\}$.

Some of the found counter-examples are given in Table 6.3.2 below. The first column indicates the set of six worker speeds to be partitioned into two groups of three workers each. The intuitive partition, given by $\{\{v_1, v_3, v_5\}, \{v_2, v_4, v_6\}\}$ results in the eigenvalues, given in the second and third columns. Columns four through six list the optimal partitioning, together with the resulting eigenvalues. Finally, column seven lists the optimal eigenvalue, corresponding to the speed of convergence to the fixed point, and the last two columns give statistics measuring how close the worker speeds in question are to each other.

Notice that scaling the speeds of workers by any constant factor affects neither Λ_{T_i} nor Λ^*. Thus, a combination of the standard deviation of the set of worker speeds and of the $v_{\max} \div v_{\min}$ statistics are necessary to keep track of how close the worker speeds

Table 3: Some Counter-Examples of Theorem 60 For Two Triples

Workers	**Intuitive**		**Optimal**					$v_6 \div$
1,2,3,4,5,6	**135**	**246**	**Groups**	Λ_{T_1}	Λ_{T_2}	Λ^*	σ	v_1
$\frac{1}{16}, \frac{1}{8}, \frac{1}{4}, \frac{1}{2}, 1, 2$	0.242	0.044	134,246	0.177	0.044	0.177	0.74	32
$\frac{1}{8}, \frac{1}{4}, \frac{1}{2}, 1, 2, 4$	0.233	0.044	134,246	0.177	0.044	0.177	1.48	32
$1, 3, 7, 8, 9, 10$	0.589	0.548	136,245	0.5	0.577	0.577	3.56	10

are together. Computer simulations were ran over various sets of worker speeds. Even on sets where the counter-examples exist, it seems that there are no counter-examples, as long as the worker speeds are close together, both in the sense of standard deviation and $v_{\max}/v_{\min}$. This suggests the following

Conjecture 1 *If the variance among the speeds of the workers is small, and the ratio of highest to lowest speed is small as well, then an analog of Theorem 60 will hold for the set of worker speeds under consideration.*

CHAPTER VII

CONCLUSION

7.1 Discussion

First, let us compare the behavior of models with $r = 1$, $r = \infty$ and $1 < r < \infty$ on trees. In the flipping models, the initial distribution of the scatterers determines the actual path that the particle will follow. So, the initial distribution of the scatterers also influences the size of the orbit, unless T is a complete tree of any order.

However, for the models with fixed environment, the period of the particle is independent of the initial distribution of the scatterers. The only thing influenced by the initial distribution of the scatterers is the order in which the subtrees are visited in T. Yet, for the LGCA with fixed environment on any tree T, the particle will perform a depth-first search. So, the behavior of the models with fixed environment turns out to be much more regular than the behavior of the models with changing environment and finite rigidity.

Another conclusion from the results on the general behavior of the models with fixed environment is that the behavior of such models depends heavily on the drawing of the underlying graph.

Finally, the rigidity models on complete d-regular trees have low-degree (sub-quadratic) polynomial periods in the number of vertices of the underlying graph. However, in terms of r, the periods can be linear (if $d = r$) or non-linear. This analysis allows us to identify the properties that cause rigidity models to have large periods on arbitrary trees and might be helpful in analyzing the behavior of LGCA on arbitrary graphs.

Remarkably, in the vast majority of the models analyzed in this thesis, either a

depth-first search or the alike behavior emerges. Such behavior occurs in systems with random environments as well. Another feature of these models is an eventual propagation along some ray in infinite graphs. Both these results have applications, e.g.,, for the robot navigation problem. Indeed, both these results show that it is not always necessary to specifically prepare an environment to ensure these types of behavior.

Additionally, in the analysis of LLGCA on $\mathbb{Z}$, we have constructed logic gates for all models under consideration. Each logic gate we constructed functions independently of the rigidity of the surrounding environment. We have also shown that it is impossible to connect any set of gates on $\mathbb{Z}$ into a logical circuit, thus proving that at most polynomial time is required to decide whether the ant will visit a certain cell in the one-dimensional setting. Consequently, one-dimensional systems possess some degree of complexity, even though such systems turn out to be considerably less complex than their multi-dimensional analogs, which are **P**-hard.

We also analyzed partitioning a pool of workers into groups to work on TSS production lines. We showed that such problems turn out to be very difficult and resource-consuming. For example, the problem to partition the pool of workers into groups with approximately the same speed is **NP**-hard. Also, in partitioning according to the rate of convergence to the fixed point for every group, there is no nice algorithm for partitioning into groups composed of more than two workers.

7.2 Future Directions

Analyzing LGCA models on lattices and general graphs is a relatively young field. Hence, there are a great many new directions for research and interesting problems to consider. In particular, there are the lower bound results of Gajardo, Goles and Moreira [34] showing that the size of the orbit of the flipping LGCA model is exponentially large even on planar graphs. However, there is a gap between this lower

bound and the trivial upper bound obtained by counting all possible states in the system. It would be nice to close the gap between the two bounds.

It has been shown that the flipping model on $\mathbb{Z}^2$ is **P**-hard. It remains an interesting problem to specify precisely the complexity class for this model, as well as for the rigidity model. It has not yet been determined whether adding rigidity to the system in 2+ dimensions results in any extra sophistication in the computational complexity of the model.

Additionally, some key questions remain unanswered even for the simplest 2-D lattices, such as boundedness or unboundedness of the orbit. Numerical studies show very unintuitive behavior exhibited by the model even on the integer lattice in $\mathbb{Z}^2$, which leaves a wealth of questions on statistical and dynamical properties of such models.

Lastly, in the case of TSS lines, a lot of work has been done in approximation algorithms for EWPP. Perhaps it would be possible to come up with a complexity class for the problem of partitioning a pool of workers into groups to optimize the rate of convergence to the fixed point of the corresponding dynamical systems. It would be natural to look for an approximation algorithm in this area as well.

REFERENCES

[1] Ahuja, R. K., Magnanti, T. L., and Orlin, J. B., *Network Flows*. Prentice Hall, 1993.

[2] Atrubin, A. J., "An interactive one-dimensional real-time multiplicator," *IEEE Trans. Electron. Computers*, vol. EC-14, pp. 394–399, 1965.

[3] Banks, E. R., *Information and transition in cellular automata*. PhD thesis, MIT, 1971.

[4] Bartholdi, J. J., Bunimovich, L. A., and Eisenstein, D. D., "Dynamics of 2- and 3-workers "bucket brigade" production lines," *Operations Research*, vol. 47, pp. 488–491, 1999.

[5] Bartholdi, J. J. and Eisenstein, D. D., "Bucket brigades: a self-organizing scheme for sharing work," *Artifical Intelligence and Manufacturing Research Planning Workshop*, pp. 9–13, 1996.

[6] Bartholdi, J. J. and Eisenstein, D. D., "Production lines that balance themselves," *Operations Research*, vol. 44, pp. 21–33, 1996.

[7] Bartholdi, J. J. and Eisenstein, D. D., "A self-balanced order picking system for a warehouse: A case study," *Preprint*, 1998.

[8] Bartholdi, J. J., Eisenstein, D. D., and Foley, R., "Performance of bucket brigades when work is stochastic," *Operations Research*, vol. 49, pp. 710–719, 2001.

[9] Bennett, C. and Grinstein, G., "Role of irreversibility in stabilizing complex and nonergodic behavior in locally interacting systems," *Phys. Rev. Lett.*, vol. 55, pp. 657–660, 1985.

[10] Berlekamp, E., Conway, J., and Guy, R., *Winning ways for your mathematical plays*, vol. 2. Academic Press, 1982.

[11] Boghosian, B. M., "Lattice gases and cellular automata," *Future Gen. Comp. Sys.*, vol. 16, no. 2-3, pp. 171–185, 1999. Also available at http://arxiv.org/comp-gas/9905001.

[12] Boghosian, B. M. and Coveney, P. V., "A particulate basis for an immiscible lattice-gas model," *Comp. Phys. Comm.*, vol. 129, pp. 46–55, 2000. Also available at http://arxiv.org/cond-mat/9911340.

[13] Boghosian, B. M., Coveney, P. V., and Emerton, A. N., "A lattice-gas model of microemulsions," *Proc. Royal Soc. A*, vol. 452, pp. 1221–1250, 1996. Also available at http://arxiv.org/comp-gas/9507001.

[14] Bowden, K., ed., *Special issue on general physical systems and the emergence of physical structure from information theory, Int. J. Gen. Syst.*, vol. 27(1-3), 1998.

[15] Bunimovich, L. A., "Many-dimensional Lorentz cellular automata and Turing machines," *Int. J. Bif. Chaos*, vol. 6, pp. 1127–1136, 1996.

[16] Bunimovich, L. A., "Controlling production lines," in *Handbook of Chaos Control* (Schuster, H.-G., ed.), pp. 347–373, Wiley-VCH, 1999.

[17] Bunimovich, L. A., "Walks in rigid environments," *Physica A*, vol. 279, pp. 169–179, 2000.

[18] Bunimovich, L. A., "Motion of particles in random media and many-dimensional turing machines," *Multiple Valued Logic*, vol. 6, pp. 463–481, 2001.

[19] Bunimovich, L. A., "Walks in rigid environments: Symmetry and dynamics," *Asterisque*, 2003.

[20] Bunimovich, L. A. and Kreslavskiy, D. M., "Lorentz gas cellular automata on graphs," *Theor. Comp. Sci.*, vol. 306/1-3, pp. 195–221, 2003.

[21] Bunimovich, L. A. and Sinai, Y. G., "Statistical properties of Lorentz gas with periodic configuration of scatterers," *Comm. Math. Phys.*, vol. 78, pp. 479–497, 1981.

[22] Bunimovich, L. A., Sinai, Y. G., and Chernov, N. I., "Statistical properties of two-dimensional hyperbolic billiards," *Russ. Math. Surv.*, vol. 46, no. 4, pp. 47–106, 1991.

[23] Bunimovich, L. A. and Troubetzkoy, S. E., "Rotators, periodicity and absence of diffusion in cyclic cellular automata," *J. Stat. Phys.*, vol. 74, pp. 1–10, 1994.

[24] Chernov, N. I., "Statistical properties of the periodic Lorentz gas. multidimensional case," *J. Stat. Phys.*, vol. 74, no. 1-2, pp. 11–53, 1994.

[25] Cohen, E. G. D., "New types of diffusion in lattice gas cellular automata," in *Microscopic Simulations of Complex Hydrodynamic Phenomena* (Mareschal, M. and Holian, B. L., eds.), pp. 137–152, Plenum Press: New York, 1992.

[26] Cormen, T. H., Leiserson, C. E., and Rivest, R. L., *Introduction to Algorithms*. MIT Press, 1990.

[27] Dewdney, A. K., "Two-dimensional Turing machines and Tur-mites make tracks on a plane," *Scientific American*, vol. 261, pp. 180–183, September 1989.

[28] Diestel, R., *Graph Theory*. Springer: New York, 1997.

[29] Farmer, D., Toffoli, T., and Wolfram, S., eds., *Cellular automata*. North-Holland, 1984.

[30] Fisher, P., "Generation of primes by a one-dimensional real time iterative array," *Journal of the ACM*, vol. 12, pp. 388–394, 1965.

[31] Fredkin, E. and Toffoli, T., "Conservative logic," *Int. J. Theor. Phys.*, vol. 21, pp. 219–253, 1982.

[32] Fredkin, E. and Toffoli, T., "Design principles for achieving high-performance digital technologies," in *Collision-Based Computing* (Adamatzky, A., ed.), pp. 27–46, Springer-Verlag: London, 2002.

[33] Frisch, U., Hasslacher, B., and Pomeau, Y., "Lattice-gas automata for the Navier-Stokes equation," *Phys. Rev. Lett.*, vol. 56, no. 14, pp. 1505–1508, 1986.

[34] Gajardo, A., Goles, E., and Moreira, A., "Generalized Langton's ant: dynamical behavior and complexity," in *STACS 2001, LNCS 2010* (Ferreira, A. and Reichel, H., eds.), p. 259, Springer-Verlag: Berlin, 2001.

[35] Gajardo, A. and Mazoyer, J., "Langton's ant evolution in the degree 3 graphs," *Preprint*, 1999.

[36] Gajardo, A., Moreira, A., and Goles, E., "Complexity of Langton's ant," *Discr. App. Math.*, vol. 117, pp. 41–50, 2002.

[37] Gajardo-Schulz, A., *Influence du réseau spatial sue le comportement d'un système dynamique: la fourmi de Langton*. PhD thesis, University de Chile, 2001.

[38] Gardner, M., "The fantastic combinations of John Conway's new solitaire game 'Life'," *Sc. Am.*, vol. 223, no. 4, pp. 120–123, 1970.

[39] Graham, R. L., "Bounds for certain multiprocessing anomalities," *Bell System Technical Journal*, vol. 45, pp. 1563–1581, 1966.

[40] Graham, R. L., "Bounds on multiprocessing timing anomalities," *SIAM Journal on Applied Mathematics*, vol. 17, pp. 476–429, 1969.

[41] Graham, R. L., Knuth, D. E., and Patashnik, O., *Concrete mathematics: a foundation for computer science*. Addison Wesley, 2 ed., 1994.

[42] Grosfils, P., Boon, J. P., Cohen, E. G. D., and Bunimovich, L. A., "Propagation and self-organization in lattice random media," *J. Stat. Phys.*, vol. 97, pp. 575–608, 1999. Also available at http://arxiv.org/cond-mat/9905168.

[43] Gunn, J. M. F. and M. Ortuño, "Percolation and motion in a simple random environment," *J. Phys. A*, vol. 18, pp. 1095–1099, 1985.

[44] Hall, L. A., "Approximation algorithms for scheduling," in *Approximation algorithms for NP-hard problems* (Hochbaum, D., ed.), pp. 1–45, PWS Publishing Company, 1995.

[45] Hardy, G. H. and Wright, E. M., *An introduction to the theory of numbers*. Clarendon Press: Oxford, 1960.

[46] Hardy, J., de Pazzis, O., and Pomeau, Y., "Molecular dynamics of a classical lattice gas: transport properties and time correlation functions," *Phys. Rev. A*, vol. 13, pp. 1949–1960, 1976.

[47] Hedlund, G. A., "Endomorphism and automorphism of the shift dynamical system," *Math. Syst. Theory*, vol. 3, pp. 51–59, 1969.

[48] Hochbaum, D. S. and Shmoys, D. B., "Using dual approximation algorithms for scheduling problems: theoretical and practical results," *Journal of the ACM*, vol. 34, pp. 144–162, 1987.

[49] Holland, J., "Universal spaces: a basis for studies in adaptation," in *Automata Theory*, pp. 218–230, Academic Press, 1966.

[50] Kong, X. P. and Cohen, E. G. D., "Diffusion and propagation in triangular Lorentz lattice gas cellular automata," *J. Stat. Phys*, vol. 62, no. 3-4, pp. 737–757, 1991.

[51] Kreslavskiy, D. M., "Construction of logic gates for one-dimensional Lorentz gases, and their dynamics and statistical properties," *Multi Valued Logic*, to be published.

[52] Langton, C. G., "Studying artificial life with cellular automata," *Physica D*, vol. 22, pp. 120–149, 1986.

[53] Lorentz, H. A., "The motion of electrons in metallic bodies, I, II and III," *Koninklijke Akademie van Wetenschappen te Amsterdam, Section of Sciences*, vol. 7, pp. 438–453, 585–593, 684–691, 1905.

[54] Margolus, N., "Physics-like models of computation," *Physica D*, vol. 10, pp. 81–95, 1984.

[55] Margolus, N. and Toffoli, T., *Cellular automata machines*. MIT Press: Cambridge, 1987.

[56] Meng, H.-F. and Cohen, E. G. D., "Growth, self-randomization, and propagation in a lorentz lattice gas," *Phys. Rev. E*, vol. 50, no. 4, pp. 2482–2487, 1994.

[57] Packard, N. and Wolfram, S., "Two-dimensional cellular automata," *J. Stat. Phys.*, vol. 38, pp. 901–946, 1985.

[58] Papadimitriou, C., *Computational Complexity*. Addison-Wesley, 1994.

[59] Rothman, D. H. and Zaleski, S., *Lattice-gas automata: Simple models of complex hydrodynamics*. Cambridge University Press, 1997.

[60] Toffoli, T., "Reversible computing," in *Automata, Languages and Programming* (de Bakker and van Leeuwen, eds.), pp. 632–644, Springer-Verlag, 1980.

[61] Toffoli, T., "Cellular automata as an alternative to (rather than an approximation of) differential equations in modeling physics," *Physica D*, vol. 10, pp. 117–127, 1984.

[62] Ulam, S., "Random processes and transformations," *Proc. Int. Congr. Mathem. (held in 1950)*, vol. 2, pp. 264–275, 1952.

[63] Vazirani, V. V., *Approximation algorithms*. Springer-Verlag, 2001.

[64] Vichniac, G., "Simulating physics with cellular automata," *Physica D*, vol. 10, pp. 96–115, 1984.

[65] von Neumann, J., *Theory of self-reproducing automata (ed. A. Burks)*. Univ. of Illinois Press, 1966.

[66] Waksman, A., "An optimum solution to the firing squad synchronization problem," *Information and Control*, vol. 9, pp. 66–78, 1966.

[67] Wolfram, S., "Statistical mechanics of cellular automata," *Revs. Modern Phys.*, vol. 55, no. 3, pp. 601–664, 1983. Also available at http://www.stephenwolfram.com/publications/articles/ca/83-statistical/1/text.html.

[68] Wolfram, S., "Computation theory of cellular automata," *Commun. Math. Phys.*, vol. 96, pp. 15–57, 1984. Also available at http://www.stephenwolfram.com/publications/articles/ca/84-computation/index.html.

[69] Wolfram, S., "Universality and complexity in cellular automata," *Physica D*, vol. 10, pp. 1–35, 1984. Also available at http://www.stephenwolfram.com/publications/articles/ca/84-universality/index.html.

[70] Wolfram, S., "Cellular automaton fluids. I. basic theory," *J. Stat. Phys.*, vol. 45, no. 3-4, pp. 471–526, 1986. Also available at http://www.stephenwolfram.com/publications/articles/physics/86-fluids/index.html.

[71] Wolfram, S., "Random-sequence generation by cellular automata," *Adv. Applied Math.*, vol. 7, pp. 123–169, 1986. Also available at http://www.stephenwolfram.com/publications/articles/ca/86-random/index.html.

[72] Wolfram, S., *Theory and applications of cellular automata*. World Scientific, 1986. Add. info at http://www.stephenwolfram.com/publications/books/ca-wspc.html.

[73] Zuse, K., *Rechneider raum*. Vieweg: Braunschweig, 1969. Transl. as Calculating space, Tech. Transl. AZT-70-164-GEMIT, MIT Project MAC (1970).

VITA

Dmitry Michael Kreslavskiy was born in Kharkov, Ukraine on November 20, 1978. His family immigrated to the United States in February of 1991. Dmitry attended Yeshiva Atlanta, a small private high school in the Atlanta metro area. In 1994, at 15, he enrolled in Oglethorpe University via the early admission program, following the advice of his parents. In one semester, he received the Oxford Scholarship there.

After getting his high school diploma in 1995, Dmitry transferred to Georgia Tech. Being torn between mathematics, physics and computer science, he chose applied mathematics as his major field, planning to use it as a common thread in all fields of his interest. He completed his undergraduate studies in 1997, and was admitted to the Ph.D. program in Algorithms, Combinatorics and Optimization at Georgia Tech. He worked with Dr. Leonid Bunimovich, pursuing his doctoral degree.

In 2003, Dmitry married Anna Shleyfman. He hopes to continue his career in the Atlanta area.